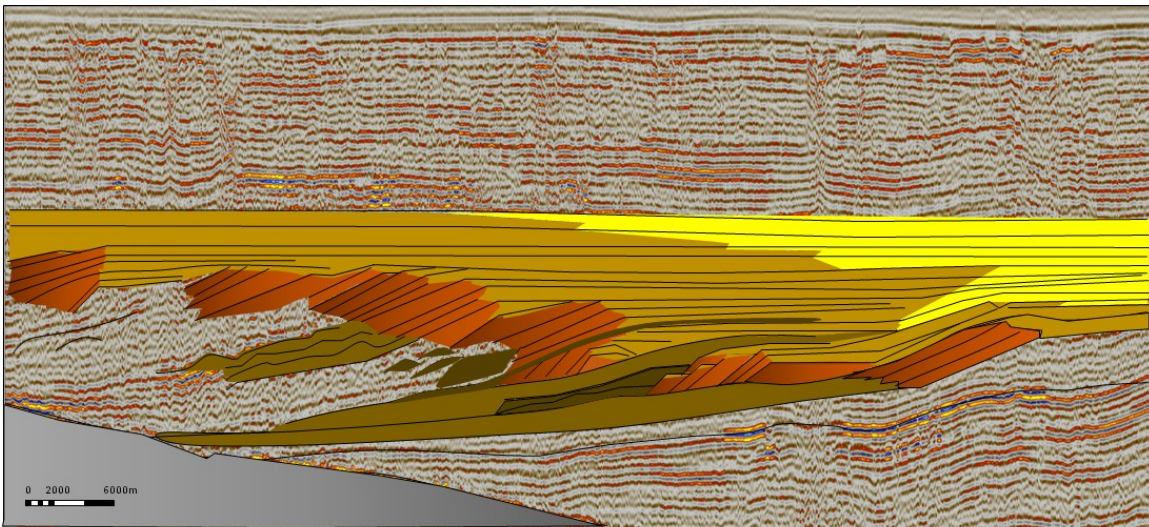# Sequence stratigraphic analysis of Eridanos deltaic shallow gas-bearing deposits in North Sea

An insight into the shallow Dutch subsurface

A thesis presented for the degree of
Master of Applied Earth Science
by

Natalia Papatrecha
npapatrecha@gmail.com

Delft, The Netherlands
21 September 2017

Delft University of Technology
Faculty of Civil Engineering and Geosciences
Department of Geosciences and Engineering

Sequence stratigraphic analysis of Eridanos deltaic shallow gas-bearing deposits in North Sea.

An insight into the shallow Dutch subsurface.

by

Natalia Papatrecha

to obtain the degree of

Master of Science
in Petroleum Engineering & Geosciences

at the Delft University of Technology,
to be defended publicly on Thurday September 21, 2017 at 13:00 .

Supervisors:	Dr. Hemmo Abels	Assistant Prof. TU Delft
	Dr. Joep Storms	Associate Prof. TU Delft
Committee:	Dr. Hemmo Abels	Assistant Prof. TU Delft
	Dr. Joep Storms	Associate Prof. TU Delft
	Dr. ir. Femke Vossepoel	Associate Prof. TU Delft

An electronic version of this thesis is available at `http://repository.tudelft.nl/`.

TUDelft
Delft
University of
Technology

Abstract

Growing interest has been expressed the last decades regarding the Late Cenozoic, gas-bearing sediments of Southern North Sea Basin. Comprising the shallow subsurface of the Dutch offshore sector, these sediments have been deposited by Eridanos fluvio-deltaic system, draining the Fennoscandian and Baltic shield through the present Baltic Sea. Three successful producing fields - A12-FA (2007), F02a-B-Pliocene (2009) and B13-FA (2011)- and five under development have triggered the conduction of several studies in the offshore area. However the deltaic environment has been characterized as highly complex owing to its influence by the onset of Northern Hemisphere Glaciation and thus the processes that governed the system have not become entirely understood. Enhanced cooling followed by the waxing and waning of the glaciers during warmer periods had an immediate impact on sediment supply, accommodation space and mineralogical input. Although the sediments have been studied in terms of chrono-biostratigraphy, no systematic investigation with respect to the three main aforementioned factors as well as the regional sequence stratigraphy and its link to the reservoir deposits has been made up to date. Therefore, this study employed sequence stratigraphy as a method to examine Eridanos conditions of deposition, investigate the interplay between accommodation space and sediment supply and explore the nature of the gas-bearing reservoir sediments. The adopted methodology is comprised of two basic pillars, observation and interpretation. The first records as clearly as possible the observations arise from the sequence analysis while the second extracts the meaningful information and interprets it in terms of temporal and spatial concepts. Using 2D seismic and well log data the basic observations were the stratal terminations, stacking patterns, seismic facies and the shoreline trajectory.

Seismic and well log interpretation showed that the delta experienced multiple events of sea level fall which forced the shoreline to regress basinward and caused sediment erosion or non-deposition. These events are bounded by nine time-significant surfaces of subaerial unconformities which constitute the depositional sequences. Normal regression comprised the dominant depositional trend, combined with aggrading-prograding patterns, leading to characteristic alternations of highstand and lowstand system tracts. Three main depositional environments which correspond to open marine turbidites (submarine lobes), delta front and delta top were identified from well logs, core descriptions and the seismic facies analysis. The study suggests that the shallow gas is located in the alternations of silty-sandstones and claystones of the delta plain which comprise the vertical stacking of parasequence topsets within the highstand- lowstand system tracts. Reconstruction of the relative sea level changes and sedimentation rates was made based on a technique introduced by this study. It uses the average thickness of each seismic unit in order to interpolate time between the three known absolute ages obtained by the literature. The graphs showed that the accommodation space was generated by a low rate of sea level rise while sedimentation rates were increasing over time. However the scarcity of time constrains in combination with the uncertainty in the estimation of seismic volumes resulted in a low resolution outcome. A comparison between the findings of this study and those of the existing literature was made. The overall depositional trends and conditions seem to be in accordance with the other surveys. Nonetheless the proposed interplay between accommodation and supply can be assigned as local since the examined area is limited compare to areas studied in literature. Limitations are traced in the quality of the 2D seismic data hampering the observation regarding the relation between the reflectors and the surfaces. Consequently, the study offers an insight into the conditions under which the gas-bearing deltaic sediments were deposited and tries to place them in the established sequence stratigraphic framework. Also it provides information regarding the distribution of the deltaic environments and identification of the reservoir rocks within each setting. The resulting interpretation can be used for prediction of the reservoir formations since the genetically-related packages where they were identified are distributed in a predictable manner within a sedimentary basin.

keywords: Eridanos Delta, Sequence Stratigraphy, Seismic Interpretation, Shallow gas reservoirs, Depositional Environments, Accommodation space, Sediment Supply

Acknowledgments

Having reached the end of my academic path I would like to express my sincere gratitude to those who contribute to the realization of this unique experience, my Master.

First of all, I would like to cordially thank my supervisor Dr. Joep Storms who tried to find a project on a subject I expressed my liking, despite the difficulties. Also his persistence on doing something I really enjoyed has been proved of high importance. Almost being my weekly supervisor, his experience was guiding me till the end. Advices on making always a planning and realizing the purpose of the project helped me substantially. Finally, his support and feedbacks were extremely appreciated.

Secondly I would like to heartily express my gratitude to my supervisor Dr. Hemmo Abels who showed immediate interest in this project. His excitement for Geology was very inspiring and motivating during my thesis as he was always trying to trigger my interest with his observations and comments. I really appreciated that he was discussing my thoughts and he was approachable almost every day until late at night.

Many thanks to Prof. Gerhard Diephuis for his priceless help and advice. His experience with respect to geophysical matters is unquestionable. He was always eager to help when I was facing "seismic" problems.

Furthermore I would like to express my sincere gratitude to Dr. ir. Femke Vossepoel for her presence in my Committee. Her immediate interest and willingness to discuss my project was highly appreciated. Mrs Vossepoel's experience on seismic interpretation and her comments and advice on the last phase of the project helped me a lot in the application of my findings.

At this point I would like to thank the Ph.D Candidate Rémi Charton for making time and discussing the issues I was facing during the project, despite his busy schedule due to his PhD completion. Also his love for Geology in the technical world of TU Delft makes his work to stand out. Finally, Ph.D Candidate Helena van der Vegt also motivated me the last period with her supporting emails and her willingness to help me.

Most of all, I want to thank with all my heart my parents and my sister for not only doing sacrifices for me in order to receive a higher education but also their every day support and strength while studying in a technical university. My sister and best friend Efilina was always advising and encouraging me till the end. Thank you Efilina for being there for me! Our Saturday coffee break was keeping me alive!

Finally, my co-student Stephan de Hoop who despite his insane workload due to the high complexity project his carrying all these months was every day next to me, supporting me, motivating me and helping me with any issues I was facing. I will never forget these long nights of work and music, stress and fun. We made it...thank you Stephan! Thank you all..

I would like to recite some lyrics of the poem "Ithaka" from the Greek poet C. Cavafys:

"As you set out for Ithaka hope the voyage is a long one, full of adventure, full of discovery. Laistrygonians and Cyclops, angry Poseidon, do not be afraid of them: you will never find things like that on your way as long as you keep your thoughts raised high, as long as a rare excitement stirs your spirit and your body..."

Contents

List of Figures

List of Tables

List of Abbreviations

2D Two Dimensions.

3D Three Dimensions.

A Accommodation space.

CDP Common Depth Point.

DT Transit time difference.

E East.

FR Forced Regression.

FSST Falling Stage System Tract.

GR Gamma Ray.

HST Highstand System Tract.

LST Lowstand System Tract.

m Meters.

Ma Million years (mega annum).

MFS Maximum Flooding Surface.

MRS Maximum Regressive Surface.

N North.

NE Northeast.

NR Normal Regression.

NSB North Sea Basin.

O and G Oil and Gas.

S Sediment Supply.

SF Seismic Facies.

SNS Southern North Sea.

SU Subaerial Unconformity.

SW Southwest.

SWS Sidewall Sample.

T Transgression.

TST Transgressive System Tract.

TVDSS True Vertical Depth Subsea.

TWT Two Way Travel Time.

W West.

Special Terms

Butterworth filter A Butterworth wavelet, originating from the electrical world, is the best approximation to most seismic wavelets and can be specified by a high and a low frequency and the filter slopes on high and low sides.

diamicton poorly sorted and poorly stratified sediments including deposits of varying genesis such as till, mudflow and other mass movement sediments. Till is a genetic term for sediment deposited directly by glacier ice without significant resorting.

dinoflagellate Unicellular aquatic organisms.

Granitic intrusive bodies An igneous intrusion (also called a laccolith or a plutonic formation) is a formation in which magma (molten rock) is trapped beneath the surface of the Earth and pushes the rock located above it into a dome shape. It has a flat base and a convex upper surface. The magma cools and solidifies, and eventually, it is exposed.

halokinesis The movement of salt and salt bodies. The study of halokinesis includes subsurface flow of salt as well as the emplacement, structure, and tectonic influence of salt bodies.

intracratonic sag basin basins that form within continental masses, possibly as the result of asthenospheric downwelling or isostatic equilibrium following termination of rifting. They are rarely fault-bounded with major fault zones but may contain internal strike-slip faulting. Sag basins are commonly circular to oval in shape and may have multiple histories of basin subsidence. They may be large and thick or small and thin. They may form over older basins and inherit only some of the previously existing structural grain.

shield a large, low-relief, exposed mass of Precambrian rock, commonly having a gently convex surface and surrounded by belts of younger rock. Shields contain rock that is more than 2,500 million years old, now changed metamorphism (see metamorphic) but originally composed of basaltic lava. Shields form the nucleus of continents; for example, the Canadian Shield, located between Hudson Bay and the Great Lakes, occupies two-thirds of Canada.

slump deposits Are mainly found in sandy shales and mudstones, but may also be in limestones, sandstones, and evaporites. They are a result of the displacement and movement of unconsolidated sediments, and are found in areas with steep slopes and fast sedimentation rates. These structures often are faulted.

1

Introduction

1.1 The Eridanos Deltaic System

Eridanos delta comprised a Late Cenozoic fluvio-deltaic environment, draining the Fennoscandia and Baltic shield. The Neogene uplift of Fennoscandia in combination with the rapid subsidence of North Sea Basin resulted in the creation of Eridanos Delta. During Mid to Late Miocene the system was evolving in the onshore part of North-Western Europe and the German North Sea Basin. Progradation was progressing from north and east with the delta reaching the Dutch North Sea Basin during Pliocene times. Therefore Plio-Pleistocene era comprised a period of extensive deposition resulting in an enormous amount of sediments in the Central Graben. These sediments are considered to be mainly climatic driven and their deposition was affected by the onset of Northern Hemisphere Glaciation. In detail they comprise alternations of silty-clay lithologies that correspond to an open to shallow marine setting. The importance of the system lies on the fact that the coarser sediments have shown high probability as reservoir rocks, hosting shallow gas. Figure 1.1 depicts a representation of the deltaic system based on Overeem et al., (2001).
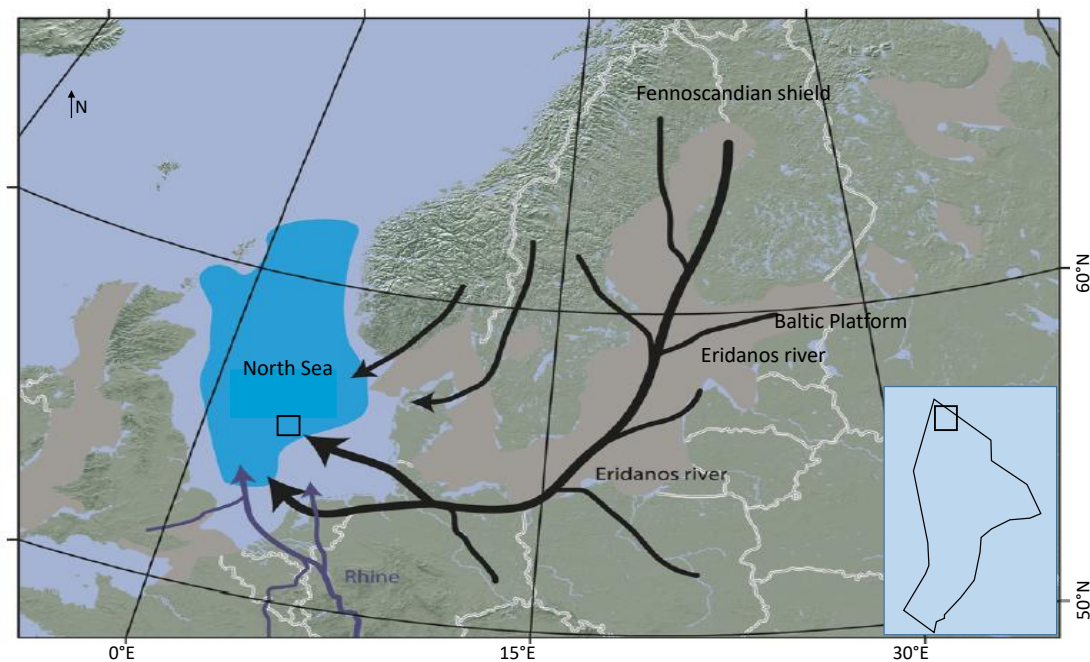
Figure 1.1: Drainage basin and delta of the Eridanos river system (black arrows). The brown background shows terrestrial environment in Middle-Pleistocene-glacial excavated areas that are nowadays seas (Overeem et al., 2001 and Cohen et al., 2014)

1.2   Literature Review & Problem Statement

Eridanos depositional environment has been a subject of investigation during the last decades with studies analyzing and interpreting the shallow Dutch subsurface. The triggering event comprised the discovery of the shallow gas accumulations, but the main reason that drew the attention is the complexity of the system owing to the climatic deterioration during the onset of Northern Hemisphere Glaciation. The body of the scientific literature has been analyzed in order to understand the fluvio-deltaic setting as well as the contribution of this research within the present studies. The following section presents the existing knowledge regarding the Eridanos delta.

Eridanos fluvio-deltaic system started developing around Oligocene-Miocene times due to extensive uplift of the Fennoscandian shield which supplied constantly the system with weathered and eroded material. The system reached the Southern North Sea basin around Pliocene, when increased subsidence dominated the basin. Deposition of open marine sediments took place this period, covering the widespread transgressive event of Middle Miocene. This event comprised an extensive hiatus with non-deposition due to dramatic sea level rise. Continuous uplift of the south Swedish Dome and southern Norway led to a westward direction of flow, with the delta reaching the Dutch offshore sector around Late Pliocene - Early Pleistocene. During this period the basin has been characterized as intracratonic, meaning that the enhanced tectonic subsidence of Pliocene had ceased or decreased significantly. Figure 1.2 presents a seismic image of the Late Cenozoic Dutch subsurface, showing the distinct Mid-Miocene unconformity and the overlying open and shallow marine sediments.

Five palaeo-environments were identified by Kuhlmann et al., (2008) who reconstructed a record of the sea-surface temperature, derived from dinoflagellate cyst (SSTDino) and the grain size distribution. The deposits above the Mid-Miocene unconformity correspond to open marine, warm conditions (blue interval), while the overlying package of sediments to a transition from open to shallow marine with alternations of warmer and colder conditions (yellow interval). The rest of the sediments represent the deltaic environment which ranges from restricted marine of enhanced cooling to shallow marine of arctic conditions (light green to dark green interval). The last package corresponds to a paralic-fluvial environment indicating the entire fill of the basin (orange interval). Evidence showing deterioration of the climate due to the onset of Northern Hemisphere Glaciation were also found at around 660ms TWT (figure 1.2), where unoriented lineaments of iceberg plough marks were observed on a seismic time slice (Kuhlmann et al., 2008).

The Middle Pleistocene increased severity of climate, owing to glaciation, affected the deltaic architecture and shaped the landscape. These conditions have been identified in 2D and 3D seismic data where analysis of the seismic facies showed an internal chaotic configuration of the reflectors, interpreted as slump deposits due to extensive sea level fall (Overeem et al., 2001). Late Cenozoic submarine slope failures known as massive transport deposits have also been identified at the center and east of the sector and their nature has been possibly attributed to the climatic-driven environmental changes (Benvenuti et al., 2012 and Thole et al., 2016). Apart from this type of sediments, westward dipping clinoforms of oblique shape, indicate progradation of sediments under conditions of high sediment supply and low rate of accommodation space. The delta was characterized by a high rate of progradation with large wedges (Overeem et al., 2001, Kuhlmann et al., 2008 , Huuse et al., 2012). Reconstruction of the sediment rates also showed significant increase in sediment supply over time as a result of the waxing and waning of the glaciers during the glacial and interglacial periods. However this rate showed a downward trend after the Mid Pleistocene as the glaciers became more stationary due to enhanced cooling (Kuhlmann et al., 2008). This is also reflected in the deltaic architecture since clinoforms of sigmoidal shape were identified, showing positive accommodation and therefore base-level rise (Overeem et al., 2001).

Furthermore, three absolute ages are known for the basinal sediments based on the integration of a palaeomagnetic and biostratigraphic study. A well to seismic tie allowed the correspondence of the three absolute ages (well A15-03) to seismic units proposed by Kuhlmann (2006, 2008). The ages are 3.6Ma for the Pliocene interval of the open marine sediments, 2.6Ma for the transitional sediments between open and shallow marine and 1.9Ma for the deltaic sediments of arctic conditions (figure 1.2).
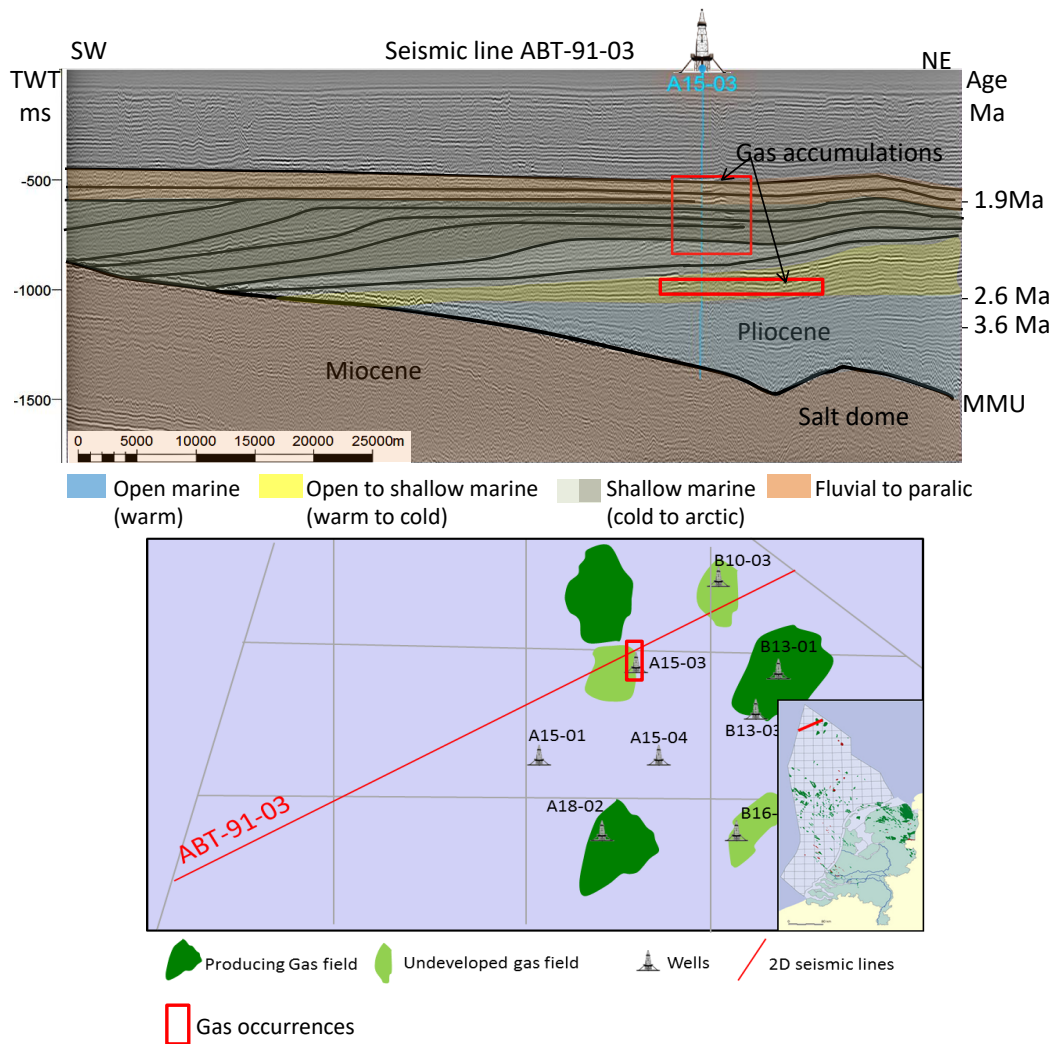
Figure 1.2: Seismic cross section presenting the existing knowledge on Eridanos deltaic sediments.The map below shows the location of the seismic line. nlog.nl

Lastly, some Eridanos deposits have been characterized as reservoirs since they host shallow gas accumulations. These gas occurrences are related to gas escapement due to uplift of a salt dome which created normal faults at the sides of the intrusion. The gas subsequently got accumulated in stratigraphic traps in the unconsolidated sediments. Two different levels of gas accumulations have been identified; one at the deeper, open marine sediments (warm conditions) and another one at the deltaic sediments were the iceberg scours were observed.

Having described what is already known regarding Eridanos deltaic sediments, it is important to mention that there is no systematic investigation in terms of sequence stratigraphy as well as the ratio of sediment supply and accommodation space under which the shallow gas-bearing sediments were deposited. Consequently, this study aims to provide a better understanding regarding the conditions under which the shallow gas-bearing Eridanos sediments were deposited.

1.3 Study Objectives & Research Question

The objective of this study is to establish the sequence stratigraphic framework of the Late Cenozoic Eridanos delta in Southern North Sea by employing sequence stratigraphy as a method to analyze the sediments and their conditions of deposition. Seismic and wireline log analysis will provide the appropriate information in order for the deposits to be classified into system tracts. Reconstruction of the relative seal level fluctuations and sedimentation rates, in combination with the determination of depositional environments comprise the main targets of this project which in turn aims to place the shallow gas reservoirs into the obtained sequence stratigraphic framework. Therefore the study objectives can be categorized as follow:

- Understand the geological setting of Eridanos delta

- Establish a sequence stratigraphic framework

- Reconstruct the rate of relative sea level changes and sedimentation

- Link the reservoir intervals with the genetically related packages of system tracts.

1.4 Area of Interest

The area of investigation is located in blocks A and B of the northern Dutch offshore sector in the North Sea and extends from the NE to the SW. It covers an area of $1338 km^2$ and it is situated adjacent to the German offshore sector at the east and to the UK at the west. The region is known for the Cenozoic shallow gas accumulations and the two successfully producing fields in Blocks A12 and B13.
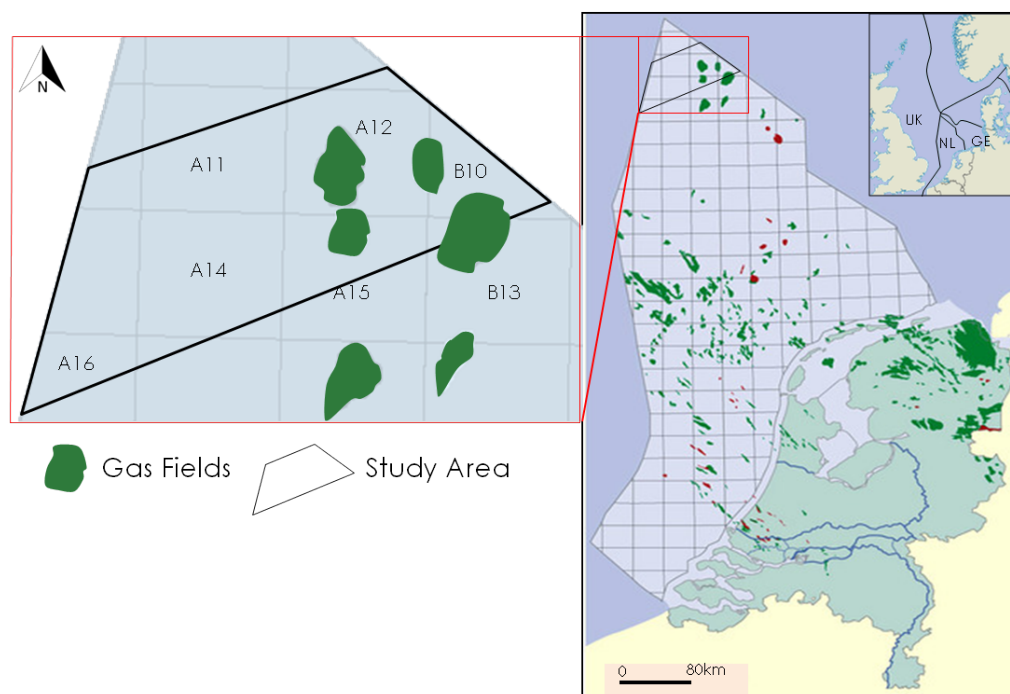
Figure 1.3: Area of interest in the Dutch offshore sector from nlog.nl Producing and undeveloped gas fields are indicated with green while the producing oil fields with red.

1.5   Study Approach & Structure

Sequence stratigraphy constitutes an important tool which organizes the sediments into genetically related packages, bounded by time-significant surfaces. These packages are the system tracts and their distribution throughout the basin can be predictable, providing critical information for the hydrocarbon exploration (Vail, 1987). The methodology selected to analyze sequence stratigraphy is the one proposed by Catuneanu (2009) which lies on observation and interpretation. The observation process uses petrophysical and seismic data in order to form a more objective picture of the subsurface. Afterwards the integration of observations starts to be interpreted, creating a seismic sequence framework. Subsequently the two types of data (2D seismic and wireline data) is tied together so as to provide a meaningful outcome in terms of geology (e.g distribution of lithofacies).

The structure of this thesis project is briefly described in the following section. The general geological setting, followed by the geological evolution of the Eridanos deltaic system is firstly described in Chapter 2. Then the adopted methodology and workflow are explained in Chapter 3. Chapter 4 contains the description and analysis of the used data, while Chapter 5 presents the seismic stratigraphic interpretation using the analysis of data from chapter 4. Chapter 6 includes the results of this study in terms of geological interpretation and Chapter 7 discusses and compares some findings with the existing literature. Finally the conclusions and future recommendations are provided in Chapter 8.

<div align="right">

2

</div>

Geological Setting

The geologic history of North Sea is characterized predominantly by two main processes, extensional tectonic movements and failed riftings. North Sea is comprised of the Northern and Southern Basin (Appendix A.1), which both were covered by two deltaic systems. The latter was affected by the Eridanos Delta which was active during the Late Cenozoic. The following section presents the tectonic evolution of the basin as well as of the Eridanos fluvio-deltaic system. Understanding of the regional geology is of great significance since it is related to hydrocarbon accumulations (Brooks & Glennie, 1987),(Pegrum & Spencer, 1990).

2.1 Geology of Southern North Sea Basin

The structural history of the Southern North Sea Basin is highly complex with the basinal subsidence being the main mechanism. Several tectonic events of uplift and erosion during Late Carboniferous, Late Jurassic and Late Cretaceous as well as mid-Cenozoic, have shaped the morphology of the region. During Palaeozoic Era SNS basin underwent two major tectonic episodes, the Caledonian and Variscan Orogeny. The former event triggered uplift of the basin resulting in high erosional rates during Devonian period (410-360Ma). Granitic intrusive bodies* deformed the thick sediment accumulations which lay several kilometers beneath SNS. In early Carboniferous times crustal extension was initiated followed by deep marine or deltaic sedimentation within the formed grabens. The rifting process stopped around 325Ma ago while a phase of thermal subsidence had started. Regarding the latter event, which initiated around 360Ma ago, caused crustal movements that intensified at about 300-290Ma during the main Variscan Orogeny. Folds and faults deformed the Carboniferous rocks and a regional uplift resulted into an erosion of sediments around 1500m thick.In the meanwhile the Mid North Sea High was formed by regional inversion. In the Permian times the SNS basin subsidence commenced and the deposition of around 2700m Permo-Triassic sediments took place.

During Mesozoic Era, extensive subsidence of the Sole Pit Basin caused the reactivation of Variscian basement faults which, in turn, triggered the earliest mid-Triassic halokinesis* of the Upper Permian salts. The end of Triassic was characterized by the prevailing of marine conditions in the SNS. The Early-Mid Jurassic amplification of the Sole Pit Basin subsidence, due to the development of growth faults, led to increased thickness and facies variability between the aforementioned basin and the East Midlands Shelf. During Mid Jurassic pervasive domal uplift took place in the Central North Sea causing the formation of erosional unconformities in the area. Around 1000m of Jurassic-Triassic sediments were eroded from the Cleaver Bank High. The phenomenon of diapirism was prevalent during Late Jurassic. Lower Cretaceous sediments are typically less than 200 m thick, but reach up to 1000 m in local zones of growth faulting, associated with sinistral fault movement (Kirby & Swallow, 1987). During the Late Cretaceous, the Cleaver Bank High became established as the main depocentre and accumulated more than 1000m of Upper Cretaceous chalk.

Cenozoic Era was a period characterized by a major phase of basin inversion that affected several basins in the NW Europe such as the Sole Pit and Cleveland Basins. Reactivation of strike slip structures

in combination with basement faults constituted the main reason of inversion. From Oligocene to Miocene the majority of the SNS basement faults were reactivated due to dextral strike slip which, in turn, triggered extensive salt movements. It is believed that most of the inversions is attributed to the Alpine Orogeny.
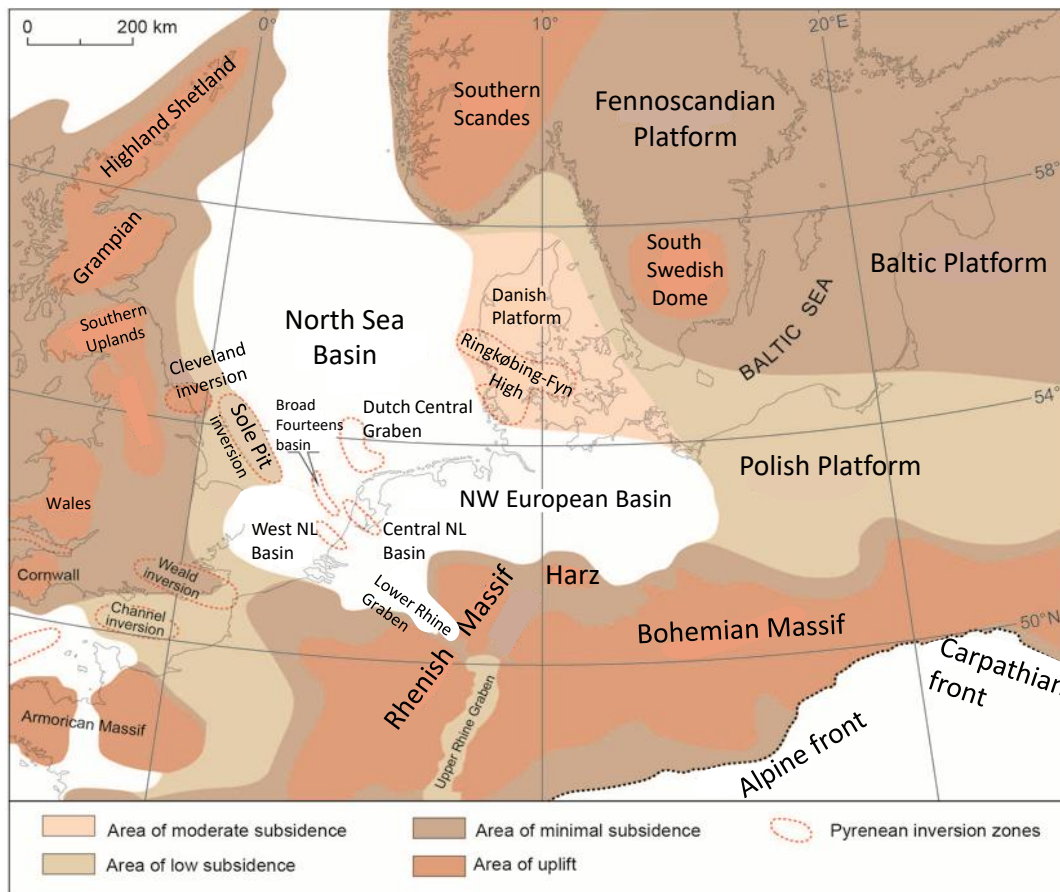
Figure 2.1: Cenozoic structural elements of North Sea.
(Knox et al., 2010b).

2.1.1 Salt Tectonics of Southern North Sea

The phenomenon of halokinesis in the southern North Sea is limited to the center of the Southern Permian Basin and it shows characteristic patterns with respect to location, orientation and maturity of the salt structures. The salt flow separates the southern North Sea into different salt domains which exhibit a specific orientation and maturity. Three of the domains consists of elongated structures each of different orientation. In the first which extends from the Central North Sea Graben to northern Germany the salt structures are oriented north to north-east and form diapiric walls. In the second from offshore England to onshore Netherlands, the salt structures trend to northwest and consist of pillows and walls. The third, in onshore Germany, shows an eastward orientation with salt walls and pillows. Salt structures of smaller scale are also present between the three major domains but with no specific orientation (Remmelts, 1995).

2.1.2 Shallow gas Accumulations

Shallow gas can be defined as gas in unconsolidated, low pressure Tertiary sandstone formations buried in depths that range from 400 to 1000m. The origin of the gas can be thermogenic, biogenic or a combination of the two. The presence of shallow gas in the Dutch offshore sector has been discovered since many years but only the last decades production from this type of hydrocarbon has taken place. Particularly three

shallow gas fields are currently producing, A12-FA (since 2007), F02a-B-Pliocene (since 2009), and B13-FA (since 2011) and development of five more fields is under consideration. In the producing gas fields no water has been encountered while gas saturation and recovery factor are typically some 50-60% and 60-75% respectively.

The origin of these gases is attributed to either biogenic or thermogenic processes. In both cases the gas is derived from organic material, with the biogenic process relying on bacterial activity (Davis, 1992). Thermogenic methane is produced from organic precursors at high temperatures and high pressures, and consequently is generated at depths greater than 1000 m. Geochemical and stable isotope analysis in combination with ultraviolet fluorescence and microbacterial investigation of core samples that were obtained from the blocks K18/L16 of the Dutch offshore sector, resulted in two different origins of thermogenic gas. The first is the methane-poor gases from a Mesozoic oil-source rock and the second the methane-rich gases from gas-producing Carboniferous source rocks (Schroot & Schüttenhelm, 2003) .

Despite the biogenic nature of the gas most of the features that are observed in the dutch offshore sector are mostly related to thermogenic gas migration from deeper sources to shallow horizons. The most important mechanism that leads to gas migration is the salt structures that are spread throughout the whole Southern North Sea. The combination of the salt domes with normal faults creates the pathways to the near surface, where fine grained claystones form a perfect seal. The reservoir consists of silty sands and is located at a depth around 300-800m, below a water depth of 30-50m. Porosity ranges from 20-35% and permeability and be characterized as good. Pockmarks, very high frequency (VHF) acoustic measurements, acoustic blanking and acoustic turbidity enhanced reflections, buried gas-filled ice-scours and bright spots which constitute some of the most well-known direct hydrocarbon indicators, are phenomena that are probably caused by glaciations, low stand channels, glacial valleys and gas charged ice scours (Schroot & Schüttenhelm, 2003).
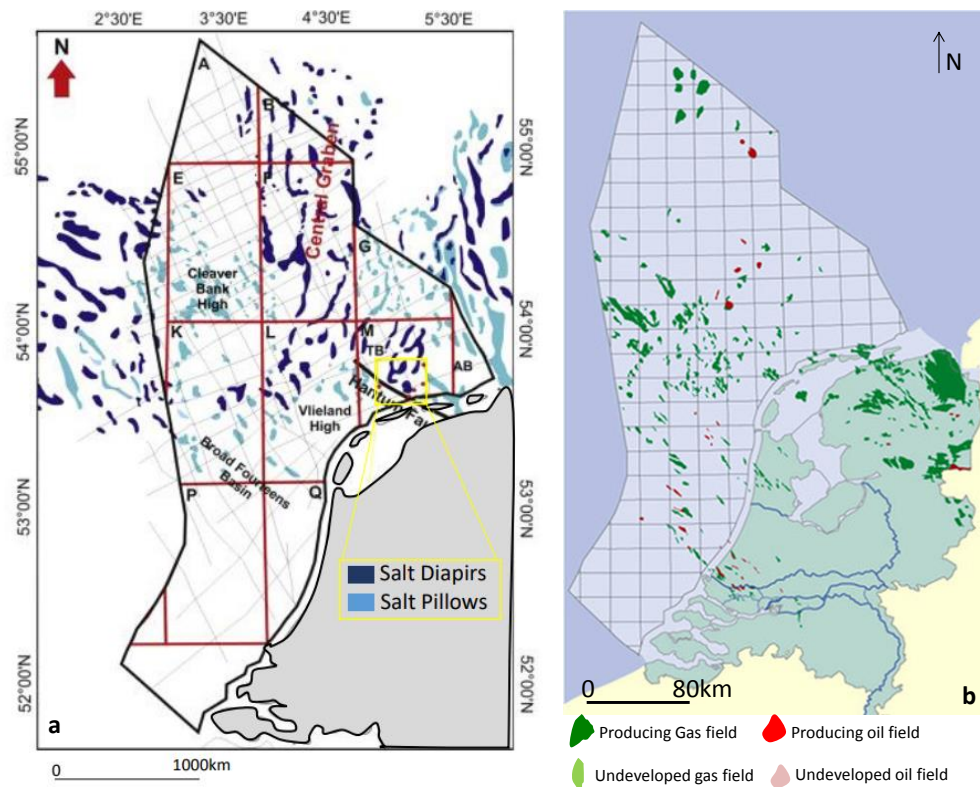
Figure 2.2: Salt diapirs and pillows distribution within the Southern North Sea area (a) (Harding & Huuse, 2015). Gas and oil fields in the Southern North Sea basin (b) (nlog.nl).

2.2   Eridanos Delta

North Sea Basin (NSB) during the Cenozoic period comprised an intracratonic sag basin*, overlying the failed Mesozoic North Sea rift system (Ziegler, 1990). The separation of Eurasian-North America plate and the Alpine Orogeny led to a tectonic regime responsible for the palaeogeographic evolution of NSB (Knox et al., 2010; Cloetingh et al., 2005). The fragmentation of the northern hemisphere plate, taking place along the North Atlantic mid-ocean ridge, resulted in an extensional regime while the continental collision during Alpine orogenesis between Eurasian and African plates generated a compressional regime. Not only were the North Atlantic margins not entirely passive but they also exhibited tectonic activity that gave rise to extensive reactivations of older features. Variscan structures of the Norwegian Atlantic coastal region showed significant vertical movements (Cloetingh et al., 1990). During Paleocene regional uplift took place in several stages, with Scandinavia having a significant but periodical uplift pattern which gave rise to a south-southwest drainage system (O. R. Clausen, Nielsen, Huuse, & Michelsen, 2000). The platform areas of North Sea Basin around Mid to late Paleocene probably comprised low-lying lands based on regional reconstructions (Vinken, 1988), (Ziegler, 1990), (Ziegler and Horvath, 1996).
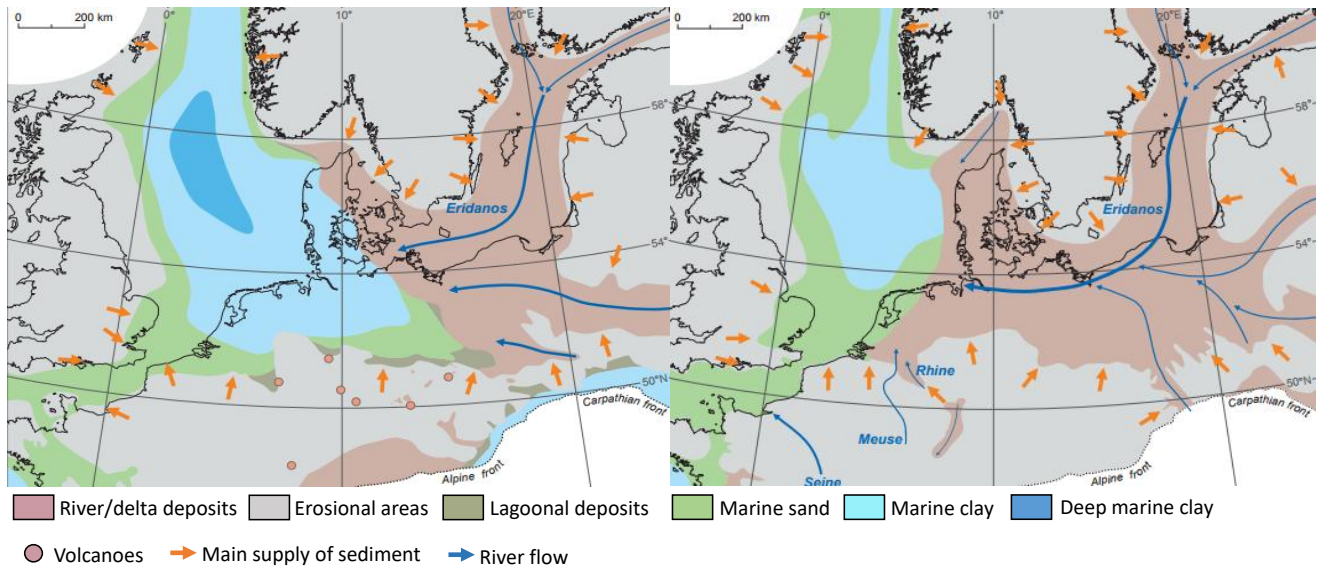
Figure 2.3: Reconstruction of the Eridanos river evolution from Mid Miocene to Early Pliocene
(P. L. Gibbard & Lewin, 2016)

Neogene times were characterized by extensive uplift and enhanced subsidence and sedimentation in the regional basins (Cloetingh et al., 2005). During this period a significant event took place around Mid-Miocene resulting into a highly marked hiatus in the base of the southern North Sea basin margin. This distinctive sedimentological gap was caused by the tectonically active Alpine Orogeny in combination with sea level fall due to accumulation of polar ice caps in the continent of Antarctica. This Alpine tectonic phase called Savian, triggered multiple episodes of basin inversion (Sole Pit Basin). The Oligocene-Miocene unconformity is more subtle in the east than in the western North European Basin since increased subsidence followed after the Savian phase. Enhanced sediment supply in the eastern part of the basin is attributed to the development of the Eridanos river. The catchment area of this river extended in the Fennoscandia, the Baltic States and western Russia.

During the Miocene Eridanos river was flowing westwards along the trend of the present-day southern Baltic sea basin based on more west-located findings of amphibole and epidote rich sands which before were deposited in the north-western Polish area. Distinct progradation was identified in the Danish Shelf during Early Miocene due to uplift and inversion simultaneously with deposition of deltaic sediments (Rasmussen, 2004). The present day equivalent areas that were feeding this system were predominantly southern Norway, Sweden and Finland. The fluvial sands and gravels in combination with the organic-rich clay beds are indicative of a meandering river associated with widespread peat accumulations. The Mid-Miocene was characterized by a significant transgressive episode with marine facies covering the Danish Shelf and the south-west Poland. This event resulted from an eustatic sea level rise due to climate amelioration (Zachos, Pagani, Sloan, Thomas, & Billups, 2001) and increased subsidence in the south-eastern embayment of the North Sea.

A significant increase in fluvial sediments took place in the northern and eastern Polish areas with the main origin of supply coming from east and north-east (Knox et al., 2010a). At the end of Mid-Miocene a shift in the tectonic regime in combination with climate deterioration resulted into a rise in sediment supply to the south-eastern embayment of North Sea through the Eridanos river (Overeem, Weltje, Bishop-Kay, & Kroonenberg, 2001). Accelerated uplift of Britain and Fennoscandia (Knox et al., 2010), possibly due to mantle processes, provided constantly weathered and eroded material (Cloetingh et al., 2005). Nevertheless sedimentation did not take place in the southern North Sea until Late Miocene (Knox et al., 2010), (Rasmussen & Dybkjær, 2014), (Thöle et al., 2014). It is worth to be mentioned that the uplift of southwestern Norway coupled with climate alternations led to extensive fluvial incision and the formation of incised valleys as much as 300m deep (Medvedev & Hartz, 2015). Enhanced incision episodes took place in the Quaternary due to further climatic deterioration. During the same period North Sea stopped to be connected with the eastern Atlantic Ocean based on the uplift along the Weald-Artois axis. The Eridanos river was flowing farther to the west (Bijlsma, 1981) passing through north Germany, depositing a characteristic group of sediments called Baltic Gravel Assemblage under conditions of relative sea level rise (Thöle, Gaedicke, Kuhlmann, & Reinhardt, 2014).
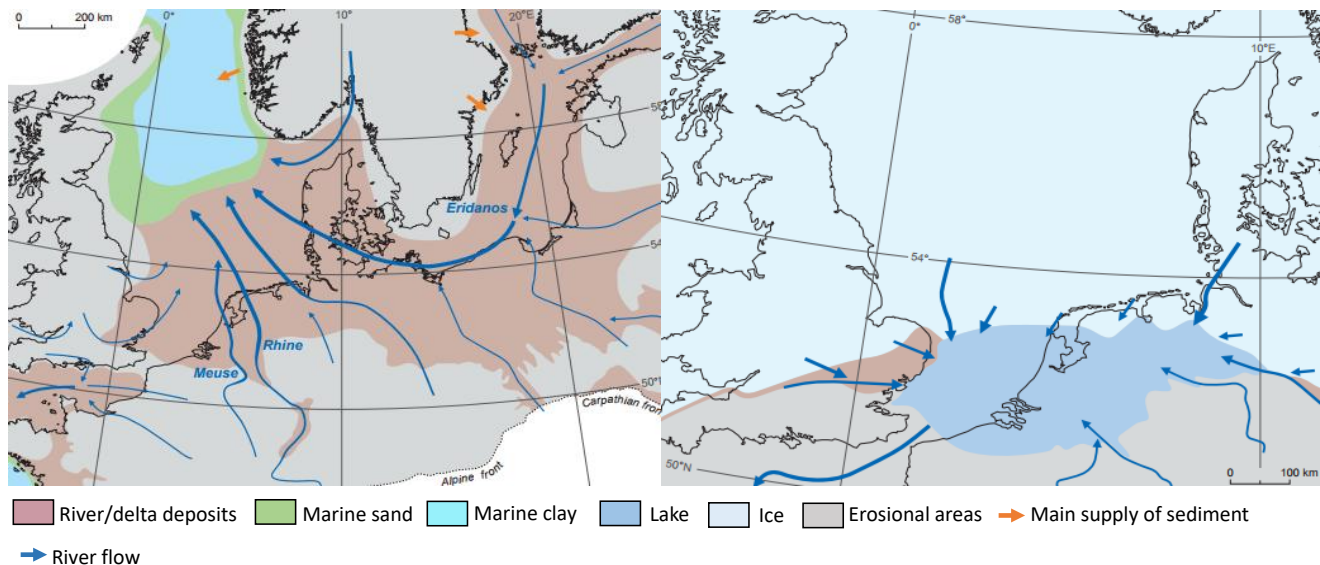
Figure 2.4: Reconstruction of the Eridanos river evolution from Early Pleistocene to Mid Pleistocene.
(P. L. Gibbard & Lewin, 2016)

During Early Pliocene sea level continued to rise and the NSB was undergoing increased subsidence while sedimentation was taking place by the Eridanos river which was carrying vast amounts of sediments to the south-eastern embayment resulting into a continuous progradational pattern (Overeem et al., 2001; Kuhlmann & Wong, 2008; Thöle et al., 2014). Subsequent exhumation of the Fennoscandia including the continuous rise of the South Swedish Dome and southern Norway led to shelf uplift and erosion. The drainage system during Pliocene can be classified as braided while the predominant material coming from the north-west was quartz-rich sands and gravels (Kesel & Gemmell, 1981); (Hall, Gilg, Fallick, & Merritt, 2015).

During Early Pleistocene period, Eridanos delta continued even more its expansion towards the west and subsequent to the north-west reaching the offshore sector of the Netherlands. The deltaic architecture and landscape was mainly shaped by the climatic variations which around Plio-Pleistocene times showed a tendency for colder conditions resulting in glaciation. The increasing severity jointly with longer duration of cold climatic conditions resulted to enhanced river incision during Mid to Late Pleistocene (P. Gibbard & Lewin, 2009). The early Middle Pleistocene period was characterized by the glacial-interglacial cycle which formed a significant amount of ice sheets in the Alps, Scandinavia, Wales and Scotland (Head & Gibbard, 2015). Even though glaciation had reached the lowland Baltic regions, it was only until the Elsterian stage that ice sheets covered the North Sea basin, southern Britain and northern Germany (Ehlers, Grube, Stephan, & Wansa, 2011). Mid-Pleistocene constituted also a period when another river become highly important in the southern North Sea region, the Rhine. The catchment area of Rhine gradually increased and its deltaic complex had already advanced to the central and southern North Sea, which was transforming into land. In this time North Sea was separated from the Channel via a substantial barrier formed by the Weald-Artois anticline to the south. On the eastern side the Eridanos river was disconnected from the Fennoscandia and Baltic regions implying that the Baltic basin had been formed probably by enhanced ice-sheet erosion. (For the evolution of the glaciation in the area see Appendix A.2)

3

Research Methodology

Eridanos deltaic deposits occupy the shallow subsurface of the northern Dutch offshore sector, which constitutes an exploration target for gas the last decades. For many years the main focus of the O & G industry comprised the deeper hydrocarbon accumulations, paying less attention to the shallow sediments. Therefore this study aims to provide an insight into the Eridanos depositional conditions by employing sequence stratigraphy as a method to built the sequence stratigraphic framework of the northern SNS basin. This method categorizes the basin sediments into genetic packages based on important stratigraphic surfaces. These genetic depositional intervals, called depositional sequences and system tracts, have a predictable stratal pattern throughout the basin (Vail, 1987).

3.1 Adopted Methodology

The methodology that was adopted in order to analyze the sequence stratigraphy of Eridanos was the one proposed by Catuneanu et al (2009) and it consists of two different aspects:

- Model-independent methodology
- Model-dependent choices.
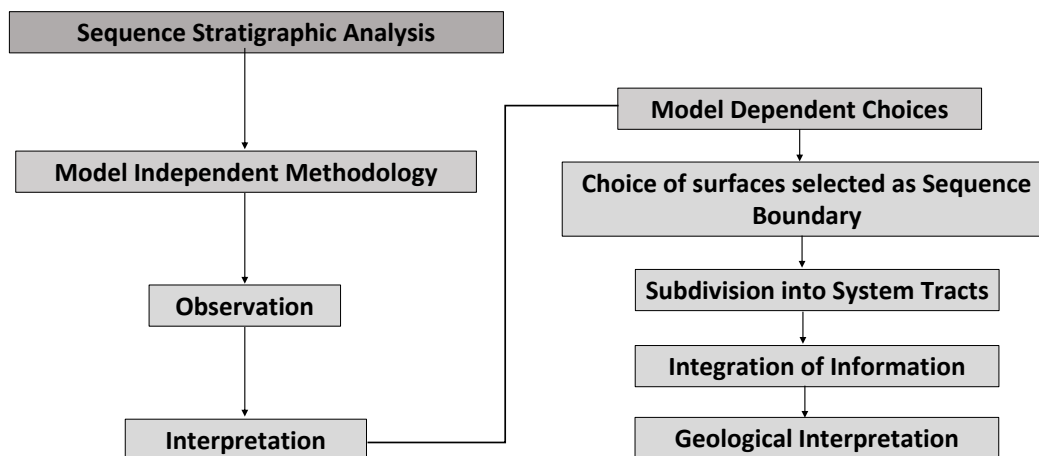
Figure 3.1: Sequence stratigraphic methodology based on (Catuneanu et al., 2009).

The Model-independent methodology gives emphasis on the basic observations of the stratal characteristics which are stratal terminations, stratal stacking patterns and stratal geometries. These main observations are fundamental for the determination of the stratigraphic surfaces and hence of the system tracts. The study adopted the aforementioned methodology because it honors all existing models and it is exclusively dependent on the data analysis by observation of the interpreter (Catuneanu et al., 2009,

2010). The Model-dependent choices define the criteria by which the stratigraphic surfaces were determined and why are characterized as sequence boundaries. This model relies highly on the quality of the available data and how well-expressed these surfaces are. The interpretation of a surface as a sequence boundary differs from one sequence stratigraphic approach to another and therefore the flexibility of the methodology lies on the quality of the surface expression which in turn depends on the depositional system, the type of available data and the scale of observation (Catuneanu et al., 2009, 2010). Although the model provides separation of the actual data (termination of reflectors) and the preferences of the interpreter (eg.nature of the sequence boundary), it is worth to be mentioned that the observations are directly related to interpretation and there is no "pure"observation in geology (Rudwick, 1996), (Miall & Arush, 2001). Hence for the stratigraphic interpretation these two aspects are coupled in order to provide a meaningful outcome. The information derived from the two types of data must be integrated in order for the petrophysical interpretation to be tied to the one from seismic. By integrating the two interpretations a geological framework can be established in terms of depositional environments and the analysis of the reservoir rocks can take place.

3.2   Workflow

For establishing a sequence stratigraphic framework, seismic and well sequence analysis was executed in three 2D seismic lines and seven wells. Due to the extensive architecture of the delta the research was conducted on two-dimensional data which covers all the examined area. Three-dimensional seismic data was not preferable since it has a smaller coverage. The selection of that type of data lies on the fact that the sedimentary surfaces comprise contrasts in acoustic impedance which in turn cause the seismic reflectors. Subsequently, the seismic reflectors represent depositional surfaces and their termination provides the base for building a chronostratigraphic framework. Regarding the well data, gamma ray logs were chosen since their response can be interpreted in terms of depositional trends.
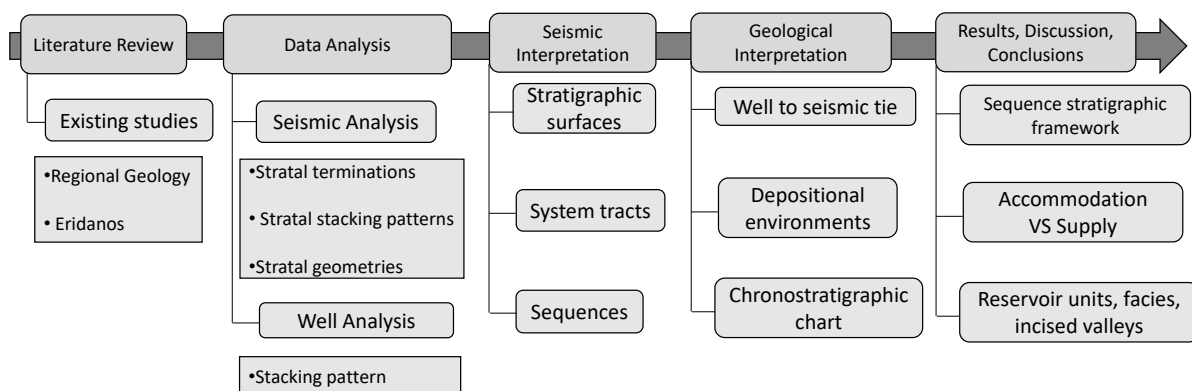
Figure 3.2: Schematic illustration of the steps for conducting the research based on the adopted methodology.

After the collection of the appropriate data, processing and analysis comprised the next steps. Processing of the data was necessary in order to enhance the nature of the seismic reflectors and therefore make the interpretation more feasible. For this stage the seismic attributes from Petrel 2014 were used based on the stratigraphic feature that was interpreted each time.

The analysis consists of the basic observations that were determined during the adaptation of the methodology. These are comprised of the stratal terminations, stratal stacking patterns, and stratal geometries. The latter includes also the seismic facies and the palaeoshelf break. The two first observations are combined to provide the stratigraphic surfaces, while the resulted surfaces and the two last observations the system tracts. Finally the combination of all the previous will provide the sequences. Additional

information will be extracted from the well logs in terms of stacking patterns in order to establish the surfaces and sequences in the gamma ray response.

The following section explains briefly the basic observations based on the use of order:

- **Termination of reflectors**: The internal geometry of the reflectors regarding their termination and relation with other reflectors. For the identification of the geometries the description from Vail and Catuneanu constitute the main guidance during the process. There are five types of termination based on the surface that the reflectors terminate: onlap, downlap, toplap, apparent toplap and truncation.
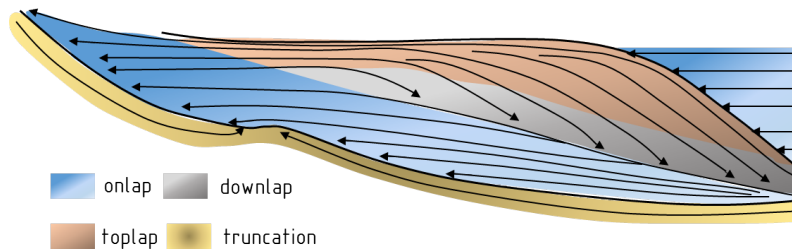
Figure 3.3: Diagram showing reflection termination patterns. Modified based on Vail, 1987.

- **Stacking Patterns**: the vertical changes in proximal versus distal trends and their classification in progradation, retrogradation, aggradation and degradation. Figure 3.4 has been modified in this study. (Zhu et al., 2012)
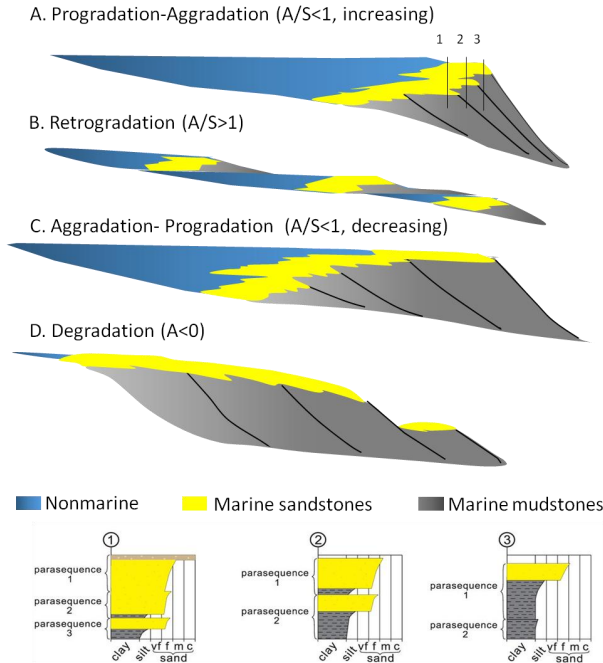
Figure 3.4: Illustration of the four stacking patterns and their relation to sediment supply and accommodation space (Zhu et al., 2012). Three wells drilled in different parts of the delta are also depicted. The first well penetrates mainly marine sandstones as it is located in the delta front. The second well contains alternations of marine mudstones and sandstones and the third well, located at the edge of the delta slope, is dominated by marine mudstones overlaid by few marine sandstones.

- **Reflection Geometry**: The nature and configuration of the reflectors in terms of continuity, amplitude and shape was determined based on the descriptions of (Badley, 1985) and (Vail, 1987). This analysis can provide important information regarding the conditions of deposition and the deltaic architecture. An example described by Catuneanu et al., (2009) mentions that a sigmoid geometry indicates positive accommodation on the shelf during progradation while an oblique geometry indicates little or no accommodation on the shelf during progradation.
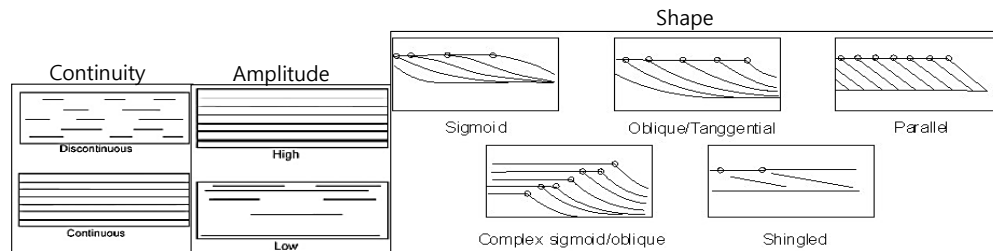
Figure 3.5: Demonstration of the three main reflectors geometries, amplitude, shape and continuity. (Badley, 1985)

- **Offlap break point**: The depositional shoreline break and its trajectory. The shoreline trajectory of the paleoshelf break is used to interpret changes in accommodation on the shelf (area located updip from the shelf break) (Johannessen & Steel, 2005); (Carvajal & Steel, 2006).
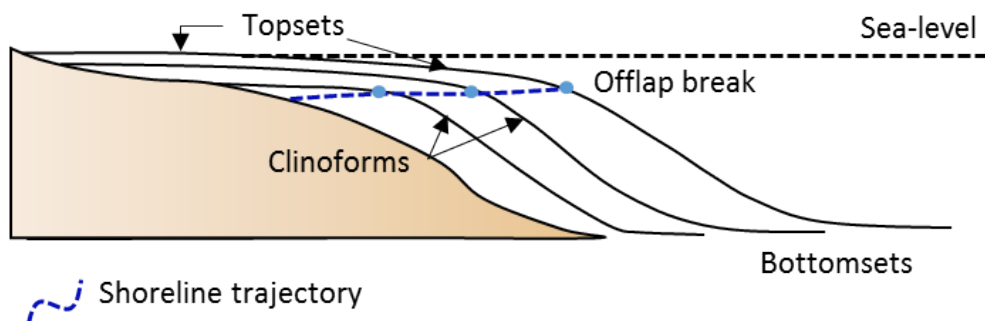
Figure 3.6: Schematic illustration of the offlap break point. Based on Emery et al., (1996)

In order to enhance the obtained information from the seismic data, well sequence analysis was also conducted so as to identify the stacking patterns and depositional trends in the Gamma Ray log. Borehole logging is another important type of data that can provide information not only of the subsurface but also in terms of sequence stratigraphy. Unlike seismic data, well data corresponds to depth and therefore the combination of the two types of data can generate a more reliable interpretation of the subsurface. For the well analysis one main observation took place based on the well log description of Catuneanu (2006) :

- Identification of Stacking Patterns

Figure 3.7 shows characteristic patterns of the gamma ray trends. Funnel shape is indicative of progradation, bell shape of retrogradation and the irregular of aggradation. The bow is a combination of the two first trends and the box car shows sharp base and top corresponding to abrupt changes.
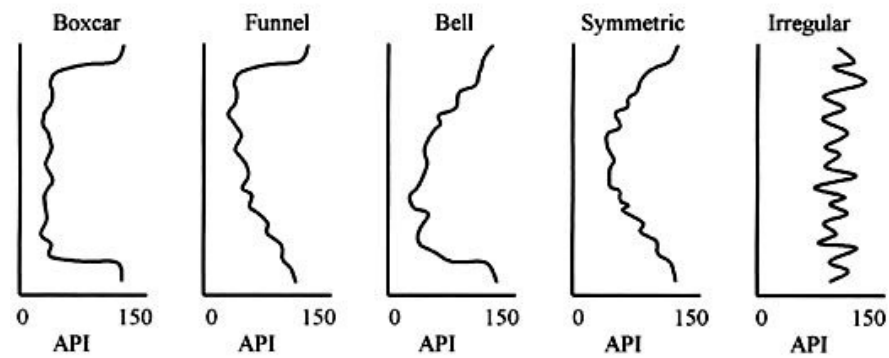
Figure 3.7: The gamma ray response based on its shape can give valuable information regarding the depositional trends and environment (Cant, 1992).

After the seismic and well log interpretation, integration of the two types of information provided the environments distribution within the delta and the link of the reservoir intervals with the regional sequence stratigraphy. The study also reconstructed: (1) chronostratigraphic chart showing the temporal distribution of the sediments and (2) the relative sea level changes based on the shoreline migration. Finally sediment volumes were estimated in order to calculate local sedimentation rates based on three absolute ages derived from literature.

4

Seismic & Well Data

For selecting the best-suited type of data on which the adopted methodology was going to be applied, the characteristics of the examined area in combination with the study objectives had to be made clear. Knowing that the scale of the delta has a length of more than 100km and a depth of 1250m, a 2D seismic data set was thought to be appropriate in order to obtain the desired lateral and vertical resolution. Apart from the seismic lines that yield a representation of the subsurface in terms of time, well log data was also being utilized in order to have tangible depth-related information.

The data was selected using the official website of the Geological Survey of the Netherlands, nlog.nl which is being managed by TNO in collaboration with the Dutch Ministry of Economic Affairs. The Data domain contains a section of models, maps and datasets that have been generated by the oil, gas and geothermal energy exploration and production surveys. The site provides interactive maps of geophysical and petrophysical data from all the surveys that have been conducted the last decades in the dutch sector. For this study a Google Earth satellite map was used depicting all the boreholes and seismic lines in the area. From the literature review was already known that the progradation of the delta had a NE-SW (some parts E-W) orientation meaning that some of the desired seismic lines needed to have same trend and some perpendicular. The borehole data had to be acquired from wells that are proximate to the lines, so as the information to be integrated in the end of the research. The lines were requested and obtained electronically via the TNO personnel, while the well log data electronically from the website without intercessor.

After the collection of the dataset, the 2D seismic lines and gamma ray logs were imported to Petrel 2014 that is provided from the Technical University of Delft in accordance with Schlumberger (Oilfield Services). For the data to be analyzed and interpreted had to be processed and undergone some modifications.

4.1 Description

4.1.1 Seismic Data

The 2D seismic dataset that was acquired for the construction of the Eridanos sequence stratigraphic framework comprised of nine 2D seismic lines (figure 4.1). The lines are part of five different surveys, conducted by three O & G companies. Table 4.1 shows the name of lines, surveys and companies and the year of data release. The seismic lines are located in the northern part of the dutch offshore sector traveling over blocks A and B. Three seismic lines were shot parallel to the prograding delta and show a NE-SW trend (SNSTI-NL-87-03, SNSTI-NL-87-02, and ABT-91-03). Lines SNSTI-NL-87-02 and ABT-91-03 crossing block A while SNSTI-NL-87-03 blocks A and B.

The aforementioned lines constituted the main data on which the adopted methodology was applied. Seismic line 51 was used for the establishment of a time-depth relation between seismic and well data, as it passes very close to the well A15-03. Finally seismic line (23) has an almost perpendicular trend to the delta progradation allowing the identification of important sedimentary features such as incised valleys. Lines 10, 15, 12 and 14 were used only for observation and not interpretation, since their orientation and

Figure 4.1: Geographic location of the nine seismic lines in the northern part of Southern North Sea.

length could not provide valuable information based on the selected methodology.

All the seismic lines are spatially referenced to the Universal Transverse Mercator (UTM) in zone 31 and have undergone migration.

Table 4.1: Detailed information of the acquired 2D seismic dataset.

2D Seismic Data			
Seismic Line	Survey	Data Owner	Data Release
ABT-91-03	Z2NOP1991A	NOPEC	01/2002
SNSTI-NL-87-02	Z2NOP1987A	NOPEC	06/1997
SNSTI-NL-87-03	Z2NOP1987A	NOPEC	06/1997
10	Z2WIN1999A	WINTERSHALL	04/2009
12	Z2WES1988B	WESTERN GEOPHYSICAL	01/1999
14	Z2WIN1999A	WINTERSHALL	04/2009
15	Z2WIN1999A	WINTERSHALL	04/2009
23	Z2WES1988B	WESTERN GEOPHYSICAL	01/1999
51	Z2WIN1999A	WINTERSHALL	04/2009

4.1.2   Well Data

Well logs and particularly gamma ray logs comprised the other type of data that was used for the deltaic sequence analysis. Namely, information from seven wells located in the northern dutch sector was downloaded from the official website of the Geological Survey of the Netherlands, nlog.nl and imported to Petrel 2014. Table 4.2 shows detailed information regarding the characteristics of the seven wells.

The wells are situated in the offshore blocks A and B and are referenced to the Universal Transverse Mercator (UTM) in zone 31 and their geodetic CRS is the European Datum 1950 (ED50). Figure 4.2 shows the location of the seven well in the northern Southern North Sea basin.

Regarding the obtained data, it consisted of three different types of files that had to be created or downloaded in order to be imported to Petrel. The well header which required the main characteristics of the well such as the well head coordinate units, well reference datum, elevation from Mean Sea Level and measured depth. The well path/deviation data and the petrophysical logs. For some wells that were used for well to seismic tie also checkshot data was imported to Petrel.

14.3km
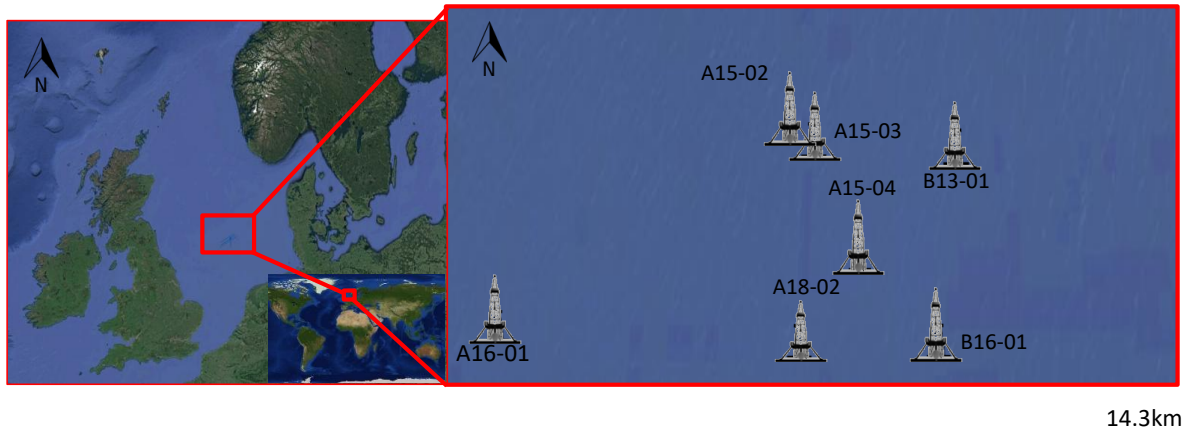
Figure 4.2: Geographic location of the seven wells in the northern part of Southern North Sea

Table 4.2: Detailed information of the acquired well dataset.

Well Log Data			
Well Name	Co-ordinates	Data Owner	Well Type
A15-02	551960, 6129283	Wintershall	Plugged and abandoned
A15-03	552567, 6128752	Wintershall	Abandoned
A18-02	551796, 6108146	NAM	Technical failure
A16-01	516154, 6108805	Total	Plugged and abandoned
B13-01	568257, 6128873	Wintershall	Plugged and abandoned
B16-01	566323, 6108475	NAM	Plugged and abandoned
A15-04	557894, 6117754	Wintershall	Abandoned

4.2   Processing

4.2.1   Seismic Attributes

For the identification of important stratigraphic features the processing of data constituted a prerequisite in order to ensure the validity and reliability of the study. Regarding the 2D seismic data, due to low quality imaging, the seismic reflectors had to be enhanced using the surface attribute features of Petrel 2014. The appropriate type of attribute was selected based on the nature of the stratigraphic features that had to be identified (discontinuities, unconformities, incised valleys). The attribute of Relative Acoustic Impedance (RAI) that corresponds to the stratigraphic methods was used for the stratal terminations and the surface determination. The First/Second Derivative, Time Gain and Trace Gradient which comprise signal processing attributes were selected for the terminations, the identification of incised valleys and the establishment of seismic units. Figures 4.3 and 4.4 show the original seismic image and the image on which the seismic attributes were applied. The attributes were used in all four main seismic lines, SNSTI-NL-87-03, SNSTI-NL-87-02, ABT-91-03 and (23). The latter also underwent removal of multiples.

Relative Acoustic Impedance (RAI) attribute is based on the physical rock property of acoustic impedance and can be computed from the integration of the real seismic trace (Pereira, 2009). Particularly it is running the sum of regular sampled amplitude values, calculated by integrating the seismic trace. The result can then pass through a high-pass Butterworth filter to reduce potentially introduced low-frequency noise. The selection of this attribute lies in the fact that it shows apparent acoustic contrasts and indicates sequence stratigraphic surfaces such as sequence boundaries, unconformity surfaces and discontinuities.

The First Derivative attribute constitutes the time rate change of the input trace and resembles a phase
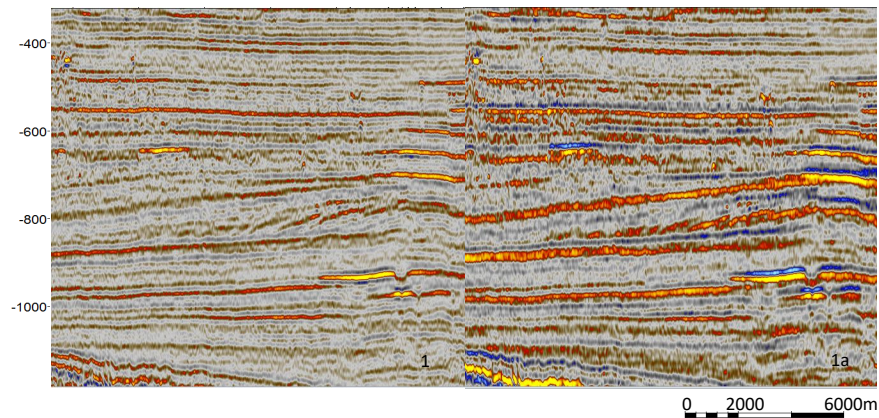
Figure 4.3: Comparison between the original seismic image (1) and the one where the Relative acoustic impedance seismic attribute has been applied (1a)

shift of 90º for the collection of traces (Pereira, 2009). Being independent of user-defined parameters, first derivative can be useful to improve reflector sharpness and correlation between seismic data and lithology-indicative well log data (Zeng & Backus, 2005). If a 90º-phase wavelet is applied to a nearly zero-phase seismic data, the vertical resolution increases with a decrease in thin-bed interference. This can have significant improvements for lithologic, stratigraphic and depositional facies interpretation. Thin layers analysis also becomes easier because reflectors have increased consistency and sharpness, leading to a better amplitude-lithology correlation (Zeng & Backus, 2005).

Trace Gradient attribute computes the gradient along a trace between consecutive samples. It gives the amplitude difference across the output time sample and has the highest value at points with the greatest rate of change. High values of trace gradient are related to consecutive points, having great changes in amplitudes. This attribute is useful to distinguish between seismic units and can be correlated to areas with abrupt changes in lithologies and related to differences in acoustic impedance (Pereira, 2009).

Attenuation of the seismic energy and errors during the seismic acquisition can be compensated with the implementation of a spherical divergence correction in the seismic processing stage. Time Gain attribute is implemented for specific time-dependent corrections, which are necessary for interpretation (Pereira, 2009).
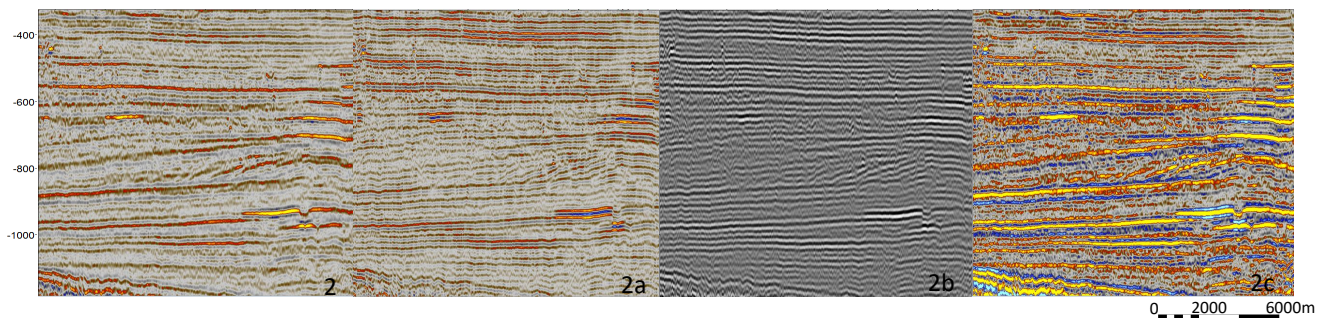
Figure 4.4: Comparison between the original seismic image (2) and the applied signal-processing seismic attributes of First/ Second derivative (2a), Trace gradient (2b) and Time gain (2c).

4.2.2 Time-Depth Relationship

One important process of the adopted methodology is the integration of the seismic interpretation with the well data. In particular this study tries to tie the major stratigraphic surfaces that were identified on seismic with the signal of the gamma ray log. Due to the fact that the former is expressed in two way travel time while the latter in depth, a relationship of the two different data set had to be established in order to become comparable. This was succeeded by converting the velocity of the strata in the well to TWT and thus the depth-time relation can be provided by an integrated sonic log, which is calibrated with wellshoot time-depth pairs. For that process, a synthetic seismogram was generated in order to establish this relation between time and depth. The well data obtained from the well A15-03, was including checkshots, sonic logs and density logs.
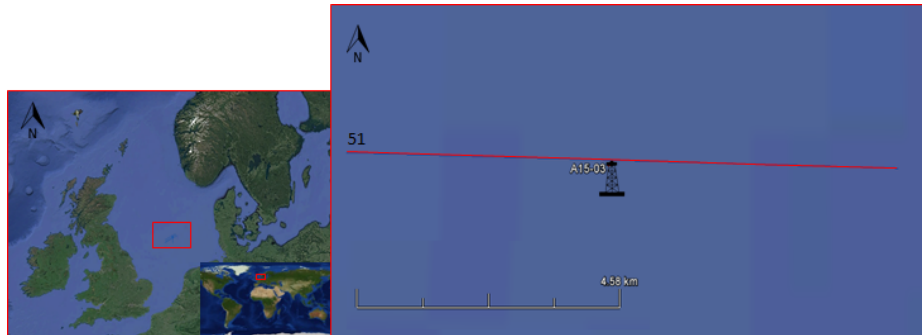
Figure 4.5: Geographic location of seismic line 51 and well A15-03.

Well Calibration & Synthetic Generation

The first step to establish a depth-time relation is to calibrate the sonic log by using checkshot data. This procedure is highly important since the readings in altered formations can generate incorrect DT values which then will produce a faulty synthetic seismic trace. After the sonic calibration the generation of a synthetic seismogram can take place utilizing the velocity data from the sonic log and the density from the density log. This trace nearly approaches the trace from the seismic line that passes close to the well from which the well data has been obtained. This study uses seismic line 51 as an input to the generation of the trace since it is located very close to the well A15-03. The steps that were execute are summarized below:

- Establish a depth-time relation by using integrated sonic, wellshoot data and a smooth drift curve

- Convert velocities and density values to TWT

- Calculate zero-incidence reflection coefficients

- Use Butterworth filter* for bandpass

Seismic Well Tie Process

After the generation of the synthetic seismogram the process of well to seismic tie took place. The match between seismic traces and synthetics was executed manually by printing on a A3 landscape paper the seismic traces of Line 51 and placing the position of the well A15-03 to the Common Depth Point (CDP). Then the synthetic seismogram was placed on top of the original seismogram. As shown in Figure 4.6 there is a minor character mismatch between the two traces. Although the very strong hard kick at around 0.5s fits rather well with the seismic trace, the synthetics have to be shifted slightly upwards in order for a match at the very prominent soft kick of 0.98s synthetic TWT to be established.

By accomplishing a well to seismic tie it is possible to correlate the two different types of data and link the seismic surfaces and units to the gamma ray trend. Figure 4.6 also illustrates the placing of the synthetic seismogram on top of the seismic image that corresponds to seismic line 51. Knowing now the relation between the two different traces it is feasible to identify the depth at which the reference seismic surface occurs in the well.
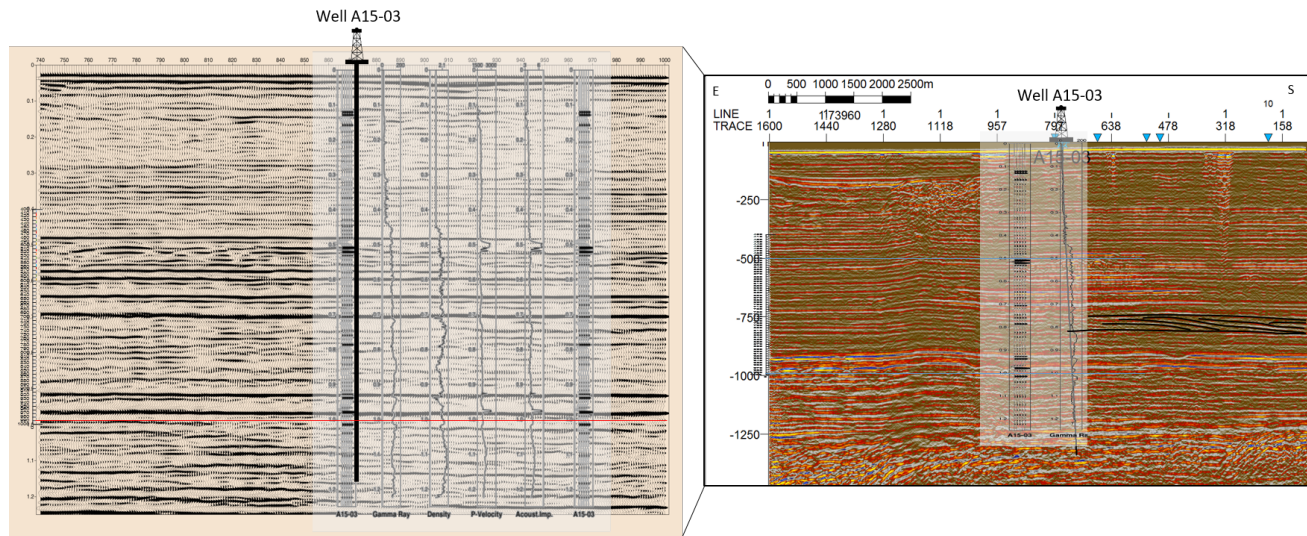
Figure 4.6: Illustration of the generated synthetic seismogram and its tie to the seismic traces of seismic line 51. The well position is between CDP 871 and 872.

4.3   Data Analysis

Prior to seismic interpretation the actual data has to be demonstrated. This is necessary in order to establish a distinct line between observation and interpretation. The plain data should be depicted in case another study is about to be conducted, using the same methodology and dataset as this study. Figure 4.7 presents seismic line ABT 91-03 in two different scales (with and without compression). The chosen depicted seismic attribute is the Second Derivative and the colors are slightly enhanced. The seismic line has undergone compression in order to be analyzed. By compressing the image, the geometry and scale of the reflectors is exaggerated, making the observation of some features easier. For instance dipping reflectors in the unstretchable image have very low dip angle while after the compression in height and width they show higher dipping angle. In that way they become more visible and it is easier to distinct them from horizontal and very low dipping reflectors. Furthermore, for the identification of the
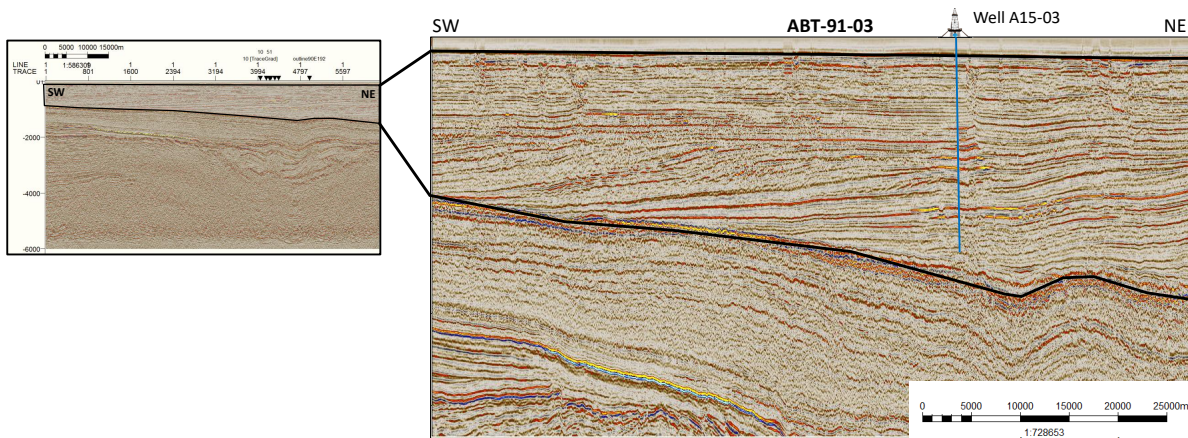
Figure 4.7: Presentation of the compressed original seismic line ABT-91-03

reflections' geometries and characteristics, it was considered useful to divide the seismic image into five sections based on the development of the delta since the line in reality is 78km long. Figure 4.8 shows the five parts that later in this section are going to be analyzed separately starting with the first sediments that correspond to the shallow marine deltaic environment.
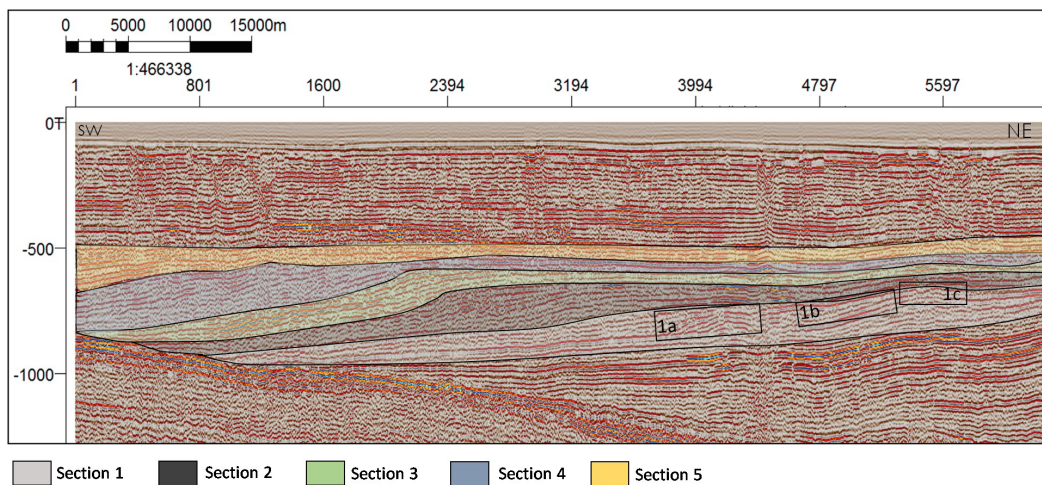
Figure 4.8: Seismic image of line ABT-91-03 has been divided into five sections in order to be handled easier. NOTE: the five sections were placed to make easier the analysis, they do not carry a scientific meaning.

4.3.1   Seismic Sequence Analysis

Seismic sequence analysis is a data analysis method which uses seismic sections in order to organize the seismic reflections into genetically-related packages that correspond to depositional sequences and system tracts. The first step of the analysis is to observe where two reflectors converge since there will be a reflection termination. Then the identification of the stacking patterns has to take place in order to understand the vertical stacking and relation of the reflectors. Subsequently, the geometrical patterns of the reflectors in terms of amplitude, continuity and shape will provide an insight into the seismic facies. The seismic facies give an indirect information regarding the deltaic architecture and their integration with well data will lead to the establishment of the depositional environments (see Chapter 6). The most important pattern that has to be observed is the offlap, created by reflectors that dip at a higher angle than those above and below. The Offlap pattern indicates the depositional shelf break, separating shallow water from deeper. Other patterns correspond to deeper water sediments (e.g. submarine onlap) and other to shallower (coastal onlap). The following section presents the basic observations of seismic line ABT-91-03 (for seismic line location see subchapter 4.1). For the other two seismic lines see Appendix B.1 and B.2.

Stratal Terminations

Stratal terminations represent geometric patterns of the seismic reflectors and can be defined based on their relationship with the stratigraphic surfaces on which they terminate. As it has already been mentioned in Chapter 3, there are five main type of terminations, onlap, downlap, toplap, offlap and truncation. The two first types of termination terminate above a seismic surface while the rest below.

   First Section: In the first section four different types of reflectors were observed and interpreted in terms of stratal terminations. Onlap, downlap, apparent toplap or offlap and truncation are the diagnostic geometries. As shown in Figure 4.9-1a, the initially horizontal strata terminating against inclined reflectors (blue arrows) corresponds to onlap. These inclined reflectors terminating downdip against a continuous, slightly inclined strata are characterized as downlap (black arrows). The apparent toplap is indicated with red arrow which shows the termination of a reflector against an overlying strata. The yellow arrows correspond probably to an offlap but due to the low quality of the data their nature cannot be clearly depicted. Figure 4.9-1b shows two onlap patterns with initially inclined strata terminating progressively updip against a surface of greater initial inclination. Features of truncation are also visible in the image 4.9-1c with two reflectors being cut off by an overlying reflector.
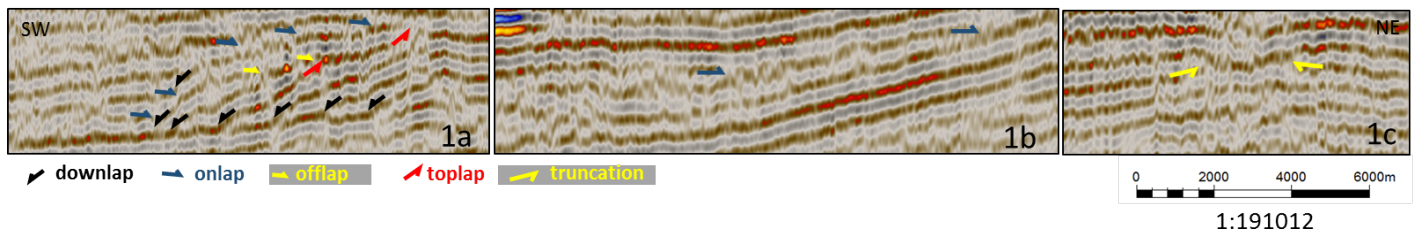

Figure 4.9: Demonstration of the reflectors terminations in the first section.

   Second Section: In the second section the identified geometries correspond to downlap, onlap erosional truncation and apparent toplap. The lower part of the section is characterized by high-angle dipping reflectors which represent downlap (black arrows). The upper part is comprised of horizontal strata terminating against a surface of high dipping angle which corresponds to an onlap (blue arrow). Some reflectors also seem to be cut off by a surface of high angle resulting into an erosional truncation termination below the surface (yellow arrow). The next part of the section is less understood but due to the presence of high angle reflectors terminating abruptly into another reflector, the geometry resembles an erosional truncation or apparent toplap below that reflector. Also the whole section shows high angle

dipping reflectors terminating downwards into a downlap. Probably two apparent toplap (red arrows) can be spot at the end of the section since there are reflectors of great angle which stop below a surface. Finally there are some onlaps terminating against the downlaps (there is a possibility of an offlap geometry in the most basinward position of the section but due to poor seismic quality it remains uncertain).
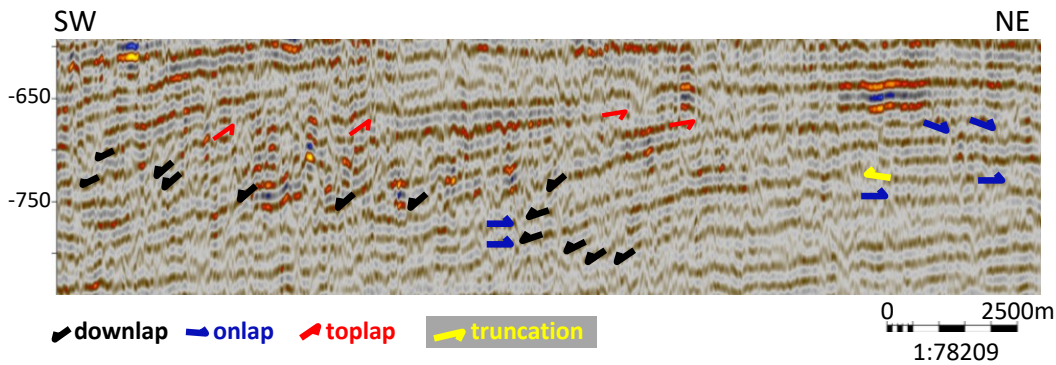
Figure 4.10: Demonstration of the reflectors terminations in the second section.

Third Section: The third section consists of three different type of reflectors, downlap, onlap and toplap. The first geometry can be spotted where high angle reflectors terminate against low angle strata. The onlap is placed in the low angle reflectors which terminate against the downlapping strata. Although the upper part of the section has lower resolution hampering the observation, some toplaps can be observed where the strata terminates against an overlying surface. It is hard to understand if there are also apparent toplap or truncation. The only certain observation is that these reflectors are situated below the surface they terminate on.
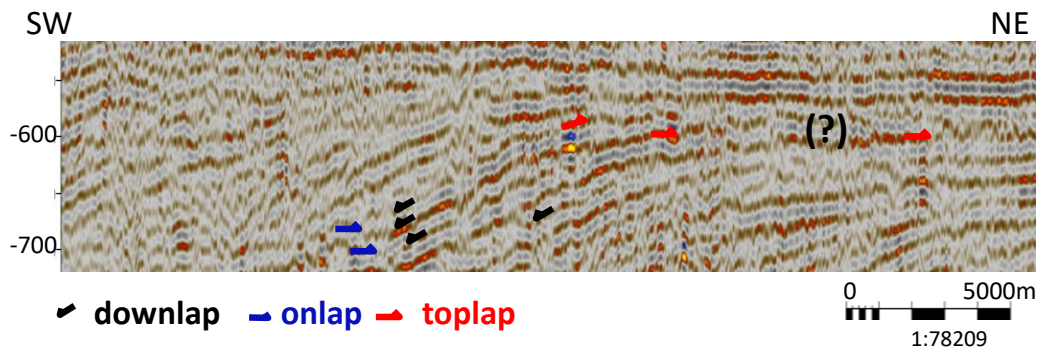
Figure 4.11: Demonstration of the reflectors terminations in the third section.

Forth Section: In the forth section the seismic quality deteriorates significantly, hindering the observation of the terminations. The low quality of the data is probably attributed to the Late Pleistocene tunnel valleys that are located in the very shallow part of the section. Therefore Figure 4.12 presents the observations that were also common in the other two seismic lines (SNSTI-NL-87-03 and SNSTI-NL-87-02). The main observation that was tried to be identified here was the termination of high angle reflectors downdip and updip. The section shows reflectors of high angle but their termination in the upper part is
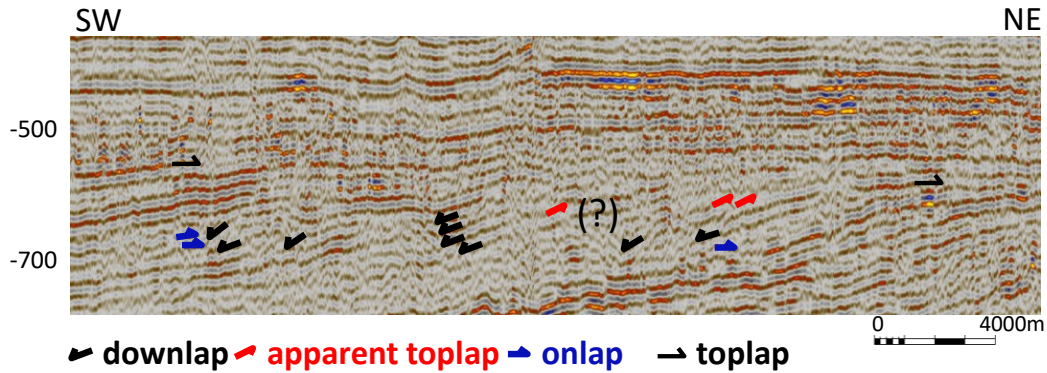
Figure 4.12: Demonstration of the reflectors terminations in the forth and fifth section.

not clear. It corresponds more to an apparent toplap and toplap since these reflectors terminate or stop below an overlying strata. Their downdip part terminates against other strata resulting into a downlap. Probably there are some onlaps in the section but with very high angle. However because their nature it not fully understood they will not be placed.

Fifth Section: The fifth section faces similar issues with the previous one due to low-quality data. Some highly inclined reflectors are visible but their termination is uncertain. Particularly, their downward termination is against a strata with different dipping angle but upwards is not clear. Probably it ends in an apparent toplap or toplap but generally the observation has high uncertainty. Some low angle reflectors can be spotted at the end of the section terminating against the downlap.

Stratal Stacking Patterns

The stacking patterns describe the vertical changes in proximal versus distal trends and can be classified as progradational, aggradational, retrogradational and degradational (J. C. Van Wagoner, Mitchum, Campion, & Rahmanian, 1990). For the identification of these depositional trends the image was analyzed in combination with the stratal terminations (Fig. 4.13). The section starts with the upward vertical stacking of the reflectors which terminate in a downlap geometry. The downlapping of the reflectors as well as their upward movement are indicative of a progradational-aggradational pattern (yellow indication). Namely, based on Catuneanu (2006) the downlap is commonly seen at the base of prograding clinoforms. However due to the presence of reflectors of lower height the trend turns into degradation which brings more proximal trends near distal. The section continues with a gradual stair-like stacking which ends in an onlap. Knowing that an onlap geometry always corresponds to rise in base-level, this implies a retrogradational pattern (green indication). Again the reflectors show a building out direction without a significant vertical stacking. This pattern probably corresponds to progradation (yellow indication) by the dowlap geometry. The upward vertical stacking of the next reflectors shows a retrogradational trend with the strata moving up and inwards. This trend continues even more upwards resulting into aggradation. The section continues with an upward and out vertical stacking corresponding to progradation which evolves to aggradation-degradation (downlap of reflectors with decreasing height). The section ends with the upward and out stacking of the reflectors resulting into progradation.
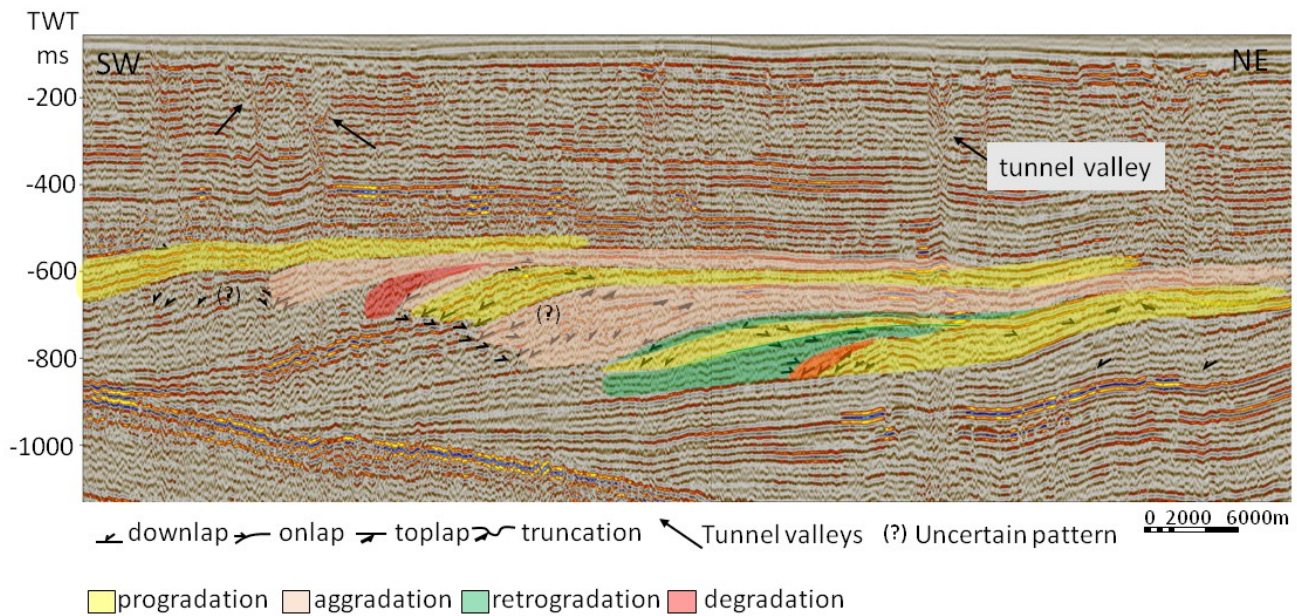
Figure 4.13: Illustration of the identified stratal stacking patterns based on the vertical stacking of the reflectors.

Stratal Characteristics & Geometries
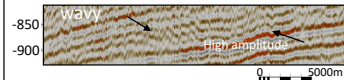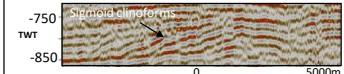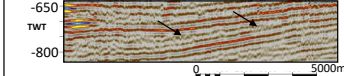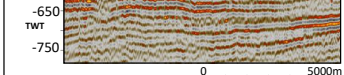
The stratal characteristics contain the observations regarding the amplitude, continuity and shape of the reflectors, as well as the paleo-shelf break and its trajectory which comprises a key geometric element in a prograding package of sediments based on Catuneanu et al., (2009). The analysis of the stratal geometries can provide an insight into the seismic facies as it is described below:
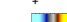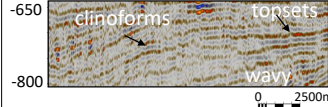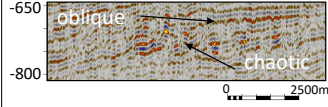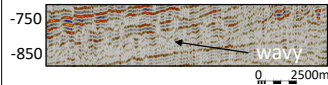
Seismic Facies Analysis

The first section is characterized by three seismic facies and two type of internal configurations, inclined sigmoidal reflectors and subparallel, subhorizontal strata. The former dipping geometry represents well-developed, prograding clinoforms which pass basinward into flatter lying reflections known as bottomsets. The bottomsets are characterized by onlapping and subhorizontal or wavy configuration. In some cases the more distal low-angle reflections are in depositional continuity with the clinoforms whereas in other they form separate depositional packages onlapping the clinoform front (Emery & Myers, 2009). Low-angle, subparallel strata can also be observed landwards, representing topsets.

The second section is similar to the previous one except for the presence of chaotic internal configuration and oblique reflectors. Generally in this section the strata is less continuous and the amplitude lower. The chaotic geometry can attributed to slump deposits while the oblique patterns are a type of clinoforms. The presence of flat, subparallel reflectors landward corresponds to topsets. Consequently, the three different seismic facies of deep marine, slope and plain can also be observed in this section.

The third section shows well-developed inclined strata representing prograding clinoforms which range from sigmoid oblique to oblique. The topsets in this section are either not well preserved or expressed due to their thickness. The amplitude is very low and the reflectors are not so continuous compare to the other sections. On the contrary, moving basiwards, the amplitude increases significantly and the reflectors onlap the clinoform front. Wavy to subparallel internal geometry can be observed, corresponding to bottomsets (turbidites, submarine lobes).

Seismic Facies	Amplitude	Continuity	Shape	Key Feature	Interpretation
SF1a	Moderate to High	Continuous	Wavy to subhorizontal parallel		Deep Marine Submarine lobes & fans
SF1b	Moderate to High	Semi-Continuous	Sigmoidal clinoforms		Slope Foresets
SF1c	Moderate to High	Semi-Continuous to Continuous	Divergent Low–angle subparallel		Coastal Plain Topsets
	Moderate to Low	Continuous	Subparallel to parallel		Delta Plain Topsets

Seismic Facies	Amplitude	Continuity	Shape	Key Feature	Interpretation
SF2a	Moderate to Low	Semi-Continuous to Continuous	Wavy Sigmoid clinoforms Subhorizontal		Slope Foresets
SF2b	Moderate to Low	Discontinuous to Semi-Continuous	Oblique Chaotic		Slope Foresets Slumps
SF2c	Low	Discontinuous	Wavy Sunhorizontal Subparallel		Deep Marine Submarine lobes & fans
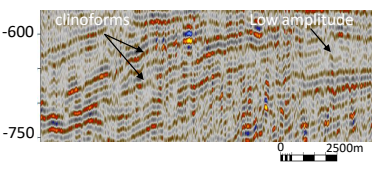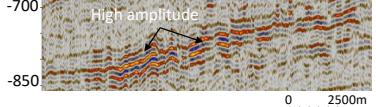
Seismic Facies	Amplitude	Continuity	Shape	Key Feature	Interpretation
SF3a	Moderate to Low	Semi-Continuous to Discontinuous	Oblique Tangetial clinoforms Subhorizontal		Slope Foresets Coastal Plain Topsets
SF3b	High	Semi-Continuous To Continuous	Wavy Subparallel		Deep Marine Submarine fan

Figure 4.14: Presentation of seismic facies identified in the three sections and their possible interpretation.

Incised Valleys

The study by using the seismic lines perpendicular to the delta progradation tried to identify possible erosional features such as incised valleys. The only seismic line that has a direction as such to provide this information is line 23. Figure 4.15 shows the location of the line with respect to the area of interest and the other seismic lines. For identified this type of feature the trace gradient attribute has been applied to the line which has also undergone processing by removing the multiples. In the line there are some reflectors which can correspond to incised valleys since they have characteristic U and W shapes. Figure 4.15 also shows these reflectors and their shapes after the removal of the multiples. By considering these shapes incised valleys the study identified one last seismic facies that corresponds to the deltaic setting.
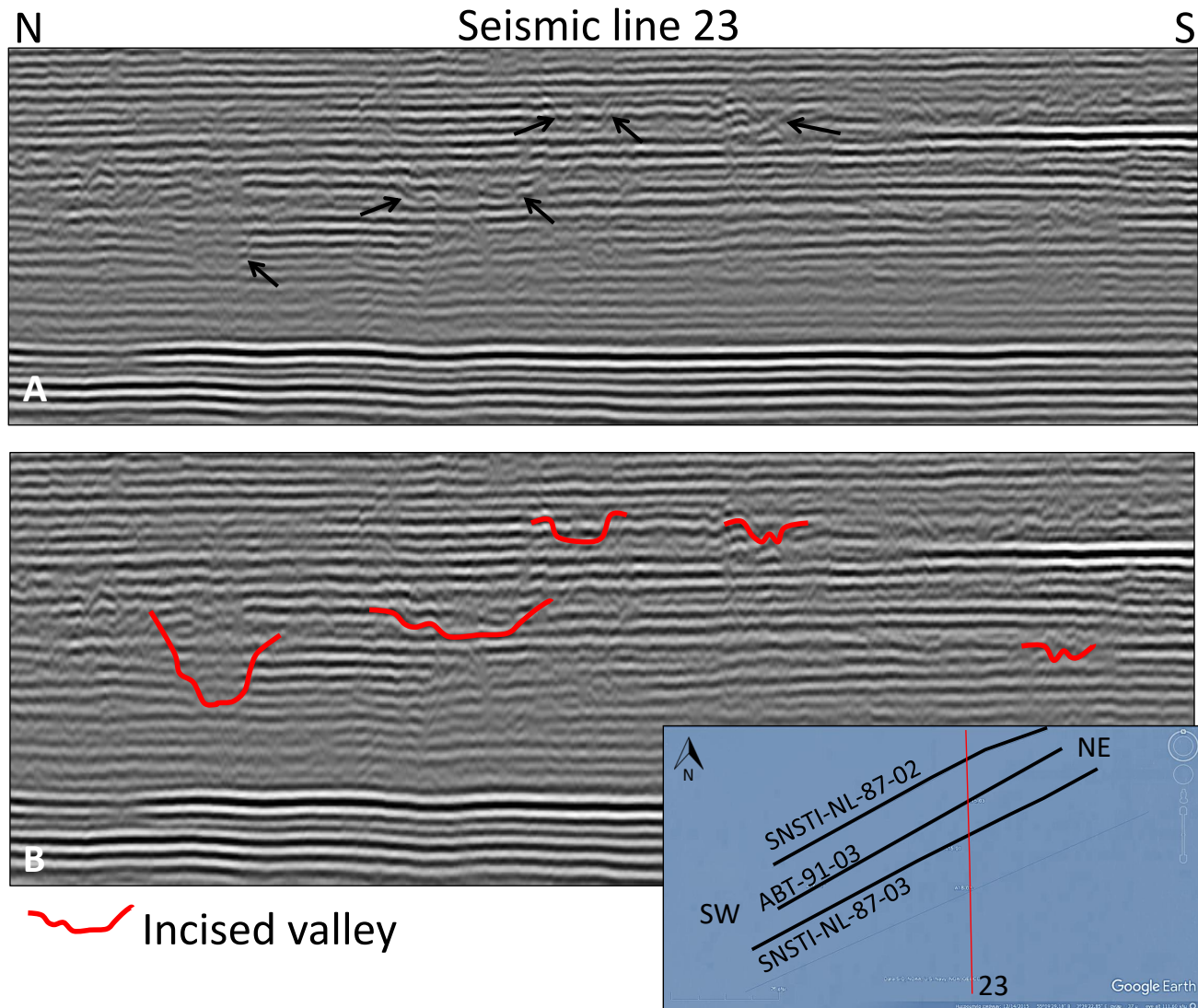
Figure 4.15: Illustration of seismic line 23 without the features (A) and (B) with the identified incised valleys-black arrows indicate the location of the features. The multiples have been removed and the trace gradient attribute has been used for the recognition of these features.

Consequently, four types of seismic facies were identified and presented in seismic line ABT-91-03 and 23. The North-eastern side is the more landward deltaic position with the development of topsets and clinoforms and the South-western the basinward with deep marine deposits. Figure 4.16 shows a schematic illustration of the possible deltaic environments and the seismic observations as an evidence (for seismic facies distribution see figure B4-5 Appendix).
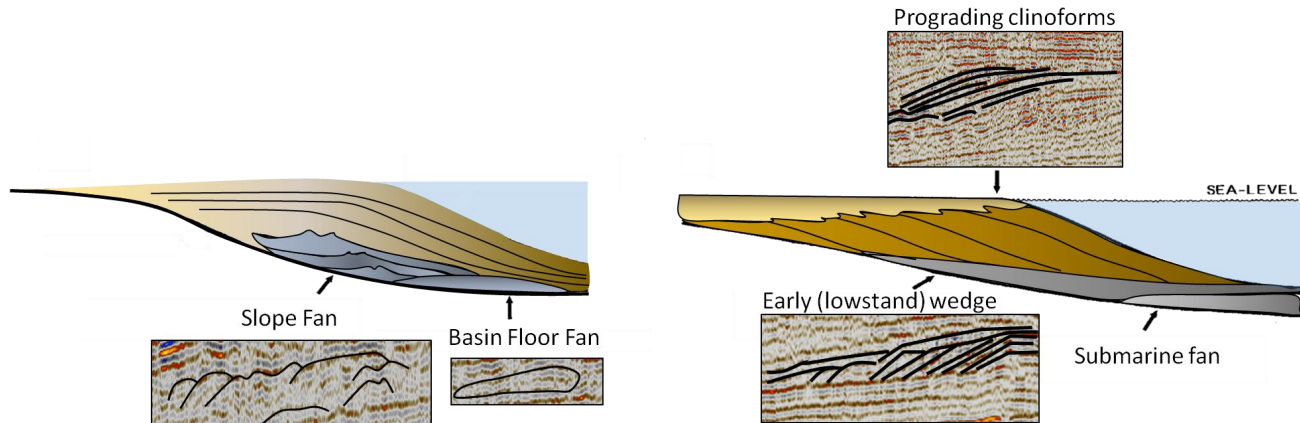
Figure 4.16: Correspondence of the identified seismic facies to possible depositional environments (Mattern, 2005)

Paleo-shoreline trajectory

One of the most fundamental observations in terms of reflectors' geometry, based on Catuneanu (2006), is the paleo-shelf break point and its trajectory in a prograding package. Identification of depositional trends is of great importance since they provide the required constrains in order for the sequence stratigraphic surfaces to be determined. Trends that are recorded below and above a surface can be obtained by constructing the shoreline trajectory. Changes in the shoreline reflect the interplay between base level fluctuations and sediment input. The different types of shoreline shifts can group packages of strata that are characterized by a specific depositional trend and therefore they result into particular stacking patterns known as system tracts (Catuneanu, 2006).

The trajectory of the paleoshelf break (Steel & Olsen, 2002) is used to interpret changes in accommodation on the shelf (area located updip from the shelf break) (Johannessen & Steel, 2005). In this study the shoreline shifts were determined based on the offlap break which is characterized as the topset edge and is associated with the position of base level. The topsets are mainly composed by shallow water sedimentary facies and the offlap break practically corresponds to the shoreline (Tropeano, Pieri, Pomar, & Sabato, 2002). Figure 4.17 illustrates the general shoreline trajectory which subsequently is going to be analyzed for each of the five sections.

First Section: The section starts with a prograding package of strata where the offlap break point moves upwards and out towards the basin. The inclined reflectors representing clinoforms are stacked on top of each other and are followed by reflectors of decreased height resulting into a downward position of the paleoshelf break point. The last part of the section is not well depicted but it is possible to distinguish some reflectors which have a gradual landward trend terminating against the clinoforms. The offlap break point is hard to be identified.

Second Section: The second section is more complicated than the first one due to either erosion of strata or strata thinner than the seismic resolution. There are some inclined reflectors which seem to have been eroded by a more pronounced reflector or their topsets are very thin. The paleoshelf break point can be observed in two to three prograding reflectors showing an updip shift, however the reflectors are in a

lower position than the last upward trend of the previous section. The section continues with the upward movement of the offlap break point but at the end of the section it starts to show a downward trend.

Third Section: In the third section the prograding package of strata shows a gradual upward trend of the topset edge point and continues into an up and out trend in the next section.

Forth Section: The low quality of the data in the forth section resulted into two different shoreline trajectories.In the first case the paleoshelf break point moves outwards and not up and in the second case it moves first downwards and then upwards and out due to the presence of some lower reflectors which seem to offlap on inclined strata.

Fifth Section: The fifth section shows similar difficulty with the previous one, not allowing a detailed analysis of the shoreline migration. However the paleoshelf break point can be observed in some reflectors at the end of the section which show an upward trend.
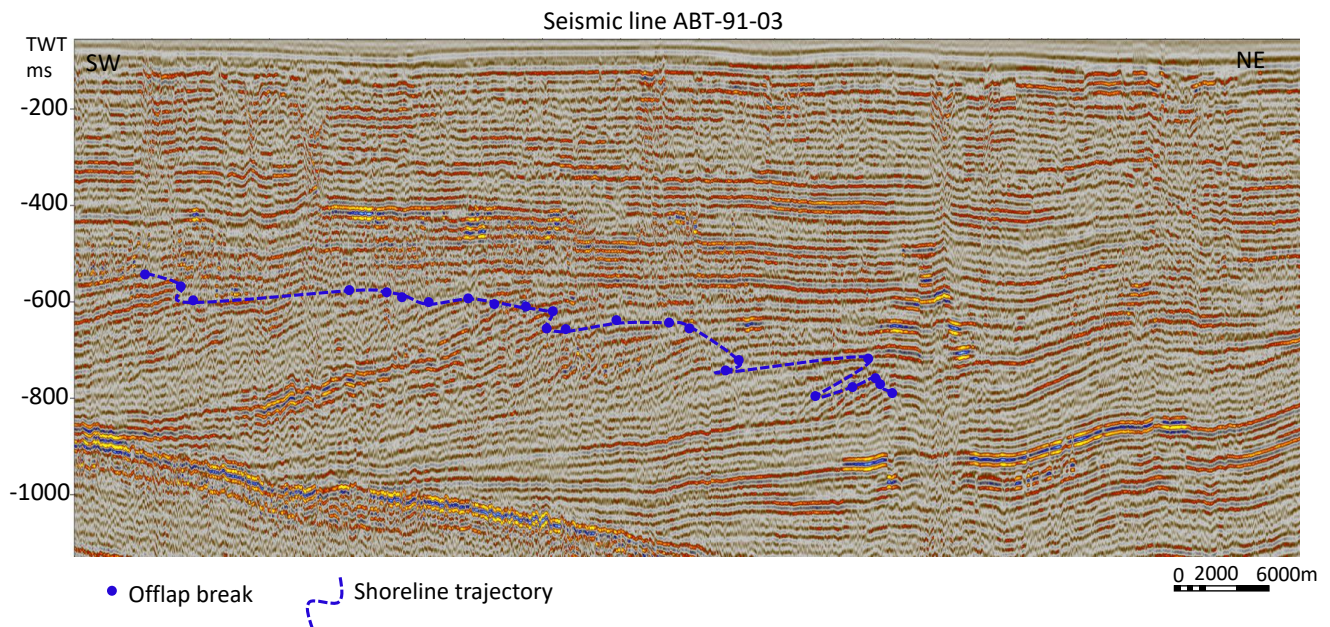
Figure 4.17: Shoreline trajectory identified based on the migration of the offlap break point.

Having identified the offlap break migration a curve presenting the changes in relative sea level has been reconstructed. Particularly, the graph was reconstructed by measuring the vertical changes of the offlap break point in the examined seismic image. For this purpose the "one to one" relationship of two way travel time and depth was used. This relationship is used by the literature for the shallow Cenozoic sediments of North Sea based on Kuhlmann et al., (2007) who mentions that " (O. Clausen & Huuse, 1999), (Japsen, 1999) and (Van Der Molen, 2004) found a linear relation between the velocity and the depth for the Paleocene to Pliocene sedimentary succession for the eastern and central North Sea with an interval velocity of approximately 2000 m/s. This relation implies that the seismic two-way travel time (TWT) in milliseconds (ms) corresponds to the depth in meters, i.e. 1000 ms TWT corresponds to 1000 m". Based on this relationship the two way travel time was translated immediately into depth. Also for the construction of the curve this study assumed a constant subsidence rate or significantly low based on the literature which mentions that the sedimentary basin around the period of Pleistocene was an intracratonic basin of low subsidence rate "Pleistocene subsidence rates are relatively low (<35cm/kyr; Cameron at al., 1992). Consequently, the basin can be considered to have been intracratonic (Bally, 1980)" (Huuse et al., 2012). However the curve represents sufficiently the general changes in sea level.

Regarding the nature of the curve is worth to be mentioned that due to the reduced quality of the data the curve can be characterized as "coarse" with high frequency, meaning that could also miss internal, smaller fluctuations. Due to an update in the graph, for higher resolution in chapter 6, where it is also being analyzed, this more simplistic graph can be found in the Appendices (see figure C11 Appendix).

4.3.2   Well Sequence Analysis

Sequence stratigraphic analysis of wireline logs is a significant process since it provides tangible information of the subsurface. The objective of this type of analysis is related to the depositional controls on sedimentary successions (Emery & Myers, 2009). One of the best logging tools that measures depositional parameters is the gamma ray log. This type of log measures the radioactivity of the rock and constitutes a direct function of the clay-mineral content, providing an insight into the depositional energy of the sediments.

Stacking Patterns

This study analyzes the gamma ray response of well A15-03, in terms of stacking patterns. The log response is highly related to the location of the well since it varies significantly based on the facies it penetrates (e.g clinoforms, topsets or bottomsets). Figure 4.7 at the beginning of this subchapter indicates the position of the well in the seismic image. The well passes through completely different facies ranging from deep to shallow marine (clinoforms, topsets). These differences in depositional conditions are depicted in figure 4.18, which presents the gamma ray log of well A15-03. As it is indicated in the figure, three stacking patterns were identified and linked into the delta.

The first interval ranges from 1140m to 965m depth. Starting from the bottom until 1105m depth the gamma ray response shows alternations between higher and lower values corresponding to a bow trend (or symmetrical). Namely, two successive bow trends can be identified consisting of a coarsening-up trend, overlain by a fining up trend. The specific motif is representative of a basinal setting where progradation and retrogradation of mud-rich fan system takes place (Emery & Myers, 2009). The section continues with lower but consistent values upwards resulting into a box car type of reading (also known as cylindrical). This motif is characterized by a sharp-based low-gamma ray unit with an internally constant gamma ray reading. The section ends with an alternation of bow and irregular trend after the box car interval, representing the changes from progradation to retrogradation and finally aggradation. Consequently the entire interval corresponds to a basinal setting.

Continuing from the last bow trend of the previous section the new interval ranges from 965m to 770m depth. This interval is characterized by large alternations of the bow (symmetrical) trend with well developed prograding and retrograding patterns of coarsening and fining upward trends. The bases and tops are abrupt and the entire interval represents submarine depositional units. The bow trend is followed by a small interval of box car with constant interval values and sharp base and top. This motif consists of coarser (cleaner) lithologies implying a shallowing of the system. Finally the section ends with an irregular trend of higher gamma ray values than the previous trend. The irregular motif is characteristic of an aggrading pattern of a shaly or silty lithology. It is typical of a shelfal or deep water setting.

The interval ranges from 770m to 675m depth. The previous aggrading pattern is followed by a retrograding trend with an increase in the gamma ray reading. The shape of this trend can be characterized as irregular and the lithology becomes more clay-rich. The following trends can also be characterized as irregular, separated by some coarsening trends in between. However the readings show lower values compare to the previous trend. The general trend is more constant with the less clay-rich intervals in between. Based on similar examples of Emery et al., (2009) this pattern can represent a silty-sandy progradation parasequence set. The next trend is a typical bell shape pattern with a gradual upward increase in gamma ray readings, representing a retrograding unit. The unit reaches very high gamma ray values which subsequently decrease sharply into lower values. Probably it corresponds to a transgressive shoreline-shelf unit or to a stacking of smaller coarsening up parasequences.
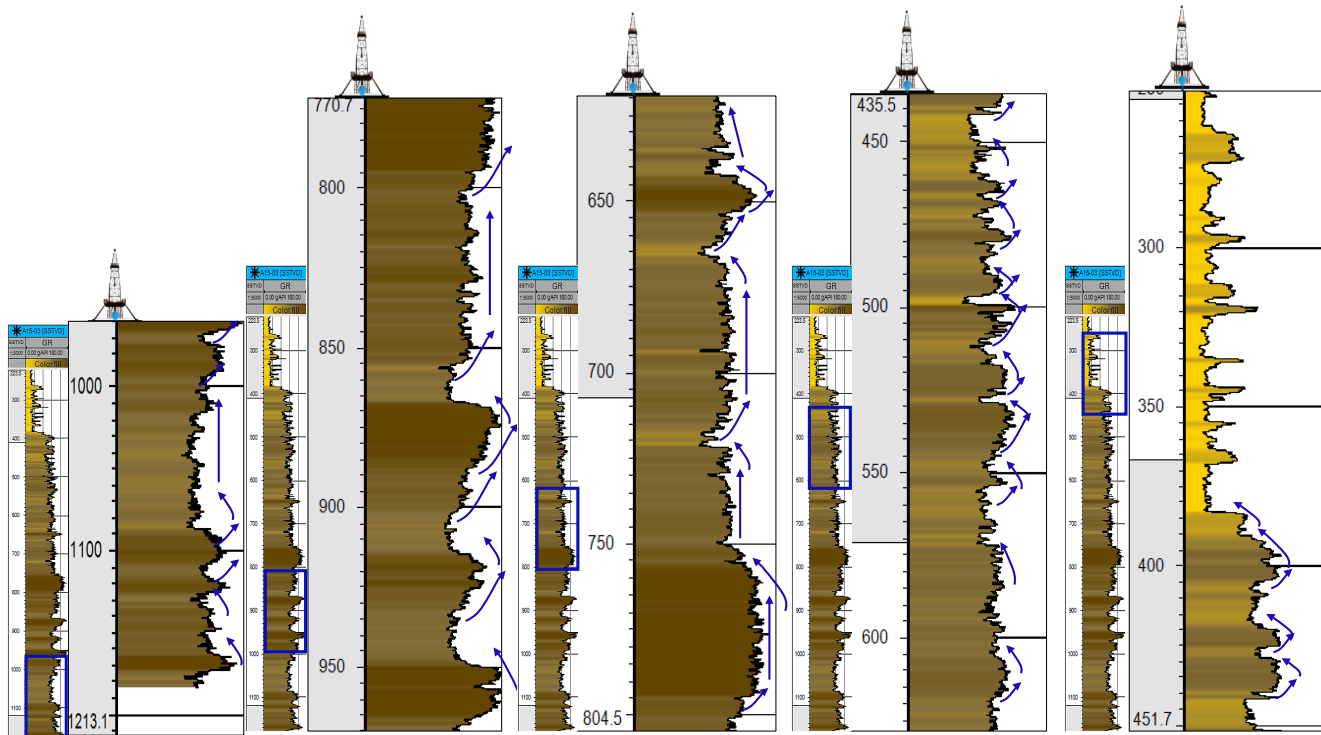
Figure 4.18: Stacking patterns (blue arrows) identified in the depicted gamma ray intervals of well A15-03.

The interval ranges from 675m to 435m depth. This section shows different characteristics compare to the previous ones. The aforementioned intervals show larger constant trends without so many variations. However, moving upwards in the section the patterns become smaller but more frequent with many variations. The interval starts with some prograding retrograding patterns which evolve to coarsening and fining upward alternations. Bell, funnel and box car trends can be observed along the log, implying a prograding and retrograding set. The majority of the transitions between the various shapes have sharp, abrupt bases and tops. Figure 3.7 shows the shapes and some examples of the nature of the base and top.

The last interval ranging from 435m to 255m depth shows a distinct transition in the gamma ray trend from a more clay -influenced lithologies to almost clay-free. This significant change in clay content implies and a change in the depositional energy and hence the depositional environment. The interval at the beginning continues with the small alternating units of progradation and retrogradation. However this section has more distinct and quite larger intervals of coarser units that form a box car pattern. This implies the transition to cleaner shallower lithologies. The section continues and ends with extensive box car trends of much coarser units with some clay-rich spikes. The boundaries are even more sharp and abrupt than any other section. Due to the location of the well and its patterns this trend probably represents fluvial channel sands Consequently, well A15-03 penetrates a basinal setting at depths ranging from 1140m to 850m with an upward shallowing trend around the 800m depth. The readings between 750m and 400m depth show small prograding and retrograding units, indicative of deltaic stacked topset parasequences. Finally the system probably changes into a fluvial with coarser formations representing channels.

<div align="right">

5

</div>

Seismic & Well Log Interpretation

5.1 Seismic Stratigraphic Interpretation

Seismic Stratigraphy is a technique that is used to interpret stratigraphic information provided from seismic data. The technique in combination with Sequence Stratigraphy can give a critical insight into the depositional evolution of a sedimentary basin. The fundamental principle based on Emery et al., (2009), lies in the fact that the seismic reflectors follow the bedding of the strata and therefore they approximate time lines. The seismic reflectors are generated by contrasts in acoustic impedance, a rock property caused by changes between the bedding interfaces and not the lateral facies. The tool of sequence stratigraphy "groups the seismic reflectors into packages that correspond to chronostratigraphically constrained genetic depositional intervals. These intervals constitute the depositional sequences and system tracts (Vail, 1987)".

5.1.1 Stratigraphic Surfaces

The significance of the stratigraphic surfaces lies on the fact that they describe fluctuations of the base level with respect to changes in sedimentation at the shoreline. The determination of stratigraphic surfaces took place by combining the observations of stratal terminations and depositional trends such as stacking patterns and shoreline shifts. Stratal terminations are coupled with specific depositional trends, providing critical information for the type of syndepositional shoreline shifts which in turn allow the recreation of base-level changes at the shoreline. Some stratal terminations have a direct link to the shoreline shifts, such as the onlap which is indicative of transgression or the offlap of forced regression. However there are cases where a type of stratal termination corresponds to two different trends. For instance downlap or apparent toplap can form during normal or forced regression. In this case supplementary features have to be identified in order to reach the link between the two type of observations.

The section starts with the downlap of prograding clinoforms and the upward movement of the offlap break which corresponds to a normal regressive shorline. It continues with the apparent toplap of the reflectors since the forsets are present but not the topsets. This means that probably the thickness of the topsets is less than the vertical seismic resolution. As it is already mentioned, this type of termination corresponds to two syndepositional shoreline trends. However, the presence of offlapping reflectors at the end of the prograding package can lead to the interpretation of a forced regressive shoreline. This interpretation can also be enhanced by the presence of truncated reflectors at the landward part of the topsets. The section ends with onlapping reflectors which are indicative of base-level rise and correspond to a transgressive or normal regressive event. It is also worth to be mentioned that the onlap at the base of the section, terminating against the clinoform front, corresponds to a marine onlap of deeper facies.

The second section is characterized by downlapping reflectors which correspond to foresets. Generally downlap is indicative of normal or forced regressive shoreline, here due to the presence of an onlap geometry a normal regression trend can be concluded. Based on Catuneanu (2006) all types of onlap indicate rise of base level. The section continues with an apparent toplap which can be linked to both fall or rise of base level. Owing to an upward movement of the paleoshelf break with vertical stacking of topsets a

<div align="center">

37

</div>
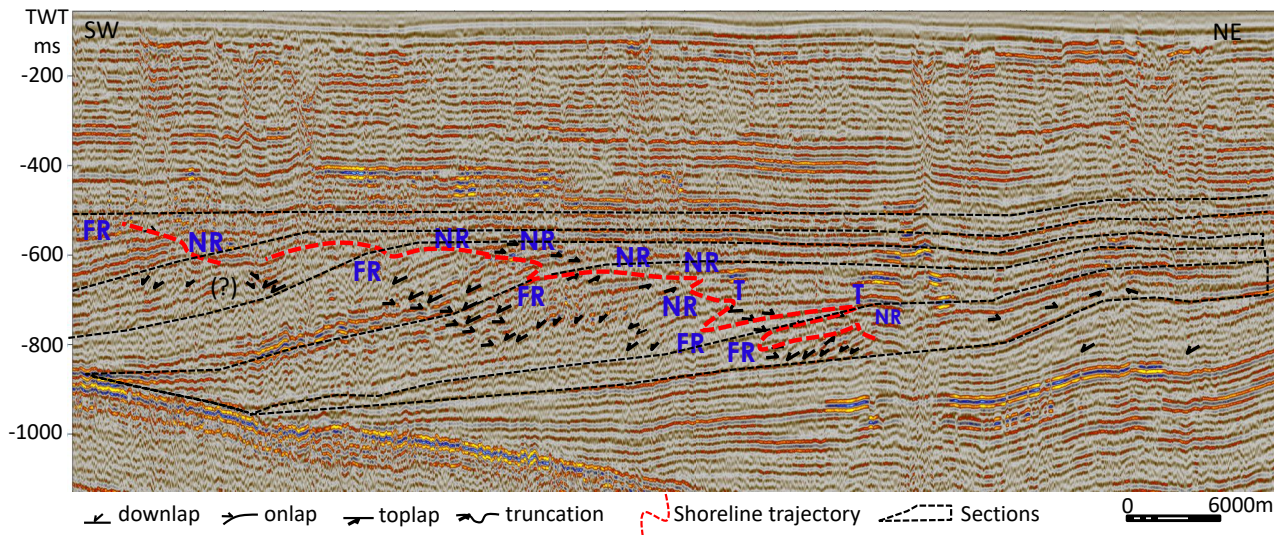
Figure 5.1: Illustration of the shoreline trajectory and the resulted depositional trends based on the stratal terminations and the offlap breaks.

normal regressive shoreline can be concluded it. Between the two type of normal regressions (prograding clinoforms and aggrading topsets) a transgressive event must have taken place which probably eroded the prograding package at the beginning of the second section. This can also be seen in the offlap break point which is more landward after the transgression and then moves seawards in the next normal regression. Nevertheless the transgressive event probably did not last enough to create a distinct retrogradational stacking of strata. The section finishes with downlapping reflectors and apparent toplaps without the formation of topsets corresponding to a forced regressive event. However because of the chaotic internal configuration of the reflectors this part of the section has higher uncertainty.

The third section shows two types of stratal termination, downlap and toplap. The downlap which represents the termination of foresets in a prograding package of strata does not continue upwards with the full development of topsets resulting into an apparent toplap geometry. Probably again the thickness of the topsets is less than the vertical seismic resolution. However some clinoforms continue upwards in a topset formation and a toplap termination. Based on these characteristics and the upward movement of the paleoshelf break point the depositional trend must correspond to normal regression.

For the forth section the interpretation is quite uncertain but owing to the presence of more distinct forsets the shoreline trend can be approximated. The section shows downlap geometry and lowering of the paleoshelf break position as well as decrease in the height of clinoforms, resulting into forced regression. Generally the topsets either are not well-developed or they are below the seismic resolution. However the fact that there are visible foresets without the corresponding topsets extensive progradation must have take place. Some reflectors seems to stop on top of each other in an offlap termination leading to a forced regression shoreline. The last sections faces the same difficulty with the previous one. A downlap termination with a possible toplap is the identified geometries. The upward trend of the offlap break results into a normal regressive shoreline. At the end of the last inclined reflector a lowering of the height of a reflector can be observed meaning a possible forced regressive shoreline.

The outcome of the previous interpretation provides critical information regarding the interplay between sedimentation and base level fluctuations at the shoreline. Based on Catuneanu (2006) the recognition of the depositional trends results into four main events which can be identified during a complete cycle of base-level shifts. For that reason the reconstruction of the sea level curve took place showing the changes at the shoreline:

- **Onset of forced regression**: this event represents the beginning of the fall in base level at the shoreline and indicates the change from sedimentation to erosion in the delta.

- **End of forced regression**: signifies the end of the fall in base level at the shoreline and corresponds to the change from degradation to aggradation in the fluvial to shallow-marine environments.

- **End of regression**: this event represents a shift in the depositional trends with rising of base level at the shoreline which leads to transgression.

- **End of transgression**: the last event marks the transition from transgression to regression during base level rise at the shoreline

Table 5.1: Stratal terminations and syndepositional trends in terms of base level and shoreline shifts.

Stratal termination	Shoreline shift	Base level
downlap	NR	Rise
apparent toplap	FR	Fall
offlap	FR	Fall
onlap	NR	Rise
downlap	NR	Rise
onlap	T	Rise
apparent toplap	NR	Rise
apparent toplap	FR	Fall
downlap	NR	Rise
toplap	NR	Rise
offlap	FR	Fall
downlap	NR	Rise
toplap	NR	Rise
offlap	FR	Fall

By combining the information from the seismic image regarding the syndepositional trends and the reconstruction of the sea level changes the identification of the four main events took place which in turn control the formation of all sequence stratigraphic surfaces. Namely, the end of forced regression corresponds to a fall in base level and is marked by the Subaerial Unconformity. The end of regression is marked by the Maximum Regressive Surface, while the end of transgression by the Maximum Flooding Surface:

Subaerial Unconformity as an erosional surface marks the end of forced regression and is characterized by forced or normal regression below the surface and normal regression or transgression above. The terminations of the strata below the surface corresponds to truncation and toplap and above to onlap. Based on these criteria this study recognized six subaerial unconformities.

Maximum Regressive Surface is associated with the end of regression, marking the change from regression to subsequent transgression of the shoreline. Hence, this surface separates prograding strata below from retrograding strata above. The change from progradational to retrogradational stacking patterns takes place during the base-level rise at the shoreline, when the increasing rates of base-level rise start outpacing the sedimentation rates. It is characterized by normal regression below the surface and transgression with onlap above.

The Maximum Flooding Surface marks the end of the transgressive shoreline and therefore this surface separates retrograding strata below from prograding strata above. The diagnostic characteristics are transgression below the surface and normal regression above. In terms of stratal termination below can be found truncation while above downlap.

Figure 5.2 shows the stratigraphic surfaces that were established in this study. Overall eight subaerial unconformities (with their possible correlative conformities) were identified with the deeper one marking
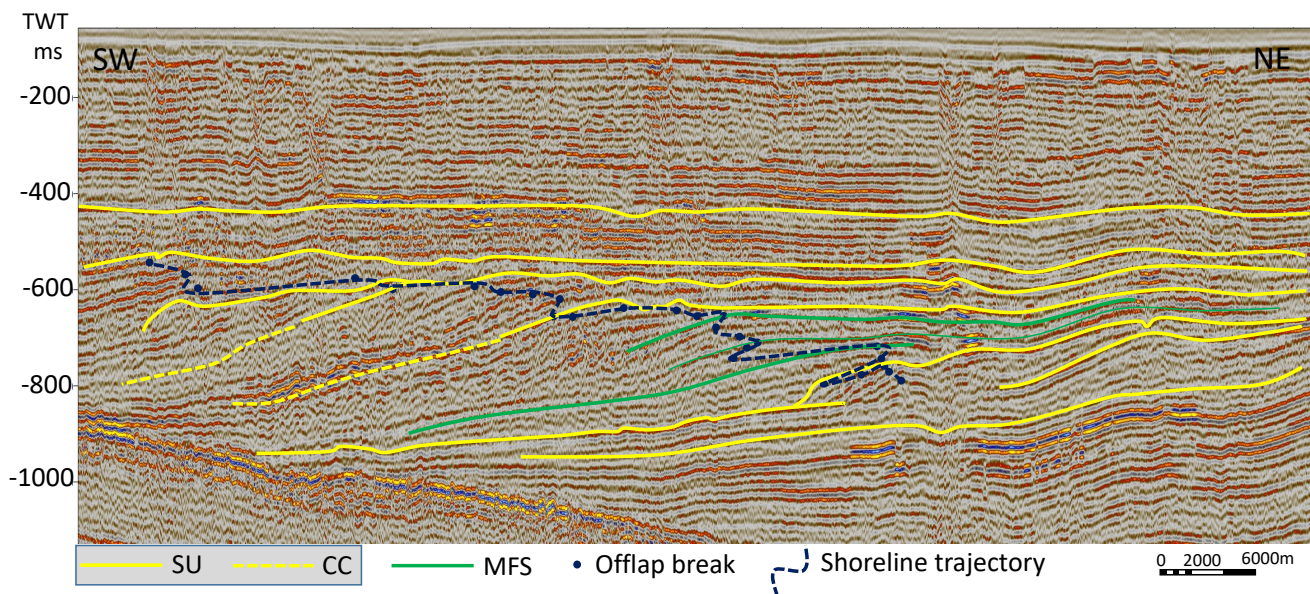
Figure 5.2: Presentation of the stratigraphic surfaces as these were determined based on the methodology of Catuneanu et al., (2006)

the transition from basinal to shallow marine setting. It is characterized only by downlapping reflectors since the progradation of the delta has not reached the examined area in this part of the seismic image. The nature of the next surface is controversial. The observations are not enough to exclude the possibility of a maximum flooding surface which also is characterized by downlapping reflectors above the surface. However due to the intact continuity of the surface in the basinward direction and the truncation of a reflector landward, the surface can be classified as subaerial unconformity with well-preserved correlative conformity. The following subaerial unconformities are related to erosional events during sea level fall with the last one representing the fill of the basin. Three surfaces are candidates for maximum flooding surfaces and are related to sections of condensation. The identification of three maximum flooding surfaces does not exclude the possibility of more than three. Maybe they are not well-preserved or they are not well-developed and thus are below the seismic resolution.

Finally the study identified seismic facies related to possible incised valleys in a perpendicular to progradation seismic line (23). The U and W shapes of the valleys have been tried to be linked to the stratigraphic surfaces of the main seismic lines (parallel to progradation). An incised valley of characteristic U shape has been identified at the same level with the first two subaerial unconformities. However the continuity of these surfaces into the perpendicular seismic line is difficult since there is a mismatch in depth between the lines. The pronounced hard kick of the sea floor is located in a shallower depth in seismic line 23 than that of the other seismic lines. This results into an upward shift in the reflectors making it hard to link the subaerial unconformities with the incised valleys. Nevertheless the study tried to understand the continuity of the reflectors based on charactaristic high amplitude reflectors in both lines. It is worth mentioning that the uncertainty is quite high due to this mismatch (see figure B3 Appendix).

5.1.2   Sequences

The establishment of all the stratigraphic surfaces that were possible to be identified allows the determination of a sequence. Based on Catuneanu (2006) a sequence represents "the product of sedimentation during a full stratigraphic cycle, irrespective of whether all parts of the cycle are formed or preserved." The selection of which type of stratigraphic surface describes best a sequence depends on the quality of the data but also the history of the sedimentary basin. If the well preserved strata corresponds to sections of condensation then the maximum flooding surfaces it would be a better choice as a sequence. However, this study based on the evolution of Eridanos delta suggests the subaerial unconformity (with its correlative conformity) as a sequence. The choice was made considering two factors. The first is the influence of Eridanos by the onset of Northern Hemisphere Glaciation which caused deterioration of the climate and lowering of the sea level. The other is based on the obtained data which shows an overall trend of degradation and progradation rather than retrogradation. Either the retrograding strata has been eroded or due to the climatic conditions the transgressive event did not last long resulting into thickness less than the vertical seismic resolution. The subaerial unconformity is considered the most important kind of stratigraphic hiatus in the rock record, and it is commonly selected as the nonmarine portion of the sequence boundary. A sequence bounded by subaerial unconformities is known as Depositional Sequence.
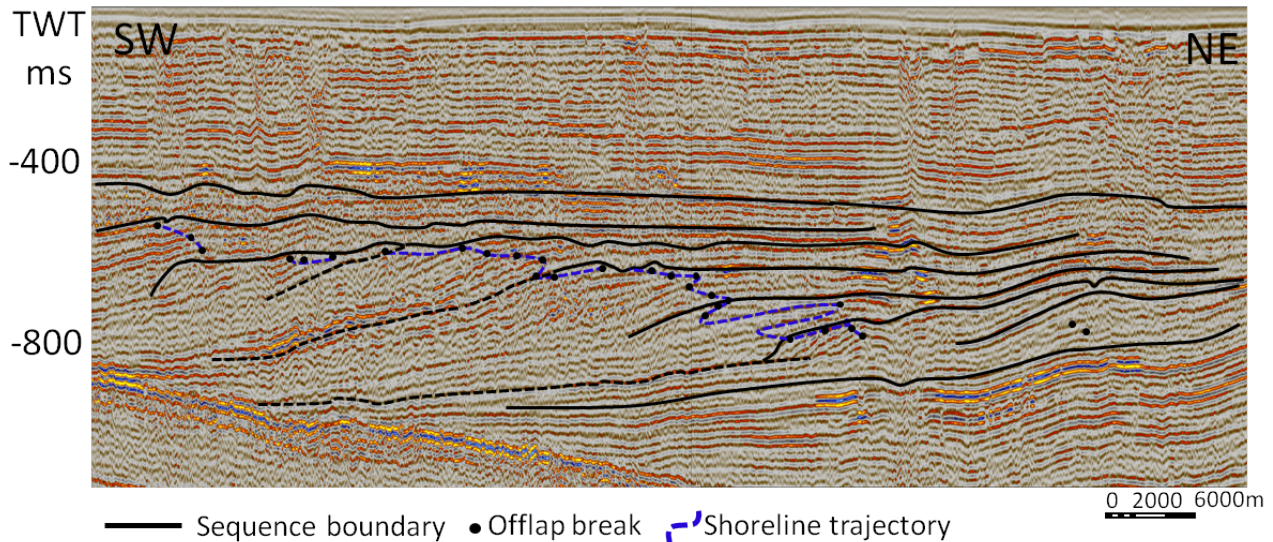
Figure 5.3: Illustration of the sequences defined by this study. They correspond to depositional sequences as they comprise erosional or non depositional surfaces known as subaerial unconformities (and their correlative conformities.

The following figure, which is depicting the vertical changes in sea level, is the same as the one described in the section of stratigraphic surfaces and it is used to show that the subaerial unconformities comprised the sequence boundaries of this study. It is worth mentioning that the second of the transgressive surfaces meets the requirements to be elevated in the standards of a depostional sequence based on Catuneanu (2006) who states that "subaerial unconformities may also form during shoreline transgression, where extreme wave energy results in coastal erosion (Leckie, 1994).

5.1.3 System Tracts

The sequences defined in the previous section can be divided into genetic packages of lower hierarchy, the system tracts. This genetic type of deposits corresponds to a specific depositional trend of the shoreline. Systems tracts are interpreted based on stratal stacking patterns, their position within the sequence, and the types of bounding surfaces (J. Van Wagoner, Mitchum Jr, Posamentier, & Vail, 1987), (1990); (J. C. Van Wagoner, 1995). This study used the identified stratigraphic surfaces in combination with the stacking patterns that have been already analyzed in the subchapter 4.3 to place the genetic packages of system tracts. Owing to the large scale of the delta smaller genetic units may exist in between those identified but the seismic quality do not allow such identification. Also the more landward part of the image may also contain responses of the sea level fluctuations with the corresponding system tracts but again the data is hampering the interpretation, or the seismic line has not captured them.
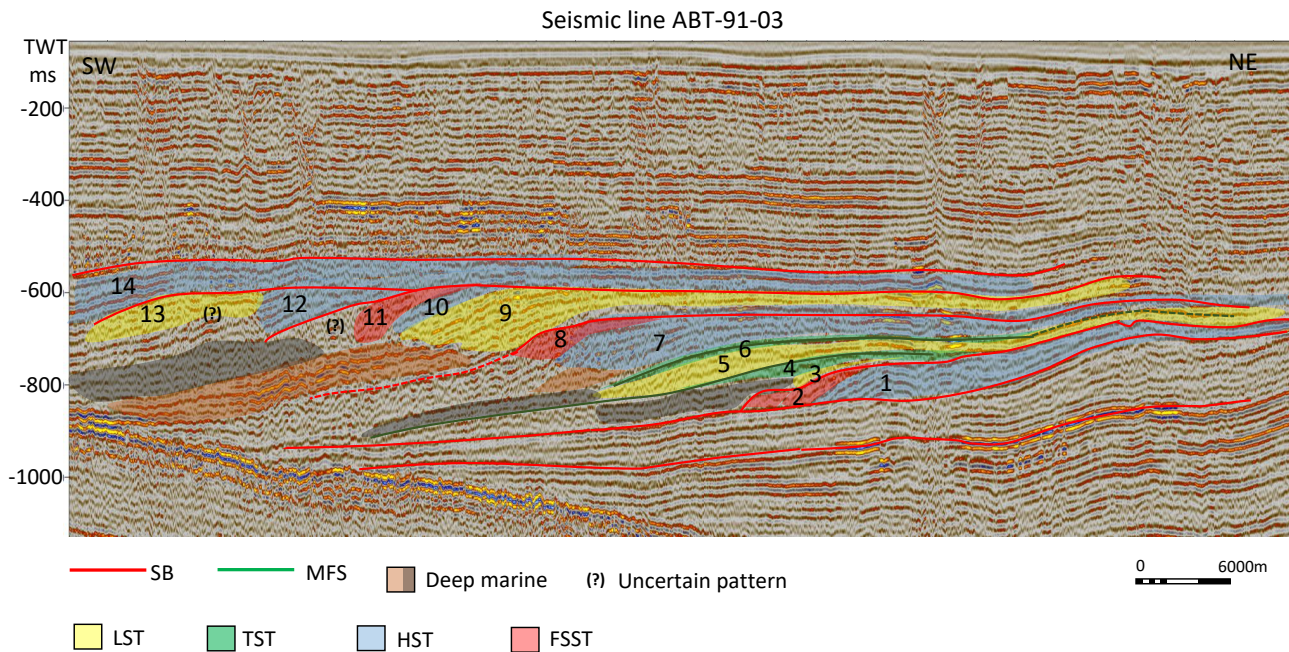
Figure 5.4: System tracts proposed by this study.

    The seismic image starts with a sigmoid prograding package (1) of strata and the vertical stacking of parallel topsets, indicative of an up-building (aggradational) trend. The upstepping shelf-break trajectory which has been described as normal regressive implies creation of shelfal accommodation during progradation. The description approximates a highstand or lowstand system tract with not so clear distinction between the two. The depositional pattern has been characterized as aggrading-prograding with the creation of clinoforms and topsets with sediment supply almost being in balance with the rate of creation of topset accommodation volume. The presence of a possible basin floor fan or slope fan attached to clinoform front may correspond to a lowstand wedge. However it can also be a highstand system tract and the slope and basinal lobes may be a result of the following sea level fall which corresponds to a falling system tract package. The aforementioned genetic package (2) is in accordance with the forced regressive shoreline, the stratigraphic surface above it, as well as the downstepping of strata marked by offlap terminations. The next genetic package (3) is in the transition to an upcoming sea level rise with a normal regressive shoreline. Therefore a lowstand system tract can be attributed for this unit which is followed by retrograding strata (4) and the landward shift of the shoreline. A transgressive system tract can best describe this type of unit. After the transgressive event the position of the shoreline is quite uncertain but is definitely regressive. The package (5) can be characterized as lowstand system tract with the formation of a lowstand wedge and basinal deposits. Nevertheless this classification is also uncertain due to the pos-

sible erosion of the package. Owing to its general geometry can best be described as a LST. The surface above this genetic package has completely different geometry than the eroded clinoforms resulting in a short transgressive event (6) since the system tract itself is absent or at least not visible by the seismic. Subsequently, progradation again takes place with a regressive shoreline and the upward vertical stacking of strata (7). The regression can be described as highstand with the shape of the trajectory resembling a convex up pattern known for the decelerating sea level rise. The rate of progradation increases with time while the rate of aggradation shows the exact opposite trend. The highstand system tract is followed by a falling system tract (8) since the shoreline is forced to regress. However attention has to be paid due to the chaotic geometry of the reflectors and the offlap termination. The resolution at this part is quite poor hindering a less uncertain interpretation. The next section (9) is characterized by a slow rise in sea level and the subsequent formation of clinoforms. Progradation constitutes the dominant depositional trend and the overall shape can be characterized as oblique. This oblique prograding package shows toplap terminations at the top and downlap terminations at the base, and a more horizontal shelf-break trajectory (Mitchum Jr, Vail, & Sangree, 1977). This type of progradation is characterized by the lack of topsets, and indicates little or no accommodation on the shelf during progradation (Catuneanu et al., 2009). The genetic package can be characterized as Lowstand system tract. Here it is worth mentioning that the basinal deposits show a significant increase in amplitude and have an extensive spread. These deposits can be characterized as lowstand turbidites. The shoreline continues the normal regressive trend. Little if any topset accommodation volume is created at this time, and the bulk of the sediment bypasses the topsets to be deposited on the clinoforms slope. Slope instability and occasional fan deposition is likely to occur and the bottomsets of the early lowstand prograding wedge may contain interbedded turbidites. The following genetic package (10) is characterized by an almost constant regressive shoreline (or normal) with a convex up shape corresponding to a highstand regressive trajectory. In this section the clinoforms are more well-developed than the topsets which either are not well-preserved or well-developed due to the following degradation. The rate of accommodation over sediment supply is negative resulting into a falling system tract (11). In this part of the study the interpretation is more "improvised" and imaginary due to the lack of evidence.

Reaching almost the end of the seismic line the type of strata corresponds to a lowstand/highstand system tract (12/13). There are some downlapping reflectors which probably represent clinoforms of an early lowstand wedge which later develops as a lowstand wedge with the creation of a clinoforms-topset package. However the last package (14) with the up-building reflectors may also represent a highstand tract due to an aggrading pattern. The clinoforms do not continue sufficiently in order to distinguish the depositional pattern. To conclude, the general trend of the delta is characterized by successive alternations of lowstand and highstand system tracts in combinations falling system tracts in between. The transgressive system tract is not rejected, as there is a possibility that it was not well-preserved or it was formed more landward or it is below the seismic resolution.

5.2   Gamma Ray Interpretation

5.2.1   Stratigraphic Surfaces

Having established the depositional trends in the gamma ray response, the key stratigraphic surfaces can be identified in order to subsequently subdivided into system tracts. For that purpose the stacking patterns play an important role since the surfaces are going to be placed between the transitions of the different patterns. It is worth mentioning that the location of the well with respect to the deltaic architecture is crucial in order to be aware of the nature of the surfaces that are about to be established. The fact that a surface is not identified in the wireline log data does not imply that it is not present in the deltaic strata.

Namely, maximum flooding surface in proximal locations can be identified by the transition from a retrograding unit to an overlying prograding unit since it marks the most landward position of a transgressive shoreline. Therefore this surface corresponds to a gamma-ray maximum. Maximum progradation surface can be recognized by the exact opposite trend, marking the transition between a prograding unit and an overlying retrograding unit. Hence this surface corresponds to a gamma-ray minimum (Emery & Myers, 2009). Attention must be paid to the recognition of the subaerial unconformity which is difficult to be identified in the well data. In order for the surface to be recognized it requires facies dislocation, with proximal facies overlying more distal. Based on Emery et al., (2009) it can be more easily identified on the front of highstand clinoforms and where shelfal erosion has been significant (i.e incised valleys). When the well is passing through clinoforms the gamma ray trend "jumps" to a more coarser lithology. Nevertheless this abrupt change can be seen if the well passes through the final clinoform of the highstand system tract. In the case of topsets there is also an abrupt change to coarser lithologies when clean topset strata overlies offshore mud.

The gamma ray log is analyzed in sections as these were divided in subchapter 4.3 for the identification of the stacking patterns. The first section from 1140m to 965m depth was determined as basinal strata with prograding retrograding patterns and an abrupt change in response to lower readings at 1090m depth. This change probably corresponds to an erosional surface. After this sharp shift to cleaner facies the readings remain quite constant until a prograding retrograding pattern starts again at 1000m depth. In the lowest value of the gamma ray the maximum regressive surface can be placed.

The next section ranging from 965m to 770m depth probably corresponds to turbidites based on the seismic facies analysis and is characterized by distinct changes between prograding and retrograding strata. This turbidites seem to have been deposited at the toe of progradation since a possible lowstand prograding wedge with lower gamma ray values follows these type of deposits upwards.

The following section is characterized by more frequent but smaller changes in the gamma ray trend resulting into the identification of more surfaces compare to the previous sections which represent basinal deposits. The section ranges from 770m to 675m depth and the first surface is placed in 755m depth where the readings show a sharp shift from fine to coarse lithology. Therefore this surface corresponds to a subaerial unconformity. The next surface is found in 720m depth and corresponds to a maximum regressive surface since in that level a prograding unit reaches its lowest value moving afterwards to retrogradational patterns. The last retrograding event leads to high values of gamma ray with the highest resulting into a maximum flooding surface. The last significant event in this section is characterized by the abrupt change of the gamma ray response to cleaner facies. The last retrograding unit does not show gradual transition to lower readings but it has this sharp shift resulting into a subaerial unconformity.

The next section ranges from 675m to 435m depth and it consists of even more frequent but short scale changes in the gamma ray readings. The first surface, placed at the gamma ray maximum of 620m depth, represents the maximum transgression of this unit which is overlaid by a prograding unit. The next transition to a cleaner lithology is not gradual but abrupt, marking the change from a much finer to a much coarser lithology. Due to this sudden shift in facies a subaerial unconformity can be placed at 560m depth. A following retrograding event around 535m depth reaches a maximum which probably corresponds to a maximum flooding surface. Moving upwards, alternating progradational and retrogradational patterns end into an abrupt event at around 500m depth. This sharp shift in lithology must correspond to a subaerial unconformity. The section ends with the continuous shallowing upward trend and a funnel shape trend which corresponds to a subaerial unconformity at 450m depth. The last section from 435m to 255m depth shows one main retrograding event which corresponds to a maximum flooding surface around at 435m depth.

5.2.2   System Tracts

The system tracts of well A15-03 are determined based on the aforementioned analysis of stacking patterns and stratigraphic surfaces. The placement of the system tracts in the gamma ray starts from the depth where an upward shallowing trend appears, separating deeper facies from the approaching prograding delta. With the possible turbidites being at the toe of progradation, the first gamma ray trend ranging from 855m to 800m depth corresponds to a lowstand or highstand system tract with very small funnel shape intervals showing coarsening upwards and progradation. Due to an increase in the gamma ray trend and a transgressive or normal regressive trend the following system tract can be characterized as HST/TST since its exact nature is cannot be determined. The system tract ends with a subaerial unconformity that is overlaid by a LST owing to a decrease in the gamma ray values. The LST is followed by constant values of an irregular shape indicating aggradation and thus a HST. The gamma ray reading from depth 665m shows a distinct decrease in values and the system stops at the sharp change where a subaerial unconformity has been placed. Above the subaerial unconformity a LST has been determined with a small retrograding-prograding trend and a maximum regressive surface before the upcoming transgressive or normal regressive event. The latter corresponds to a HST/TST with a candidate maximum flooding surface. The following system is a HST with also maybe a short LST event. The system finishes with an abrupt shift to cleaner lithologies indicating a subaerial unconformity. The next section shows characteristic prograding trends resulting into a LST and a possible HST.The last section contains a TST above the previous subaerial unconformity with a possible maximum flooding surface. Finally a LST follows the TST with distinct blocky gamma ray response of a clean lithology.
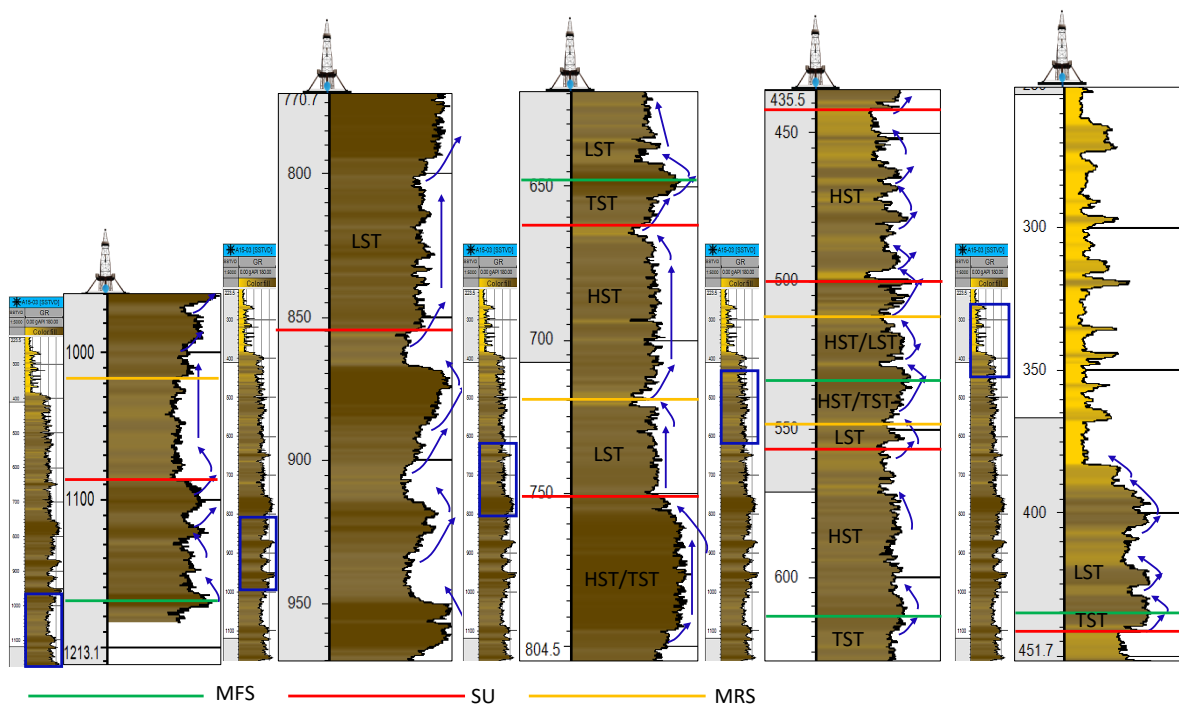
Figure 5.5: Stratigraphic surfaces and system tracts on the gamma ray log of well A15-03.

6

Geological Interpretation

6.1 Well to Seismic Integration

The match between well and seismic data constitutes one of the most important procedures in order to accomplish a geologic interpretation. The integration of the two type of data can provide critical and less uncertain information of the subsurface. In this study well A15-03 was chosen for the tie because it is the most studied well by the literature and therefore the following results can be compared and verified. For that reason seismic line 51 was selected since it transects the examined well. The process has been analyzed in subchapter 4.2 and its results are demonstrated in the following paragraphs.

As it is illustrated in figure 6.1, the tie is in accordance with the one of Kuhlmann et al., (2007) who places the distinct shift in gamma ray response of 750m depth (TVDss) at the toe of the clinoforms. Kuhlmann uses inline 3270 as it is depicted in figure 6.2 which probably is the same or parallel to seismic line 51 of this study. Consequently both studies determined that at depth 750m (TVDss) the gamma ray reading correspond to the base of the prograding clinoforms (red arrow).
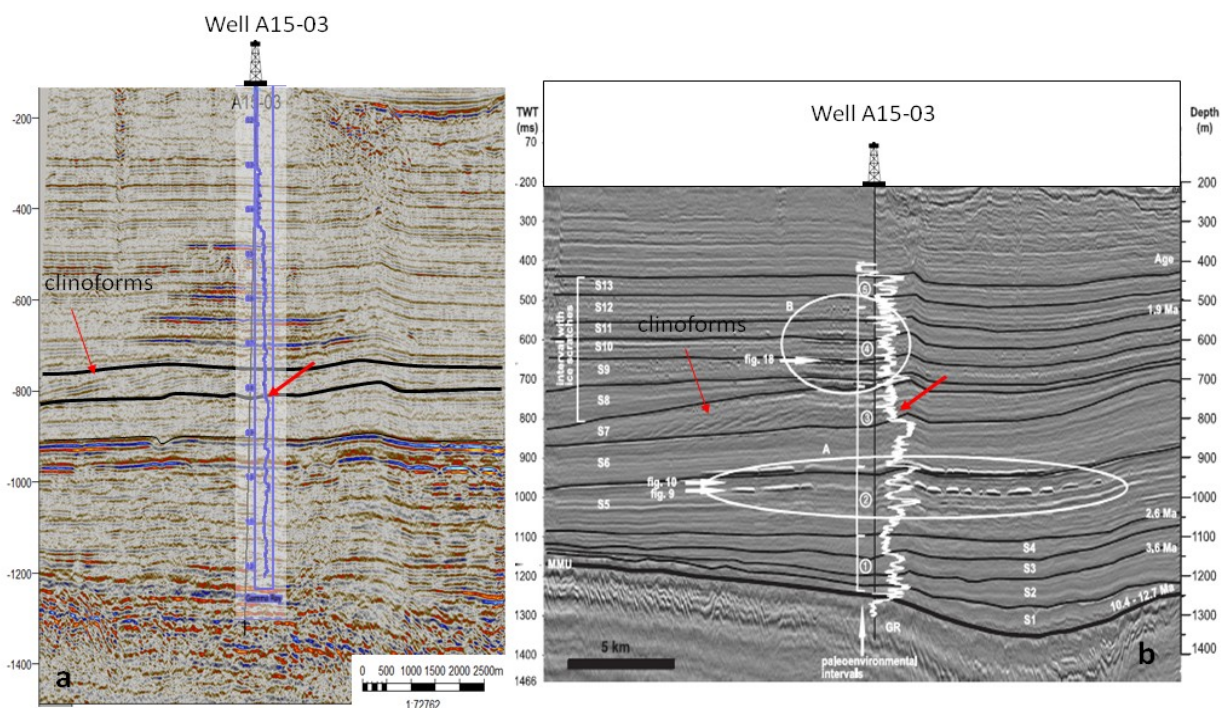
Figure 6.1: Comparison of the well to seismic tie conducted by this study (a) and the one from Kuhlmann et al., (2008) (b). The distinct, sharp change in gamma ray which corresponds to the toe of the prograding clinoforms has been placed in the same position by both studies, verifying the tie resulted from this study

47

Figure 6.2: Geographic location of the seismic line that has been used by Kuhlmann et al., (2008) in order to accomplish a well to seismic tie and the seismic line (51) used by this study.

It is worth mentioning that although the tie took place by using seismic line 51 the study tries to place the well also in the main seismic line ABT-91-03, owing to its direction parallel to progradation. Seismic line 51 is a line of limited coverage and it is almost oblique to t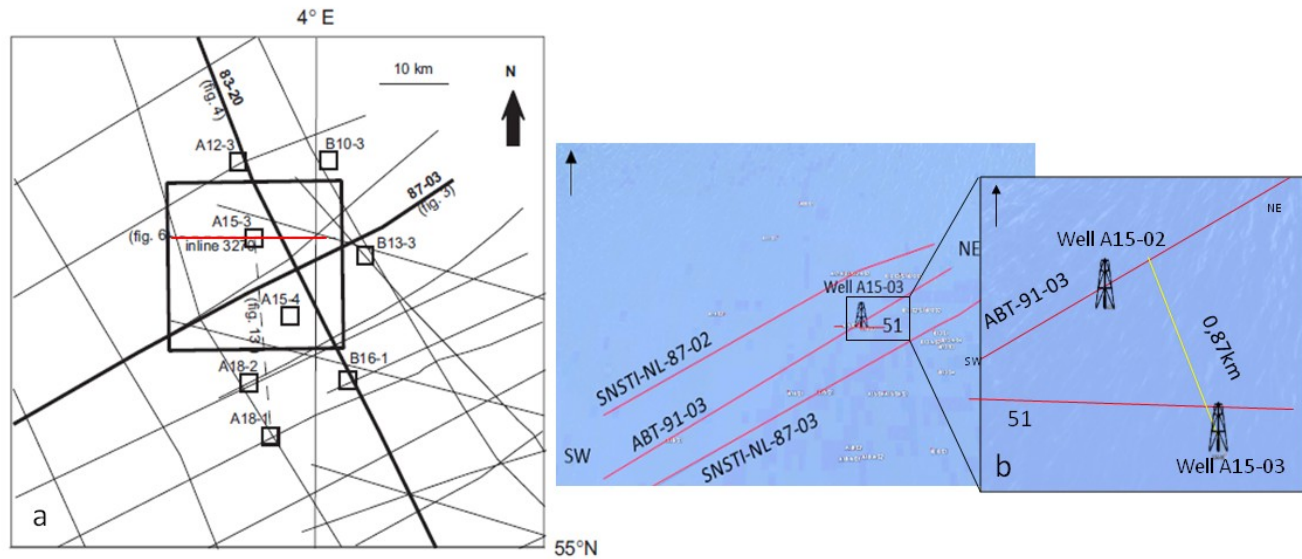he progradation of the delta. Although line ABT-91-03 does not transect the well and thereby increasing the uncertainty of the tie, due to the presence of well A15-02, which is transected by the examined line, the tie becomes possible. Well A15-02 has the exact gamma ray response with well A15-03 and it is located only some meters apart. Namely, the shortest distance between well A15-03 and line ABT-91-03 is 870m. The tie to seismic line ABT-91-03 was established based on the characteristic inclined reflectors, representing clinoforms at 800ms Two Way Travel time. These reflectors are distinct in both seismic lines and they mark the full development of the delta in the area. The transition in gamma ray in this depth is distinct since there is a shift in facies from open marine to shallow marine. Therefore the gamma ray response of this prograding unit was placed in the prograding unit of seismic line ABT-91-03. An additional indication is the characteristic bow trend alternations of the gas bearing turbidites at depth around 900m and 1000m depth which correspond to the significant high amplitude around 900ms and 1000ms TWT.

After having established a well to seismic match the integration of the two type of information is possible to take place. The first integration comprised of the seismic stratigraphic surfaces in TWT and the surfaces identified at the well in depth (TVDss). As it is depicted in Figure 6.3 the seismic surfaces are in accordance with the surfaces from the gamma ray response. The subaerial unconformities identified on seismic as erosional or non-depositional events equate to the abrupt changings of coarsening upwards in the gamma ray response which have also been interpreted as subaerial unconformities. These sharp changes in gamma ray indicates the sudden proximity of completely different facies on top of each other and therefore can be correlated to erosional events and with the shoreline being forced to move basinwards. Similar trend can be seen for the seismic maximum flooding surfaces which correspond to the retrograding units of the gamma ray log and the established MFS in depth. However some retrograding episodes in the gamma ray, where a maximum flooding surface is present, cannot be identified on seismic due to the difference in resolution between the two types of data. Maximum regressive surfaces are also present on gamma ray but not on seismic.

Regarding the system tracts the integration shows some differences compare to the stratigraphic surfaces. On seismic the first, main deltaic sequence (1) consists of two different system tracts. The nature of the first is controversial between lowstand and highstand, whereas the following is a falling system tract (2). On the contrary, the gamma ray interpretation diverges from the aforementioned interpretation. The first seismic system tract is divided into two different in the well data. The bottom one, which shows a coarsening upward funnel shape, corresponds to a LST while the upper one to a HST due to a higher and more consistent trend upwards. Despite the presence of the subaerial unconformity in the gamma ray the falling system tract is not visible. This can be attributed to the fact that the well does not penetrate these deposits or that the seismic line is 800m away from the well. The last reason can also be verified by well A15-02 which is the one transected by this line and it shows a more distinct abrupt change in lithology (for location of well A15-02 see chapter 4.1). The next system tract (4) corresponds to a transgressive tract on seismic and on the gamma ray too as well as the following transition to a lowstand system tract (5) which can also be seen in both type of data. The lower gamma ray values of the previous LST are followed by higher values which start decreasing upwards resulting into a HST. The same system tract has been also identified on seismic (7). The following section shows different systems on both data. On seismic this section (9) has been characterized as LST but the gamma ray trend shows a transgressive event at the beginning of this unit. This transgressive event is not visible on seismic or at least this study could not identify it. The section (10) continues with a LST and HST due to coarsening and then fining upwards. The next section on seismic it is characterized as a Highstand (or possible) Lowstand system tract, an interpretation which is in accordance with the one in the gamma ray response. The last section (13/14) corresponds to the fill of the basin and due to characteristic blocky shapes with a coarsening upward trend it represents probably lowstand deposits. On seismic there is not a specific interpretation, owing to absent in reflection terminations. Overall the seismic and well interpretation does not show significant deviations in terms of sequence stratigraphy. The system tracts that are situate more basinward and are not penetrated by the well were not present. The only important difference is the identification of more transgressive events in the gamma ray than on seismic.
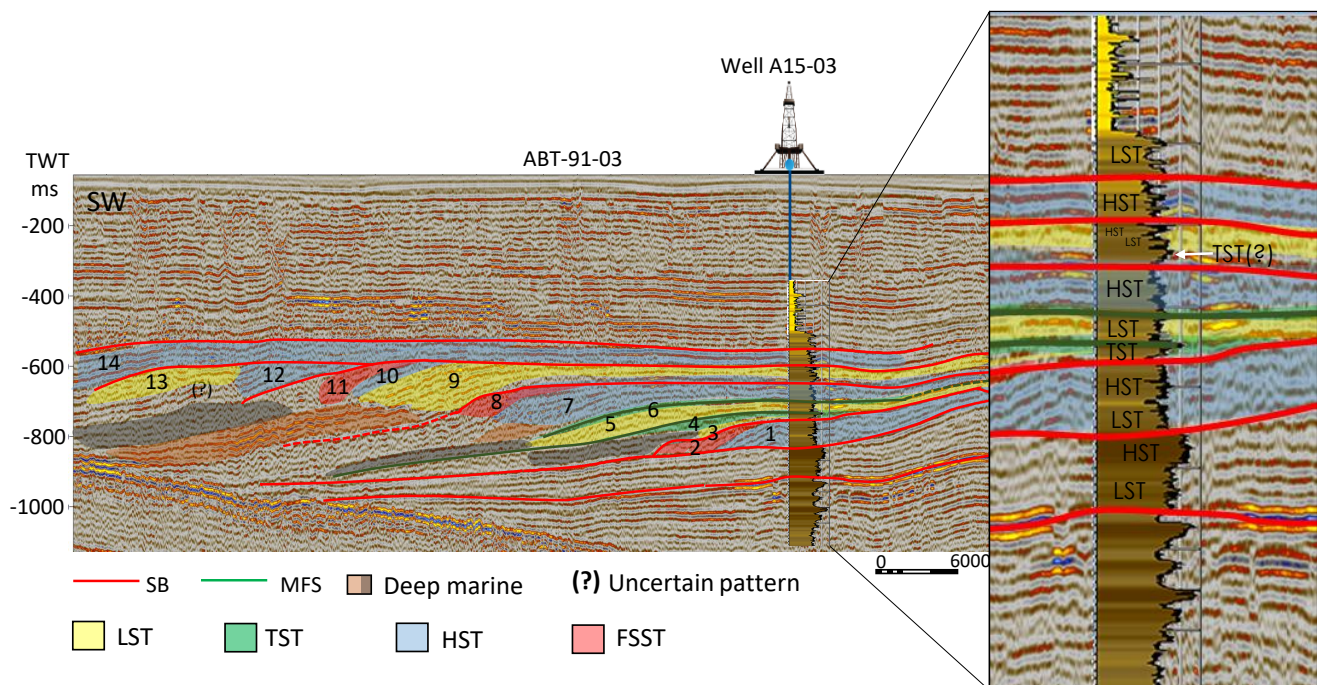

Figure 6.3: Integration of well and seismic sequence stratigraphic interpretation. The seismic stratigraphic surfaces and system tracts show a positive correlation with the equivalent features at the well.

6.2   Depositional Environments

The determination of the depositional environments is a combination of seismic, wireline log and literature. For the literature part core descriptions were used in order to understand the type of lithology and therefore the lithofacies. The following sections describe the integration of the three type of data and tries to link them to a depositional setting. For that purpose different wells were analyzed based on their location in terms of deltaic architecture. For seismic line ABT-91-03 well A16-01 represents the basinal part based on the seismic facies analysis and well A15-03 a part of the prograding-aggrading delta. For seismic line SNSTI-NL-87-03, wells A15-01 and B13-01 represent the prograding-aggrading delta and the more landward part respectively. Figure 6.4 shows the wells and the type of data used for the understanding of the depositional environments. For wells that are not transected by a seismic line the gamma ray trend was used in order to provide additional information regarding the distribution of the environments.
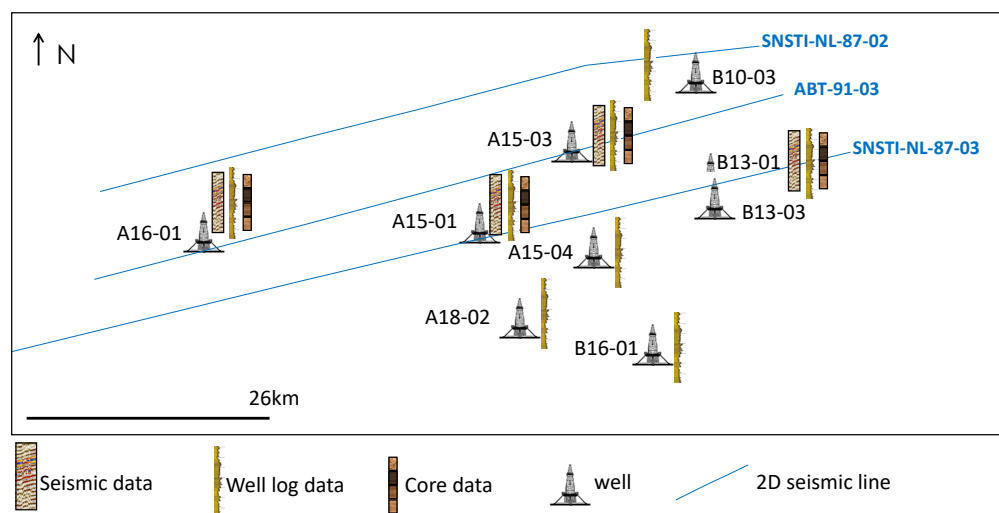

Figure 6.4: Geographic illustration of the wells used for the geological interpretation and the type of data that was analyzed by each.

The following section presents the integration of the three types of data for well A15-03. Core plugs and sidewall samples of the Upper North Sea Group comprise the core data. The description of the samples conducted by Wintershall Noordzee BV. and Panterra Geo-consultant.The determination of the depositional environments was executed for each sequence unit of this study and is presented below (for the rest of the sequence units see Appendix C.3-C.8):

Before the presentation of the main sequence units that correspond to the deltaic environment, the analysis starts with the deeper deposits that based on the seismic facies and the gamma ray readings represent turbidites. The gamma ray of this section (860m to 1000m TVDss) is characterized by troughs and peaks, corresponding to cleaner and dirtier lithologies respectively. Core plugs and sidewall samples have been taken for this interval. Four core plugs at log depths 897.03m, 907.15m, 922.95 and 940.22 have been described as claystones. A core plug at log depth around 951m corresponds to a silty claystone while the sidewall sample at log depth 1097m to a greywacke sandstone. The bow gamma trend with the core data, showing alternations of claystone and some silty sandstones, and the high amplitude seismic reflectors with erosional feature indicate an offshore environment of turbidite deposits. Based on the alternating patterns between claystone and sandstone the nature of the turbidites resembles a proximal turbidite fan with channels and levees, probably located at the Toe-of-slope. This interpretation comes in accordance with the general evolution of the environment since on top of these deposits the deltaic ones had started being deposited in the examined area.
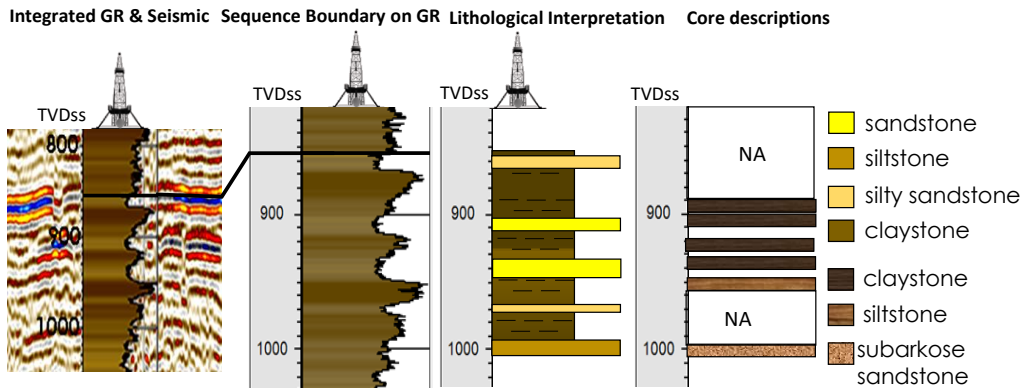
Figure 6.5: Integration of the three types of data, seismic, well and core data. The claystone-sandstone core samples are placed at log depths based on Wintershall sedimentological report.

Sequence Unit 1

The first sequence is ranging from 850m to 750m depth and is comprised of two high gamma ray trends with the shallower one reaching much higher values of around 180 GAPI. The deeper unit shows a peak at around 150 GAPI. For this unit a sidewall sample (SWS 16) has been taken at around 826m log depth and it constitutes a claystone. From this it is concluded that there is no change in lithology since the deeper trend with the lower gamma ray corresponds to claystone. Therefore the shallower trend also is a claystone but with higher content in radioactive minerals. As it is depicted in Figure 6.6 the seismic quality in this depth is quite poor due to fluid presence. The low amplitude semi-continuous reflectors does not show a characteristic pattern in order to enhance interpretation. Also there is only one core sample being taken at this interval. Due to the location of the unit between the proximal turbidites and the forthcoming clinoforms this unit must represent the transition from deeper conditions to shallower.
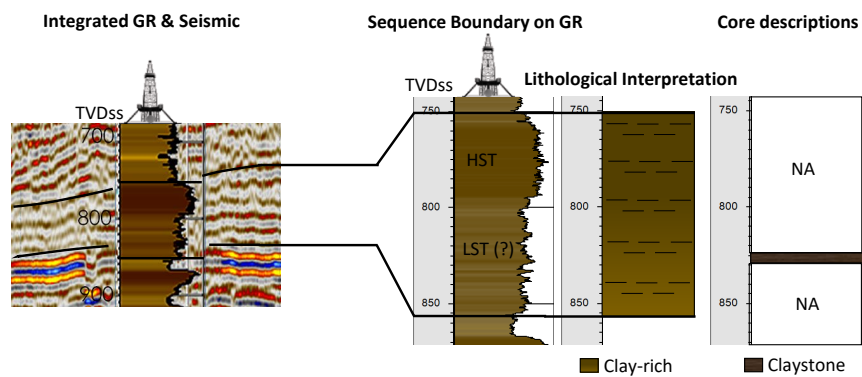

Figure 6.6: Integration of the three types of data. At this interval there is only one claystone core sample at around 820m log depths based on Wintershall sedimentological report.

Similar analysis like the one presented above was not feasible for the rest of the wells that are transected by the other seismic lines (SNSTI-NL-87-03 and SNSTI-NL-87-02), owing to sparse or absent cores and core description. Hence for wells A16-01, A15-01 and B13-01 only the gamma ray is going to be used for lithological interpretation. Each of the wells represents a different part of the delta and therefore their gamma ray response varies significantly. Figure 6.7 presents the deltaic architecture as this is extracted by the three seismic lines. It is worth mentioning that all three lines show substantial similarity in system tracts and seismic facies. Consequently the examined wells from the different lines are projected in a schematic representation of the delta (see figure C.1 Appendix).

The gamma ray readings for each well matches the interpretation of the study. Well A16-01 due to high, constant gamma ray readings without characteristic prograding trends corresponds to the offshore part of the delta. Well A15-01 shows as well a silty-clay character but less dominance compare to well A16-01. Based on seismic the well penetrates offshore, delta front and some delta top facies upwards. Well A15-02 is almost similar to well A15-03 and has been penetrated in similar position as the latter one. In this well the prograding-aggrading gamma ray patterns are more visible, representing mainly delta front and top facies. The last well B13-01 shows completely different response compare to the three other wells. Namely, is substantially more sandy-silty dominated and based on seismic it is known that it is located more landward in the deltaic environment. The gamma ray trend corresponds probably to a fluvial or deltaic plain (see figure C.2, Appendix).

Having analyzed and linked in detail the three types of data, the following geological interpretation is presented in terms of depositional environments.
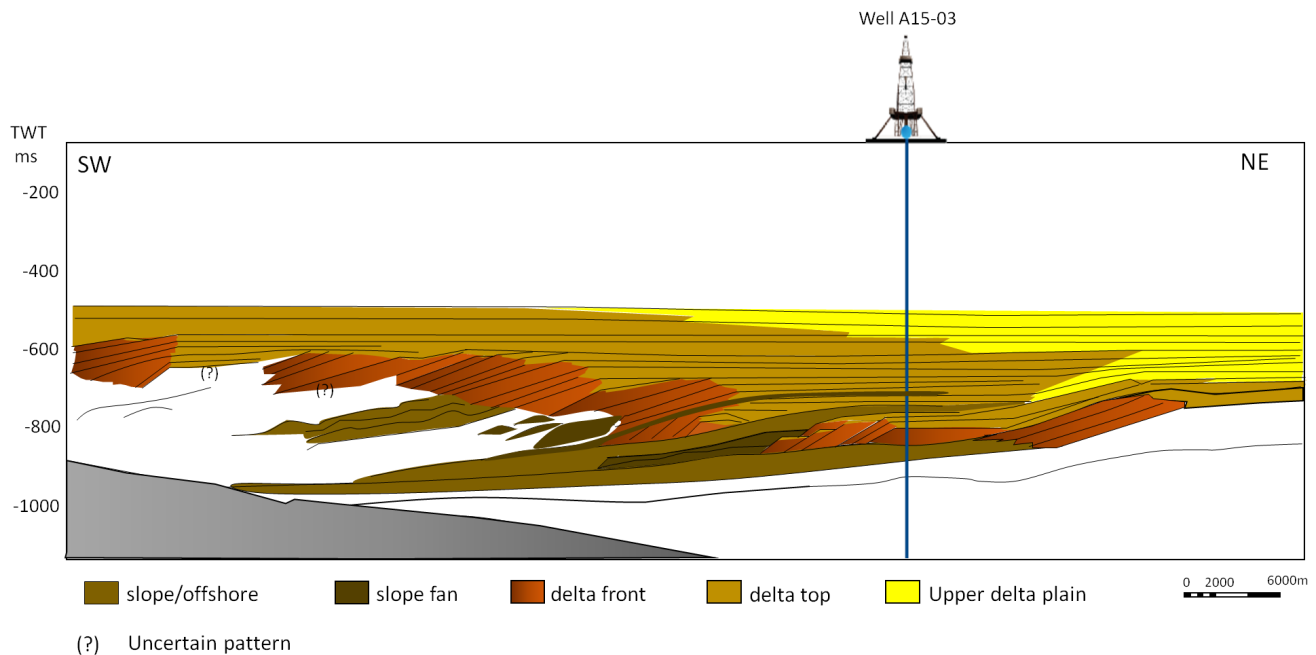

Figure 6.7: Schematic illustration of the resulted deltaic environments in the area of interest.

6.2.1   Shallow Gas Reservoir

The study also tried to link the shallow gas reservoir rocks to the reconstructed sequence stratigraphic framework and the facies distribution. For that reason, the gamma ray of well A15-03 has been used which shows the gas prospects, identified and named by Wintershall Noordzee B.V. As it is illustrated in figure 6.8 there are eight prospect where gas has been found. The gas has been accumulated in the silty-sandy reservoir rocks and it has been sealed by the intercalated claystones. These reservoirs correspond to the lowstand-highstand system tracts based on the gamma ray analysis and the claystones to highstands and transgressive system tracts. The gas has been accumulated within the stacking of parasequence topsets which are characterized by alternations between claystones and silty sandstones. The facies vary between delta front and top (delta plain on top).
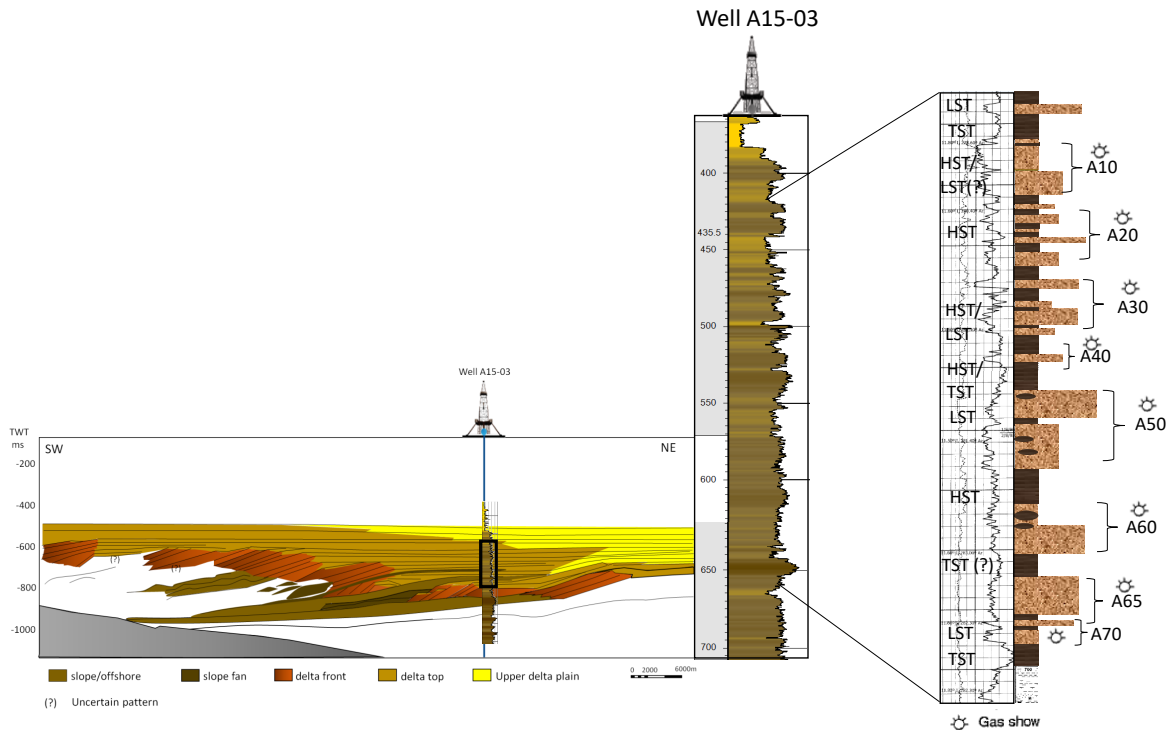
Figure 6.8: Depiction of the eight prospects identified by Wintershall Noordzee B.V. in well A15-03. Their link to the system tracts of this study as well as to the depositional environments is also presented

It is worth mentioning that wells with similar gamma ray trend as the one of well A15-03 have also shown gas accumulations. Figure 6.9 presents these wells in the surrounding area. It must not be a coincidence that wells with this characteristic trend have found gas while others even close to already producing wells (B13-03) are dry. For example well B13-01 which is located only 2.67km away from well B13-03, has been found dry while the latter contains gas. As it is illustrated by the gamma rays the dry wells do not show this intercalation of clay in between but a sand dominant trend. Probably this significant differences in the sand-clay content between the relative close-spaced wells can be attributed to the regional distribution of facies as near the dry well large incised valleys have been identified on the seismic data. Also well A15-01 which is not presented in this figure (see figure 6.4) has been drilled in the foresets of the delta front and therefore is more clay dominated without the sandy intercalation of wells A15-02 or A15-03. The well found gas on deeper parts which do not correspond to this deltaic environment. For the shallow Cenozoic sediments the well has been categorized as dry. This means that probably the reservoir can been found in the highstand-lowstand prograding-aggrading strata of the stacked parasequences topsets of the deltaic front-top environment. However it is worth to be mentioned

Figure 6.9: Map showing the Gamma Ray of wells A18-02, B16-01 and B13-03, which have similar trend and all found shallow gas. Well B13-01 despite being very close to the producing well B13-03 is dry. The gamma ray trend of the well shows the dominance of cleaner lithologies like sandstone probably due to the presence of incised valleys identified in this study.
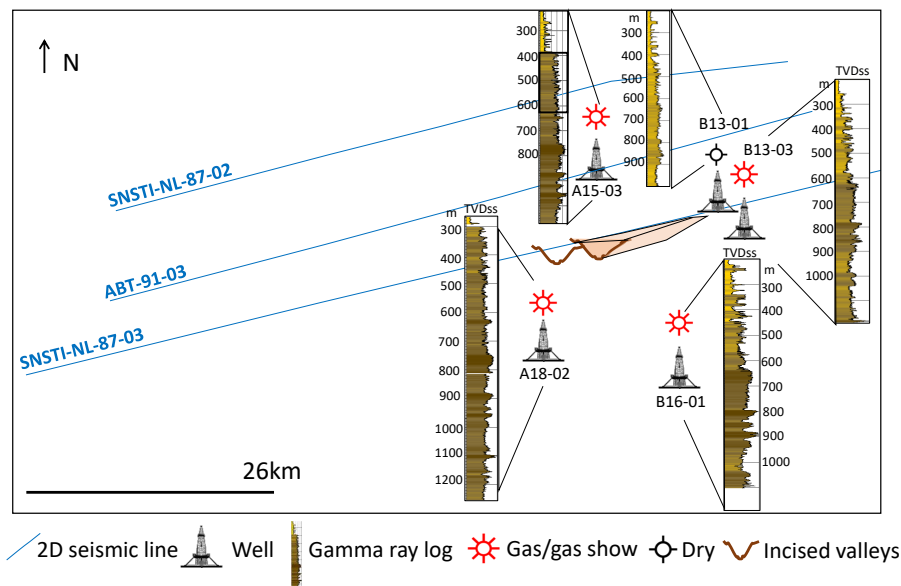
that this is a regional finding using limited and low quality data. For more detailed research high resolution 3D seismic data and a variety of well analysis has to be conducted in a larger area in order for the findings to be less uncertain.

6.3   Chronostratigraphic Chart of Eridanos

After having established the geological facies the chronostratigraphic chart of Eridanos (in the study area) can be analyzed in terms of temporal distribution. The chart provides an insight into the temporal relationship of the genetic packages and the surfaces of non-deposition and condensation. It is worth mentioning that the principal of chronostratigraphic reconstructions lies on the assumption that seismic reflectors follow bedding and these bedding planes are isochronous and thus the seismic reflections approximate time-lines (section 3.1.1; Vail et al., 1977a) (Emery & Myers, 2009). The steps that executed for the construction of the chart are based on Emery et al.,(2009) and are listed below:

- Construction of a schematic representation of seismic line ABT-91-03

- Numbering of the seismic packages in stratigraphic order

- Numbering of their component reflections

- Transferring of the reflectors to a time-scale

- Filling in the chart

For constructing the chronostratigraphic chart, firstly a schematic representation of the deltaic architecture has to be made. In this scheme the bottomsets, foresets and topsets have to be depicted in a more ideal way in order for the construction of the chart to be less complicated but not too simplistic resulting into an unrealistic representation. For that reason the reconstruction took place based on the seismic reflectors and hence the sketch is at the same scale with the seismic image of seismic line ABT-91-03. The main difference is that the topsets in the sketch are flat while in the seismic image show

some topographic elevation more landward. Also to include all the deep marine deposits was not possible since their terminations against the shallow marine strata is not clear. Therefore only some representative open marine reflectors were taken into account. In places where there is uncertainty due to low quality of the data a question mark has been placed for indication (figure 6.10). After the construction of the scheme the numbering of the seismic packages has to take place in a stratigraphic order. This process categorizes the strata into system tracts from the oldest to the youngest, making clear which package deposited before and after the main stratigraphic events of the deltaic area. Having determined the order of the genetic packages the reflections within them can also be numbered. By doing so, the interpreter can easily understand the natural succession of the events within a given time frame. Figure 6.10 shows the three first steps that have been executed by the study in order to categorize the deltaic strata in a stratigraphic order.
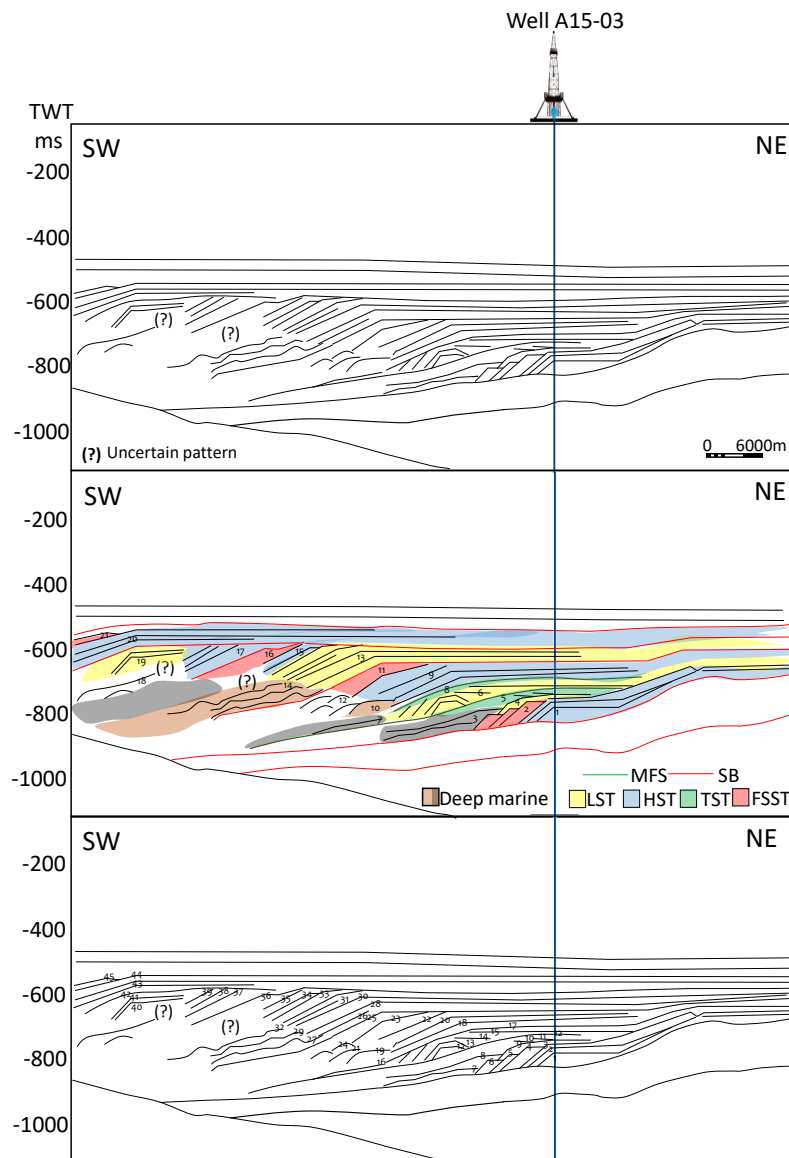
Figure 6.10: Three main steps for reconstruction of chronostratigraphic chart

   The next step of the procedure is to transfer the reflections to a time-scale. To accomplish this the seismic reflectors have to be plotted, in order of age, as horizontal lines on the chronostratigraphic chart in the same lateral position as they appear on the seismic line (Emery & Myers, 2009). The chart has as axis, time in the vertical direction while in the horizontal is the same as the horizontal axis of the seismic section. Figure 6.11 presents the construction of the chronostratigraphic chart with the first image showing the reflectors as horizontal lines and the migration of the offlap break (black dots and dotted line). Due to the presence of well A15-03 which has been tied to seismic line ABT-91-03 the scaling of the chart in absolute time can take place. The ages, obtained from the chronostratigraphic study of Kuhlmann et al., (2006), are the absolute values of 2.13, 1.9 and 1.7Ma. The age of 2.25 is a relative values placed by this study since it is known from Kuhlmann et al., (2006) that the genetic package prior to the first deltaic package is around 2.44Ma. By trying to scale the reflectors in the fixed ages the chart in some parts has to be stretch and in some to be compressed in order to fit these data points derived from the passing well.

Figure 6.11: Depiction of the chronostratigraphic chart based on Emery (2009). The stratigraphic surfaces of subaerial unconformities represent 2D areas in the chart. The main elements comprising the delta in time are stretched based on the three absolute ages of Kuhlmann et al., (2006)

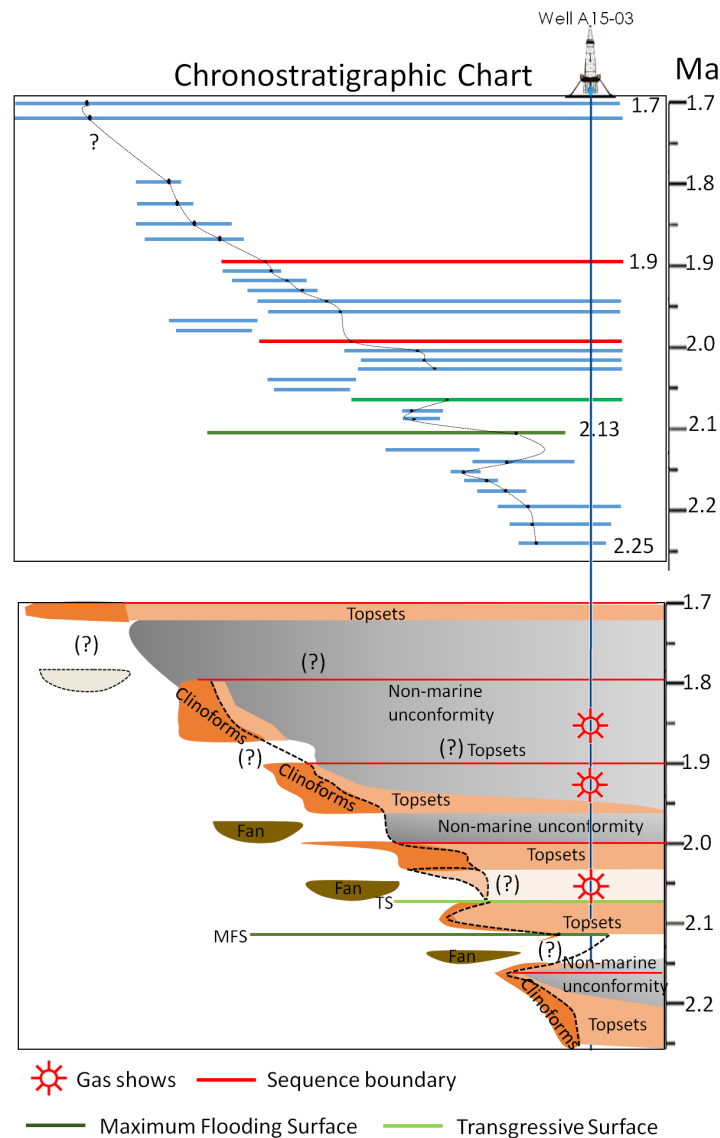Having constructed the chronostratigraphic chart the interpretation of the depicted features has to take place. The parts of the horizontal lines that are at the rightmost position of the offlap break represent the deltaic topsets while those at the left of that point are clinoforms. The horizontal lines without offlap break point are fan deposits. The transgressive surfaces are indicated with green color whereas the non-depositional or erosional surfaces with red. Based on Emery et al., (2009) the subaerial unconformities which represent sequence boundaries are represented as areas in a chronostratigraphic chart with both extent and duration. Figure 6.11 shows these areas with grey color stopping at the offlap break point. However the extent of the areas of non-deposition or erosion is quite uncertain due to the low quality of the seismic data in the youngest parts of the strata. Particularly three main events of non-deposition, bypass or erosion can be identified in the chart, an outcome that fits with the overall interpretation of the study. The last extended event of third subaerial unconformity is not clear how extensive it is. There is a possibility that is overestimated. However, taking into consideration the conditions of deposition during the deterioration of climate (onset of Northern Hemisphere Glaciation) and the presence of icebergs in the area based on Kuhlmann et al., (2007) the dimensions of this surface seem feasible. Also on seismic this part corresponds to apparent toplaps and clinoforms with downlaps without well-developed topsets. It is also worth mentioning that the chart should have been comprised by multiple onlaps of open marine deposits (fans, turbidites) but the quality of the data in the deeper part is very low not allowing understand which reflector is which, where they end and what shape they have. In the chart only the well-developed reflectors have been placed.

6.4   Estimation of Sediment Volumes

For estimating the volumes the study used the three main seismic lines as shown in figure 4.1. Since seismic units constitute different depositional trends it is meaningful not only to calculate the total sediment volume but estimate the sediment volume per seismic unit. This can then be translated to a sediment accumulation rate. To estimate the sediment volume per seismic unit, a polygon outlining the seismic unit has been drawn on a seismic line (parameterization of the concave hull of the seismic unit), corresponding to a cross-sectional area of that particular unit. An example is given in figure 6.12.
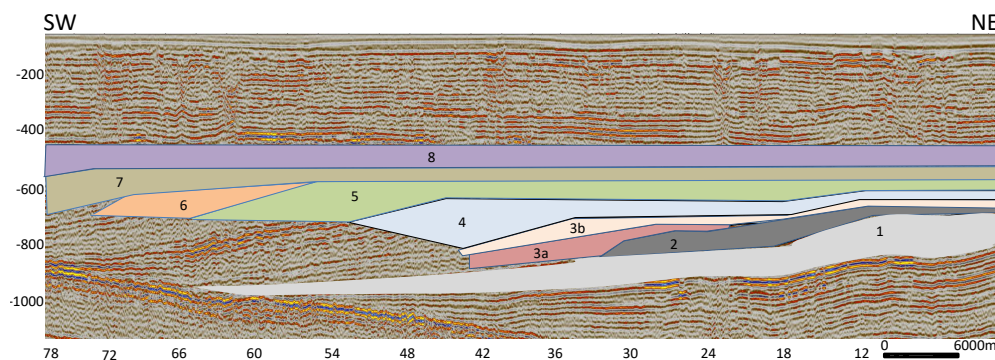
Figure 6.12: Illustration of the geometric shapes that correspond to the seismic units for the surface area calculation.

Points on the polygon are fully described by their x- and y-coordinate in a given reference frame (width and depth with respect to a fixed point/origin). These coordinates have been stored in a text file which then has been imported into MATLAB. In order to obtain the area within the polygon (concave hull), the left- and rightmost coordinates are used to define the boundary between an upper and lower curve in the XY-plane (see figure 6.14 as an example and Appendix C.10). These two curves have been integrated and the result is subtracted to obtain the actual area of the seismic unit (polygon). This has been done for all the seismic units on the three main seismic lines. The resulting areas are shown in figure 6.13.
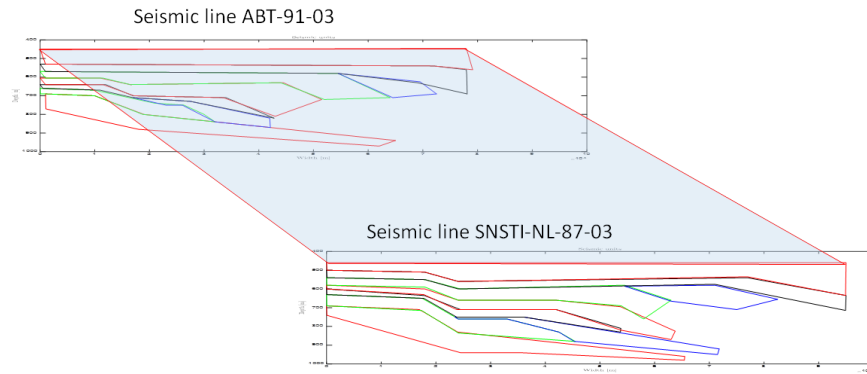
Figure 6.13: Illustration of the polygons that correspond to the seismic units in both seismic lines. (Polygon areas for both lines see Appendix C.9)

The areas have been converted to a volume by multiplying them with an averaged width, since the seismic lines are not entirely parallel. This is of course only possible if the seismic units are continuous and slowly varying in between the seismic lines, since calculating the volume in this way implies a linear change of the seismic areas in between the seismic lines. The obtained seismic volumes are given in table 6.1.

Table 6.1: Total sediment volumes per unit.

Seismic Units	Total Volumes (km^3)
Unit 1	73.2
Unit 2	28.6
Unit 3a	17.9
Unit 3b	19.9
Unit 4	56.7
Unit 5	62.2
Unit 6	12.4
Unit 7	64.9
Unit 8	108.1
Total	444.1
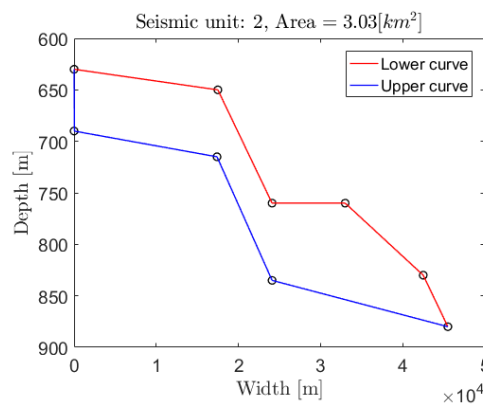
Figure 6.14: Upper and Lower curve of polygon corresponding to seismic unit 2.

In order to translate volumes to accumulation rates, time-constraints from well A15-03 has been used (Kuhlmann et al., 2006). Unfortunately only three absolute ages were determined from the palaeomagnetic study of Kulhmann. It is not sensible to merely linear interpolate these ages at the well location due to the non-linear deposition in a prograding setting (Kuhlmann & Wong, 2008). Therefore, a slightly better estimate for the ages in between the three fixed points is obtained by calculating an averaged thickness in the whole delta area. This averaged thickness has been obtained by dividing the area of that seismic unit (cross-sectional) by the effective width (see figure 6.15). The ages for the seismic units then result by weighting the seism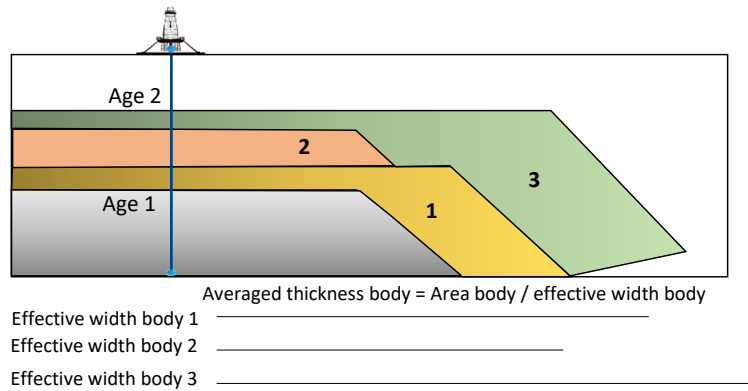ic units according to their averaged thickness, constraint by the three absolute ages. To clarify, a numerical example is given below.

Averaged thickness body = Area body / effective width body

Effective width body 1

Effective width body 2

Effective width body 3

Body	Thickness at well	Weight from well	Interpolated age
1	10	0.21	1.79
2	30	0.63	1.16
3	7.5	0.16	1.00
Total	47.5	1.00	
Body	Averaged thickn.	Weight from aver.	Interpolated age
1	50	0.31	1.69
2	28	0.18	1.51
3	80	0.51	1.00
Total	158	1.00	

$$Age_{1,m} = Age_1 - \sum_i^m w_i \Delta t_{1 \to 2}$$

$$Age_{1,1} = Age_1 - \sum_i^1 w_i \Delta t_{1 \to 2} = 2 - 0.21 \cdot 1 = 1.79$$

$$Age_{1,2} = Age_1 - \sum_i^2 w_i \Delta t_{1 \to 2} = 2 - 0.21 \cdot 1 - 0.63 \cdot 1 = 1.16$$

$$Age_{1,3} = Age_1 - \sum_i^3 w_i \Delta t_{1 \to 2} = 2 - 0.21 \cdot 1 - 0.63 \cdot 1 - 0.16 \cdot 1 = 1 = Age_2$$

Figure 6.15: Example: Absolute Age 1 is 2 Ma and Age 2 is 1 Ma giving an absolute interval age of 1 Ma. There are three units contained within the interval. Interpolating the ages linearly at the well location gives a completely distorted estimate of the ages of the seismic units, since they do not take into account the whole delta area, but merely one point. Another interpolation technique is proposed, which considers the whole depositional area, using the averaged thickness as a weight for the interpolation of the ages. The following tables describe the difference between the two interpolation techniques, which ultimately lead to different sediment accumulation rates. The sediment accumulation rates per seismic unit are calculated using the proposed interpolation technique for the ages of the seismic units based on the averaged thickness.

Sedimentation rates are in km^3/kyr, which is hard to compare to the relative sea level change (generation of accommodation space). Therefore, the sedimentation rate in m/kyr for each seismic unit has been calculated by dividing the averaged thickness by interval time of the particular seismic unit. Sedimentation rates in m/kyr can then be compared to the rate of change in relative sea level to analyze the interplay between accommodation space and sediment supply.
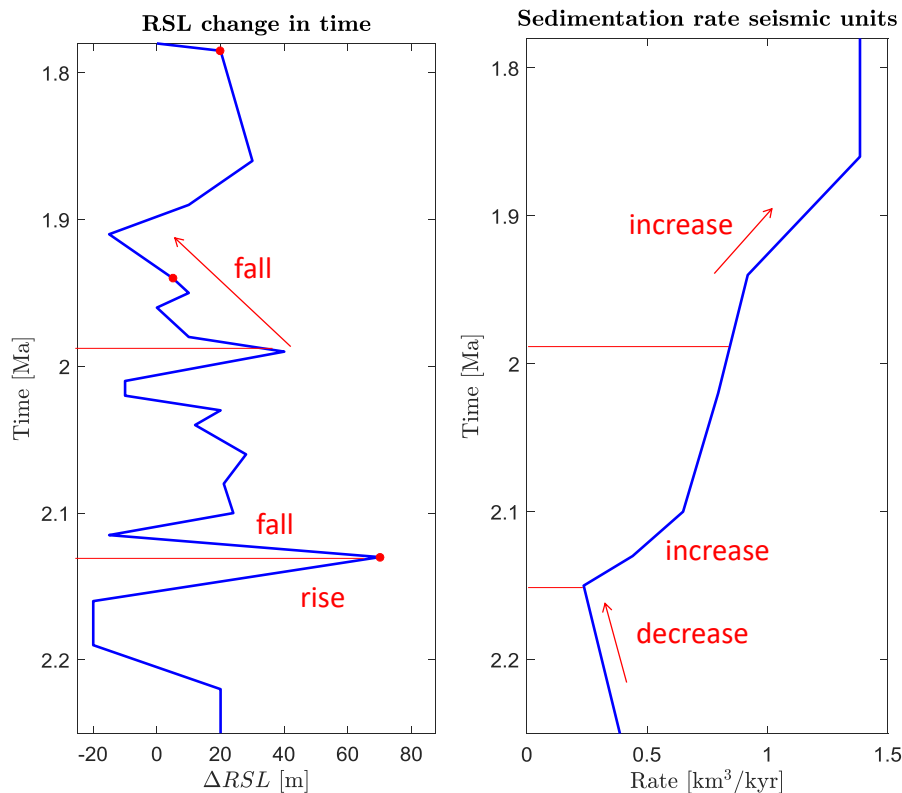
Figure 6.16: Relative sea level and sedimentation rate curves based on the average thickness technique.

Also it is worth mentioning that the curve of relative sea level changes had to be modified based on the same technique for the time between the absolute ages. The offlap breaks used to identify the position of the shoreline were attributed to a seismic unit. The new interpolated ages for the seismic units (based on the averaged thicknesses) were then used as an additional constraint (on top of the three absolute ages) to identify the change of sea level in time. Multiple offlap breaks inside the same seismic units were merely linearly interpolated within this unit. This provides a slightly higher resolution for the change of relative sea level in time. However it causes more uncertainty since the interval ages of the seismic units are not absolutely dated, but interpolated using the averaged thicknesses as weights (as described above). Figure 6.16 shows the two graphs of the updated relative sea-level changes curve and the total sedimentation rates. The two graphs differ in resolution since the one of sedimentation rates has been constructed with fewer data points compare to the relative sea level curve. The latter shows four sea level falls and one of a significant rise (four sea level rise of lower magnitude). These fluctuations are not so well captured by the sedimentation rate curve which only shows one minimum around 2.14Ma. The rest of the graph has an upward trend with some intervals of lower rising rate than other. However the importance of the graph can be spotted at around 2Ma where there is a substantial sea level fall and a continuous increase in sedimentation. As it has already mentioned by the literature this trend is attributed to the enhanced cooling of this period owing to the upcoming glaciation.

Two scenarios of the interplay between accommodation and supply are shown below. The first scenario is without any modifications, while the second scenario has been slightly modified around 2.1-2.0 Ma due to possible underestimation of the sedimentation rates. Namely, the two graphs demonstrate the relative sea level rate with respect to the sedimentation rate. The former represents the accommodation space while the latter the sediment supply. Apart from the two graphs that show the two factors affecting the deltaic setting, the depositional trends are also illustrated below each graph. These events are modeled

based on logical processes that take place between accommodation and sediment supply.

The first scenario shows the two rates plotted in thousands of years with respect to meters per thousand years. The red line corresponds to accommodation rate (sea level changes) while the blue to sediment supply. As it shown in the graph the relative sea level curve is of higher frequency compare to the one of sediment supply since the latter has been obtained by a smaller amount of data points. The former has been estimated based on the vertical migration of offlap break point and therefore the collection of data is easier than the estimation of sedimentation rates for each seismic unit. Expect for this the depositional trends depicted below do not entirely correspond to the interpretation of the deltaic environment that took place based on the methodology, adopted by the study. Although the forced regressive events fit quite well with the interpretation, the transgression events are much more than those of normal regression. This is something that diverges from the seismic interpretation. However in the gamma ray short episodes of transgression have been identified but not so extensive as these presented by the depicted graph. Due to the fact that this scenario does not fit neither the seismic nor the well interpretation has to be modified. The modification will take into account the underestimation of the sediment rates (and possible overestimation of the sea level curve).

The second scenario presented is the modified one where sedimentation rates have been slightly increased in some units where the geometric shape fitted in the units did not include all the surrounding strata. By having higher sedimentation rates and lower sea level change around 2.1Ma the model of depositional trends comes closer to the interpretation of the study, where the transgression events are thinner and the normal regression episodes dominate in the area. By comparing this model to each depositional trend obtained by seismic and well data it resembles quite well. However higher sedimentation rates with lower sea level changes than those depicted would have probably described better the deltaic setting. It is worth mentioning that the forced regressive events fit good with the interplay of the two factors (A and S).
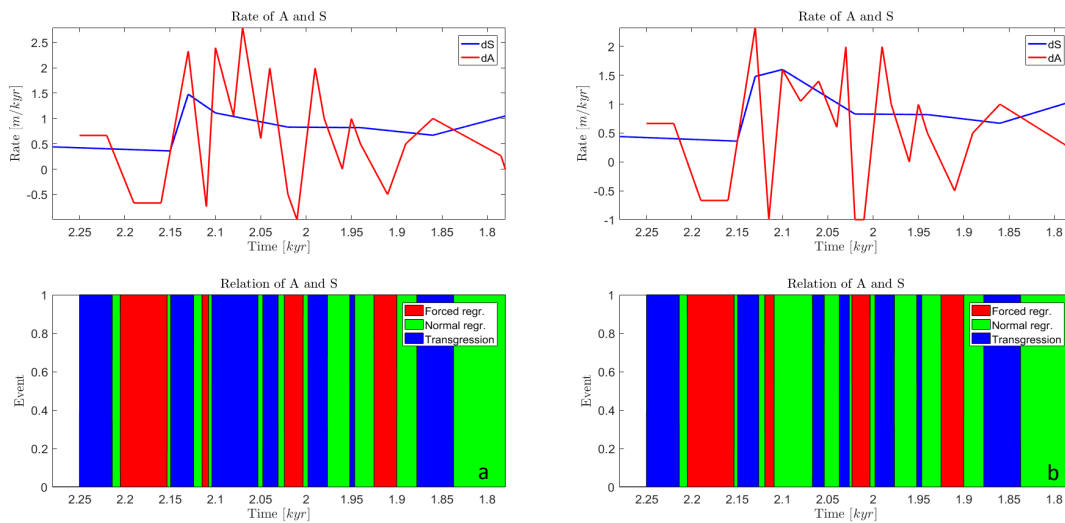
Figure 6.17: Two scenarios obtained from the integration of the relative sea level curve and the sedimentation rates. Graph a shows the sedimentation rates with respect to the relative sea level changes and the corresponding depositional trend. Graph b shows the same but with the difference that the sediment rates have been slightly increased around 2.1Ma and the accommodation space has been slightly decreased, due to underestimations and overestimations respectively.

<div style="text-align: right; font-size: 3em;">7</div>

Discussion

The main goal of the thesis project is to gain a better understanding regarding the shallow gas-bearing deposits of Eridanos deltaic system. By using sequence stratigraphy as a method and Catuneanu's (2009) methodology as a way of data analysis, the findings of the study are presented in the following section where they will be discussed, analyzed and compared with the body of scientific literature. The results of the study can be divided into seismic and geological, with the former containing the sequences and system tracts of the delta while the latter the facies distribution within the examined area. Secondary findings are the reservoir units within the system tracts and their link to the deltaic environments as well as the seismic volumes translated into sedimentation rates based on the absolute ages of Kuhlmann et al.,(2007). The first part of findings provides an understanding in terms of accommodation space and sediment supply within the area of interest since the determination of the system tracts can reflect the interplay between base level fluctuations at the shoreline and sedimentation rates. The reconstruction of sea level changes based on the offlap break in combination with the estimation of seismic volumes and hence sedimentation rates can give an insight into the prevailing conditions at the time of deposition and the temporal relation of the strata. The second part of the findings is related to the geological interpretation and it consists of the distribution of depositional environments as well as the correlation of the reservoir units of well A15-03 to the integrated system tracts (seismic and well). The aforementioned result aims to provide information regarding the spatial relationships of the sediments and the possible link of the reservoir units with specific depositional trends. The validity of the findings will also take place by comparing them with those of the scientific literature and finally discussing their limitations and improvements.

7.1   Sequences and System Tracts

The study identified nine sequence boundaries which correspond to eight depositional sequences. These sequences constitute the seismic units of this study and they belong to the shallower deltaic domain. The identification of sequences within the deeper, open marine sediments was not possible since there is absence of characteristic stratal terminations or internal shapes. The seismic units do not diverge from those of Kuhlmann et al., (2007) and Huuse et al., (2012). The latter mentions that the division of the units corresponds to sequence boundaries while the former does not mention the nature of these units. However due to the resembles with the study of Huuse it is assumed that they also correspond to depositional sequences. It is worth to be mentioned that Kuhlmann et al.,(2007) identified thirteen seismic units and Huuse et al.,(2012) fourteen since they both included the open marine sediments at the toe of progradation. Figure 7.1 shows the comparison of the units with the two studies, in seismic line 87-03 as it is the line used by literature. The black lines represent the seismic units of this study, the red of Kuhlmann (2007) and the yellow of Huuse (2012).In parts where the interpretation had an overlay the black lines were kept while where there was divergence between the units these are indicated with the difference in colors based on the study. As it can be observed, the overall view shows many similarities between this study and the others meaning that the adopted methodology and criteria of sequence recognition can provide similar results as those of the literature. The discrepancies are spotted at the first seismic units. This could be
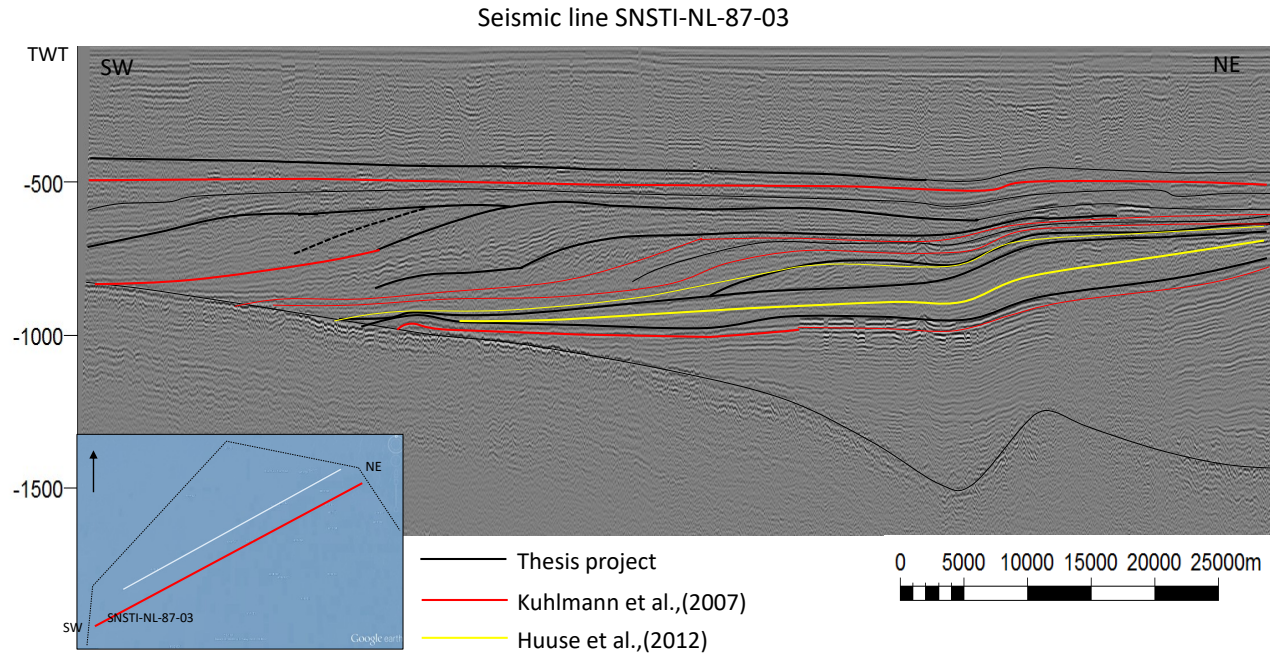
Figure 7.1: Comparison of the resulted seismic units with those identified from Kuhlmann et al., (2008) and Huuse et al., (2012).

due to different observations and/or interpretations. One of the differences is that this study does not identify the correlative conformity in the first units since the reflectors seem to stop and not continue to the open marine setting. On the contrary the two studies extend these lines until the boundary which is the Mid Miocene Unconformity. The first seismic unit for this study and Huuse's at al., (2012) starts above the last gas bearing turbidites where the high amplitude reflector can be seen. However, Kuhlmann (2007) places the boundary between the high amplitude reflectors(around 1000ms). The placement of the sequence boundary in this study was determined based on the presence of downlapping terminations since internally, the turbidites do not show a characteristic configuration. Moving upwards Huuse (2012) places one sequence boundary which subdivides the first seismic unit into two. Huuse (2012) observed onlapping reflectors and the clinoform break point in more distal position than the previous one. With these observations they place an internal sequence boundary which does not constitute a separate seismic unit but a subdivision. These observations cannot be seen in this study probably due to different data or processing.

Another difference can be seen in the first prograding clinoforms where this project places a sequence boundary at the end of the prograding clinoforms due to marine onlap onto the prograding front and offlap terminations indicative of forced regression. Huuse (2012) places the boundary as this study but with its correlative conformity in the open marine setting. On the contrary Kuhlmann (2007) places the sequence boundary in a different position, by grouping the prograding strata and the following retrograding. Moving to the center of the delta front, the forth sequence boundary of this study is of a different nature compare to the others since it is a transgressive surface which has been elevated to the standards of a sequence boundary owing to erosion of the overlying strata (Catuneanu, 2006). Kuhlmann (2007) places the sequence boundary further in the delta, where the chaotic reflectors seem to downlap. Nevertheless this study interpreted these reflectors as part of a highstand system tract owing to apparent toplaps, without separating them from the chaotic reflectors. The following sequence boundaries are matching the interpretation of the literature except for an extra sequence boundary from Kuhlmann (2007) between

seismic unit eight of this study.

Having established the sequence boundaries, the study identified smaller genetic packages within the sequences, the system tracts. This finding is very important since it provides information regarding the interplay between accommodation and sediment supply. All four system tracts are present in the delta but not in an ideal succession owing to erosion or extreme conditions due to the Northern Hemisphere Glaciation. From the integration of seismic and well data the study found that the overall depositional trend is dominated by normal regressive episodes at the shoreline and a succession of prograding-aggrading patterns which resulted into alternating highstand and lowstand system tracts. In between some forced regressive episodes were identified by the chaotic internal configuration of the reflectors, leading to a falling system tract and degradation. The transgressive system tract has only been identified at the onset of the delta progradation in the examined area, either due to data resolution, erosion or absence. Although some retrograding events can be spotted in the gamma ray, still they are very few compare to the strong prograding-aggrading character of the delta. The repetitive successions of normal regressions indicate high sediment input which consistently outpaces the rates of base level rise. Namely, normal regressions occur during early and late stages of base-level rise when sedimentation rates outpace the low rates of base-level rise at the shoreline (Catuneanu et al, 2006). The seismic facies analysis also described an oblique shape of prograding foresets implying little or no accommodation on the shelf during progradation. Nevertheless at the beginning of the delta progradation in the study area, the clinoforms are characterized as sigmoid, meaning positive accommodation which also led to two transgressive events and therefore deposition of clay in the delta front.

Unfortunately there is no scientific study with detailed analysis of the system tracts in the examined area. However some the aforementioned deltaic characteristics were observed and recored by the literature. Particularly, the research of Overeem et al., (2001), whose study area is parallel but further south than in this study also identified a dominant aggrading-prograding pattern in the overall deltaic area. They mention in the deltaic architecture that extensive areas are associated with aggradational units while some are showing a downlap configuration and therefore representing progradation. Kuhlmann et al., (2001) and Huuse (2012) mention as well that the delta was characterized by huge prograding wedges which fill in the southern basin. Regarding the deltaic architecture, Overeem et al., (2001) identified similar distinct packages of oblique clinoforms mentioning that this type of architecture is indicative of high rates of sediment supply and relatively low rate of accommodation (suggesting a fairly stable sea level and limited subsidence). Apart from this, Overeem (2001) and Huuse (2012) describe these chaotic configurations which have been spotted in all three seismic lines of this study. The former interprets them as slump deposits which are related to sea level fall while the latter as forced regressive sediments during cold, restrict marine conditions and a fall in relative sea level.

It is worth mentioning that the research of Benvenuti et al., (2012), whose study area is located more southern-east (blocks G,M and parts of F), presents the regional sequence stratigraphy and mentions that "the reflector geometries analyzed on their seismic sections and time slices show lobate prograding clinoforms with vertical thicknesses decreasing with time. This suggest that sediment supply has been high for the entire studied succession and that there was a progressive lack of accommodation creation (A'/S' less or equal than 0). This is in agreement with Sørensen et al. (1997) who suggested a progressive sea-level fall during composite sequences VI and VII (in their work) which are located in the present study area" of Benvenuti et al., (2012).

7.2   Conditions of Deposition

The study tried to generate its own sedimentation rates for each seismic unit. The technique that is used to estimate the rates is different from the one that has been used by the literature. First of all the study estimated volumes of the identified seismic units and thus the result diverges from the literature since the area of which these units are spread is more limited compare to Kuhmlann et al.,(2007). Kuhlmann for her research used the volumes from Overeem et al., (2001). These volumes are within an extensive deltaic area since the study of the latter took place in the overall dutch offshore sector. Overeem used their surface areas in order to estimate the sediment volumes. Kuhlmann (2007) uses these volumes by corresponding them to their own seismic units. However Kuhlmann's seismic units have been identified in the northern part of the dutch offshore sector, using seismic line SNSTI-NL-87-03, whereas Overeem uses a southern seismic line, SNSTI-NL-87-06. Consequently, the correspondence of Overeem's seismic volumes to Kuhlmann's probably have an uncertainty regarding the matching of a sediment rate to a specific time interval or age. For this study has to be clarified that the surface area is much smaller and therefore the rates probably have a more regional character. Secondly, the study used the three fixed, absolute ages of well A15-03, estimated from Kuhlmaan et al., (2007). It is worth mentioning that this research uses another technique to interpolate the time in between these fixed points. It is known that the time of deposition cannot be linearly interpolated in a non-linear sedimentary setting of prograding strata. This technique uses the average thickness of each seismic unit in order to distribute the time between the absolute points. By doing this the study takes into account the entire sediment volumes of the seismic units within the study area and not only the thickness from the well which may is not representative of the seismic units as their thickness increases towards the basin. The well it is drilled in parts of the deltaic topsets where the strata is thinner and flatter than the prograding wedges. Kuhlmann (2007) mentions that for obtaining their sedimentation rates they had to divide each volume by the duration of a seismic unit. "The duration of a unit was inferred from the gradient of the line between the age points. We are aware that the duration per unit is assumed to be linear between the age points, but the closer the points, the better a linear line approximates the 'true' duration" (Kuhlmann & Wong, 2008).

Figure 7.2 shows the cumulative sedimentation rates obtained from the three main seismic lines. It is hard to compare the sedimentation rates of this study with those of the literature not only because the rates of this study have been calculated within a smaller surface area but also the seismic units between the three studies are different. However the study tried to correspond its own seismic units to the one of the literature and identified some similar trends.
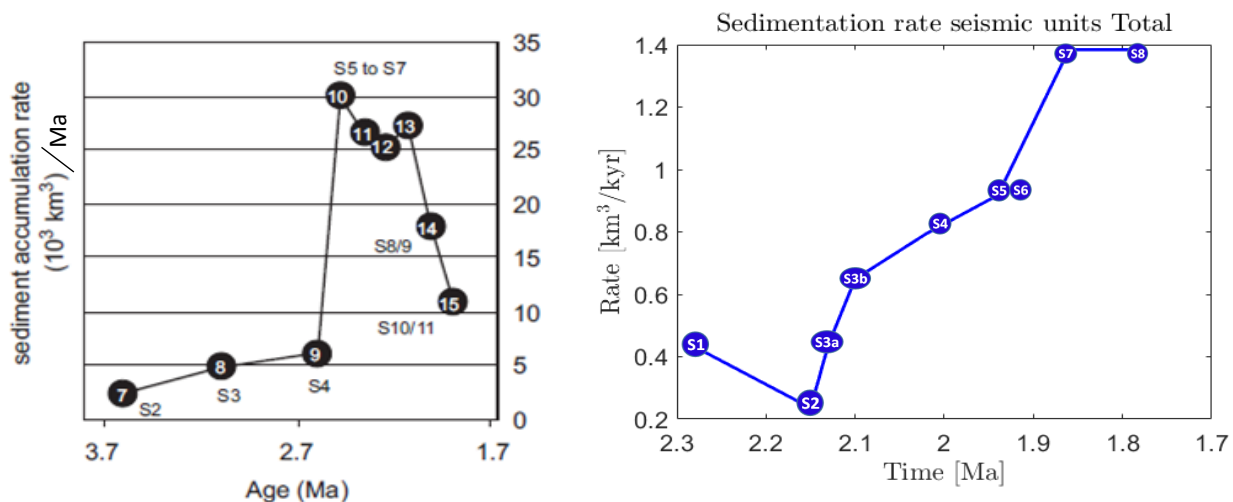

Figure 7.2: Comparison between the sedimentation rates obtained by this study (b) and those resulted by the literature (a).

The graph at the right corresponds to the sedimentation rates of this study while the left one to Kuhlmann et al., (2007). The graphs also present the seismic units for the corresponding rate of the the three different studies. The blue dots represent the seismic units of this project and the black the ones from Overeem et al., (2001). In both graphs the non-circled seismic units correspond to Kuhlmann's. Seismic units 7, 8, 9 of Overeem and S2, S3 S4 and S5 of Kuhlmann comprise the open marine sediments and are have not been taken into consideration in the following section. As it is depicted in the graphs, the one generated by literature shows three characteristic trends. Sedimentation rates during deposition of S5 until S7 reach a peak around $30 \ 10^3 km^3$. After this the rates decrease slightly to $25 10^3 km^3$. The trend increases again but not at the same rate as before and the subsequent dropping during deposition of seismic units 8/9 and 10/11 is substantially sharp with rates of seismic units 10 and 11 hitting the bottom at around $10 10^3 km^3$.

Regarding the graph of this study, it shows an overall upward trend over time, something that diverges from the literature. Unfortunately it is not possible to correlate the seismic units of this study with those of Kuhlmann's since, as it already has been mentioned, the rates for this study have been estimated for a smaller surface area (and only for the shallow marine where the reflectors were visible). However the general trend of the two graphs can be compared. As can be seen from the figure the two graphs present an opposite trend, with the one of this study showing increased rates over time. This matches with the aforementioned descriptions of the scientific literature (section 7.1) which mentions that the sediment supply must have been significantly high due to the onset of Northern Hemisphere Glaciation (Overeem et al., 2001), (Benvenuti et al., 2012), (Sørensen, Gregersen, Breiner, & Michelsen, 1997). However Kuhlmann et al., (2007) mentions that from their eighth seismic unit and onwards the sedimentation rate decreases as "the existing glaciers remained more stationary due to enhanced cooling and had consequently shorter seasonal melting periods". The result of this study do not show such a trend probably due to different methods for the estimation of sediment supply. This contradictory probably results from the different approach used by this study regarding the time interpolation and the estimation of volumes for each unit. However it is worth to be emphasized that this study estimated the sediment volumes based on the seismic surface area of each unit from the seismic data. Also for the distribution of time within the fixed absolute ages it used the average thickness of each unit for better interpolation. On the contrary Kuhlmann uses the seismic volumes obtained from Overeem, whose surface area was larger than that of Kuhlmann's. Therefore the correspondence of Overeem's seismic volumes to their seismic unit can also be of high uncertainty.

Finally, the reconstructed relative sea level curve is compared with the global sea level curve produced by Dr. James Hansen at Columbia University's Earth Institute, based on proxy datasets for the last 5 million years. The depicted interval spans from Late Pliocene to Pleistocene. Due to difference in frequency, the finer global sea level curve has to be cut and stretched in order to be magnified and be able to be compared with the curve produced in this study. Figure 7.3 shows the two graphs, with a being the curve constructed in this study and b from Dr. James Hansen (the curve has been modified by this study in order to be more clear because of the stretching). As it is illustrated in the figure the trends of sea level rise and fall seem to be in an accordance with the overall image. Starting from the age of 2.2Ma both graphs show a downward trend which later increases, reaching a peak before the age of 2.1Ma. However after the 2.1Ma the global sea level curve shows a fall and a subsequent rise whereas the graph of this study shows a sea level rise of medium magnitude which afterwards decreases before the 2Ma. From the 2Ma the curves again seem to have similar response with a rise after 2Ma and a subsequent fall around 1.9Ma. Both graphs show an upward trend after the 1.9Ma which later shifts to a downward trend of lower magnitude.

To sum up, the overall trend between the two graphs seems to be in an accordance, meaning that the offlap break interpretation at the shoreline can provide a less uncertain insight into the depositional trends.
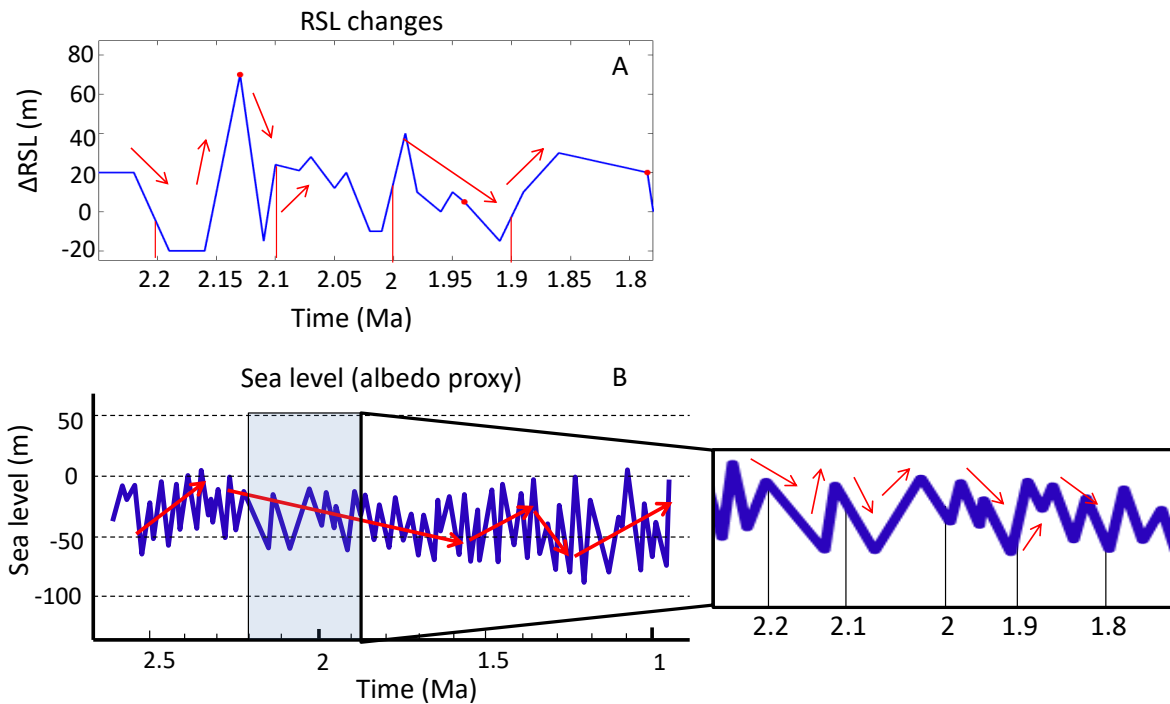
Figure 7.3: Comparison between the global sea level curve (B) and the relative sea level curve reconstructed in this study (A).

7.3   Study limitations and Delimitations

The study for reconstructing the Eridanos deltaic framework used 2D seismic lines which constitute a significant constraint during the implementation of the adopted methodology. The poor quality in all three main seismic lines, either due to gas escapement or low resolution, hampered the observation and thus the interpretation. Namely, the reduced quality affects the termination of the reflectors which comprises one of the most important and fundamental observations. The impact of this can in turn affect the interpretation and result into more uncertain findings. Many reflectors have been pull down owing to Pleistocene tunnel valleys while other seem to be missing or being disturbed. Especially in the last sections of the seismic images the geometry of the reflectors cannot easily be observed and therefore in these parts extra attention has been paid. Also another important feature that is highly dependent on the seismic quality is the offlap break point. The study tried to take the points only where a clinoform-topset package was clearly present. Determination of points that were not clear took place based on the overall interpretation of the area.

Another limitation of the study has been identified in the estimation of the sediment volumes based on the seismic units. For estimating the volumes the study assumed that the shapes (surface areas) of the seismic units between the three seismic lines does not change spatially. Also it uses the average thickness of each seismic unit in order to interpolate the time between the fixed absolute ages of well A15-03. In that way the time is not entirely linearly interpolated by is weighted based on the thickness of each seismic unit. Finally by using the average thickness the study tried to include a representative volume of a whole unit and not only a regional thickness that can be obtained from the well. Consequently the method has both drawbacks and positive aspects.

By having 2D seismic lines of higher quality the study could have resulted into a more accurate interpretation regarding the depositional sequences and system tracts as well as a relative sea level curve of higher frequency. It is believed from this study that the sea level fluctuations must have been much

more significant than the ones observed in this project. The changes in sea level must have played an important role in the deltaic setting but unfortunately the data was "too coarse" or "low" to capture these changes. Finally the core data that wanted to be used for the surrounding wells was absent probably due to absence of samples or no core descriptions in the nlog website. The core descriptions wanted to be used in order to link rocks and reservoir rocks with the gamma ray of some particular wells which have very similar trend and all have shown gas accumulations.

8

Conclusions & Recommendations

The following section presents the conclusions of this thesis project, emphasizing the most important findings and suggesting future objectives.

8.1 Final Remarks

- Nine depositional sequences have been interpreted on conventional regional 2D-seismic profiles and wireline logs of the northern Dutch offshore sector and have subsequently been divided into system tracts. All four system tracts are present but not in an ideal order since some must have not been preserved or they are absent.

- Eridanos delta throughout its main progradation in the study area experienced five forced regressive events and two transgressive. Nevertheless the gamma ray analysis identified three more transgressive events which are not visible on seismic either due to resolution or lack of preservation. Normal regression dominated the delta shoreline meaning low rate of generated accommodation and high sediment supply. These depositional trends are in accordance with the stacking patterns on logs, which show a characteristic aggrading-prograding stacking and the corresponding system tracts which have been interpreted as highstands and lowstands.

- Three main sub-depositional environments were identified in the Eridanos setting by integrating the seismic facies derived from the 2D seismic lines and the gamma ray shapes that are indicative of a depositional environment. The interpretation was tried to be enhanced by using core descriptions but the core samples along the well were not sufficient enough to reconstruct the entire lithostratigraphy of the well, nonetheless they provide some information regarding the lithology in some depths. The sub-environments comprised of offshore marine, delta front and delta top. In detail the offshore sector consists of turbidites (submarine lobes) that correspond to alternations of claystone and sandstone as derived from the core description. The delta front is characterized by pro-delta facies and the delta front itself which based on the core samples it contains intercalation of silt and sand. Finally, the delta top (lower and upper delta plain) is characterized by silty and muddy lithologies which become more sandy upwards.

- Identification of incised valleys on seismic line 23 which is perpendicular to the delta progradation enhances the interpretation of the extensive sea level falls during forced regression episodes. Owing to the high width to height ratio of the valleys (around 2.5), their nature is quite confusing. They are not deep and wide enough to constitute tunnel valleys but also they are quite large for incised valleys. However, due to the deterioration of the climate and the extended cooling of the Northern Hemisphere Glaciation these features must correspond to incised valleys but affected by the long-lasting sea level fall during glaciation.

- Shallow gas accumulations occur between 400m to 640m depth (TVDss) in well A15-03. These accumulations correspond to a vertical stack of silty sandstones which comprise the reservoir rock while the intercalated claystones play the role of the seal. The alternations of silty sands and muds are related to the vertical stacking of parasequence topsets in the delta top. Regarding the sequence stratigraphic framework they have been identified in alternations of highstand and lowstand system tracts during the aggradation-progradation of the delta.

- Sediment volumes were estimated and subsequently translated to sedimentation rates based on a technique that is proposed by this study. The geometric shape of the seismic units identified on the 2D seismic lines was used in order to calculate the surface area of each unit. The shape of the units it was considered constant between the seismic since the deltaic architecture must have stayed the same within such a short distance. By using the average thickness of each unit the study interpolated the time between the fixed absolute ages from Kulhmann et al., (2006). Therefore sedimentation rates were calculated for each unit. The total sedimentation rate shows an increase of sediments over time.

- Changes in relative sea level, constructed by the migration of the offlap break point on the seismic lines, are consistent with the interpretation of the study which shows four to five sea level falls, one main and extensive transgressive event at the beginning of the deltaic progradation in the area of interest and sea level rises of medium magnitude. These observations fit with the rate of sediment supply. High sediment supply coincides with sea level falls and forced regressive events whereas medium to high rates of supply corresponding to an increase in accommodation match with the normal regressive events.

8.2   Future Objectives

This thesis project tried to provide information regarding the shallow gas bearing deposits of the Eridanos deltaic system. A sequence stratigraphic framework of the examined area was established and the interplay between sediment supply and accommodation space has been researched in order to understand the regional conditions of deposition. The study can constitute a basic literature for future objectives as those listed below:

- High resolution 3D seismic data in the area of well A15-03 can provide detail information regarding these gas bearing parasequence topsets of the delta top. The reservoir rocks located in the topsets can be analyzed in terms of reservoir heterogeneity.

- The identified system tracts of this study can constitute a prediction tool for identification of reservoir rocks in another adjacent area were shallow gas has been found.

- Modeling of the deltaic environment based on the obtained facies can result into a reservoir modeling.

8.3   Recommendations

- For future studies it is recommended a dataset of higher quality.

- The adopted methodology from Catuneanu et al., (2009) has been proved highly effective since it takes into account the quality of the available data and it can be adjusted based on characteristics of each depositional environment. Also it helps to distinguish observations from interpretation in order to have a less biased result.

- Estimation of sediment volumes using seismic units resulting from 2D seismic lines led to low frequency sedimentation rates and thus 3D seismic data could probably provide more accurate estimations.

- The average thickness technique for interpolating the time between the three known absolute ages was an effective approach avoiding the assumption of equal time distribution within these ages. In a non-linear sedimentary environment like the deltas the sediment rates can vary significantly from one unit to another.

Appendices

A

Appendix

Appendix A contains two maps that correspond to the chapter of Geological setting. The first map shows the two Basins of North Sea (NNS, SNS) with the structural elements of the Viking Graben and Central Graben as well as the direction of the Delta progradation till it reached the Dutch sector.
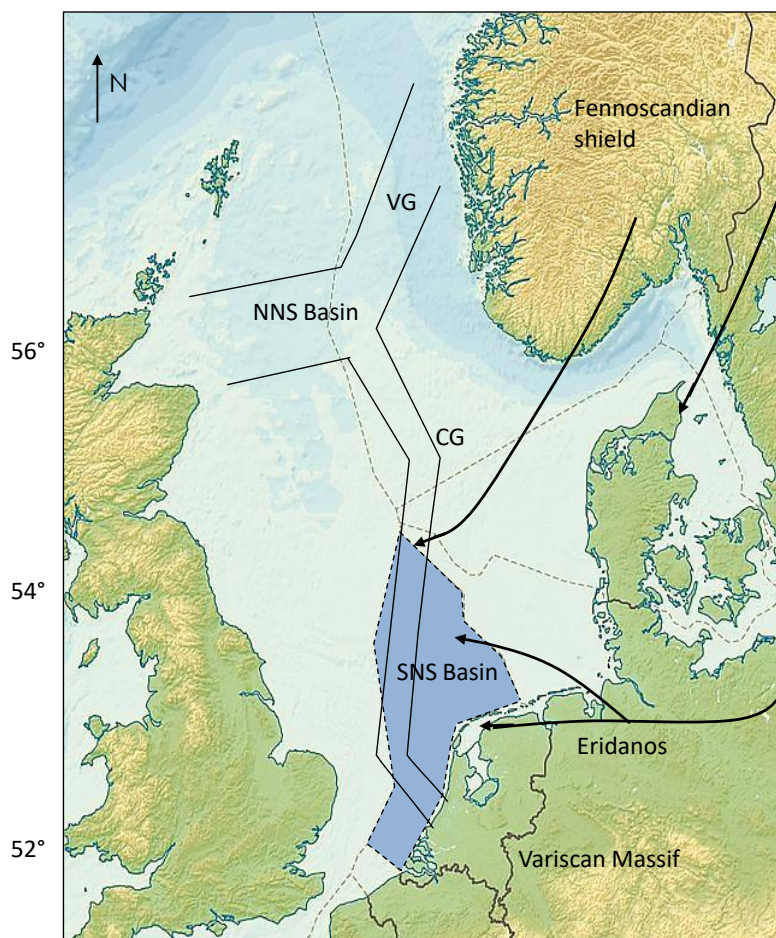
Figure A.1: Schematic map showing the basic North Sea tectonic elements and the Eridanos progradation.

The second map shows Late Cenozoic tectonic elements and the distribution of the three stages of Glaciation that affected North Sea. The three phases of glaciation took place after the ceased of Eridanos delta due to the spread of the prevailing glaciers.
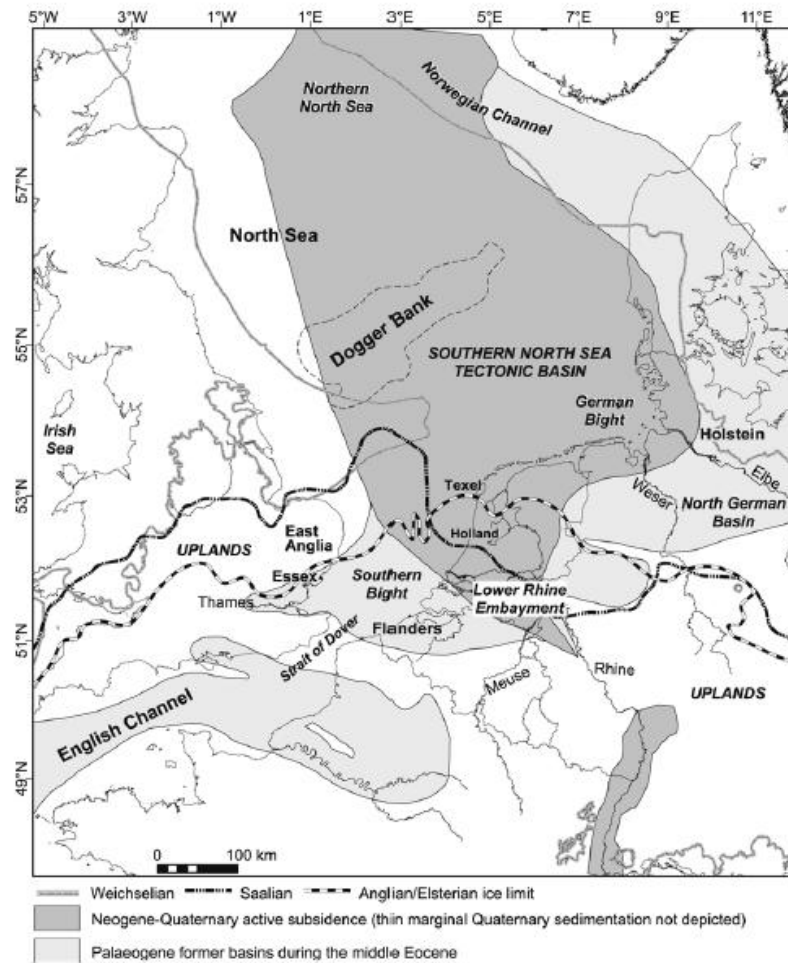
Figure A.2: Quaternary tectonic and glaciation setting of North Sea area.
(Hijma, Cohen, Roebroeks, Westerhoff, & Busschers, 2012)

B

Appendix

Appendix B contains the part that corresponds to the data analysis, showing the seismic analysis that took place in the other two seismic lines which were parallel to the delta progradation.
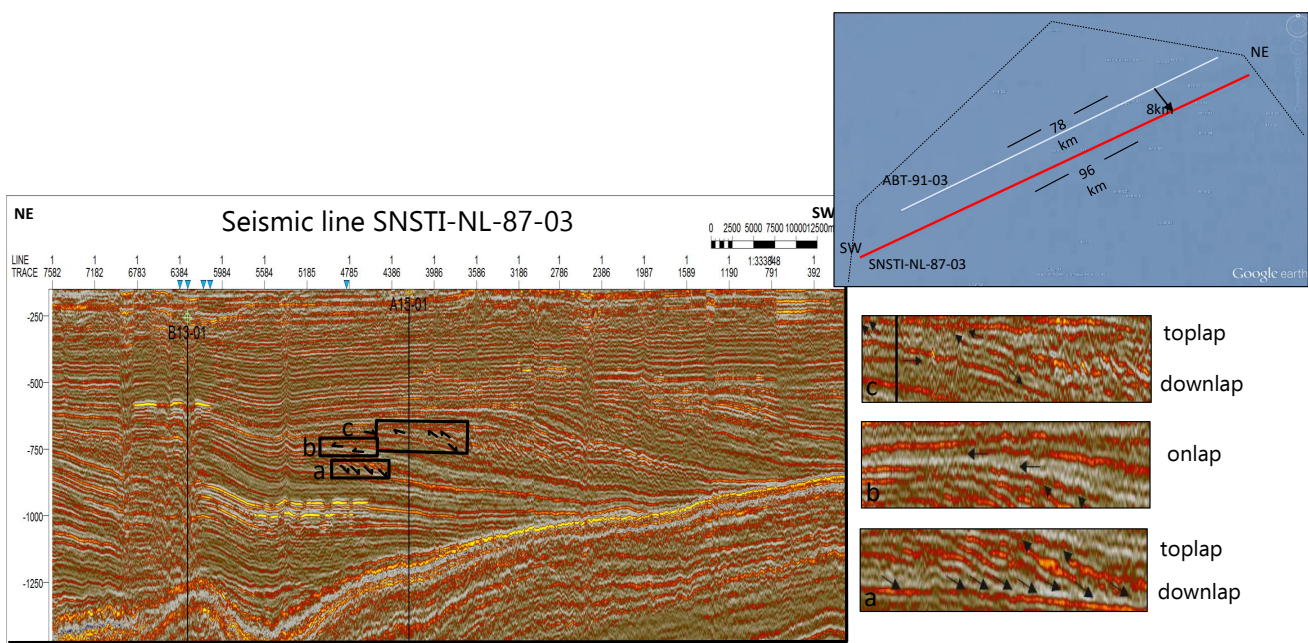
Figure B.1: Identification of stratal terminations on seismic line SNSTI-NL-87-03

Analysis of stratal terminations in seismic line SNSTI-NL-87-02. The geometries of the seismic reflectors are similar those of the other two seismic lines.
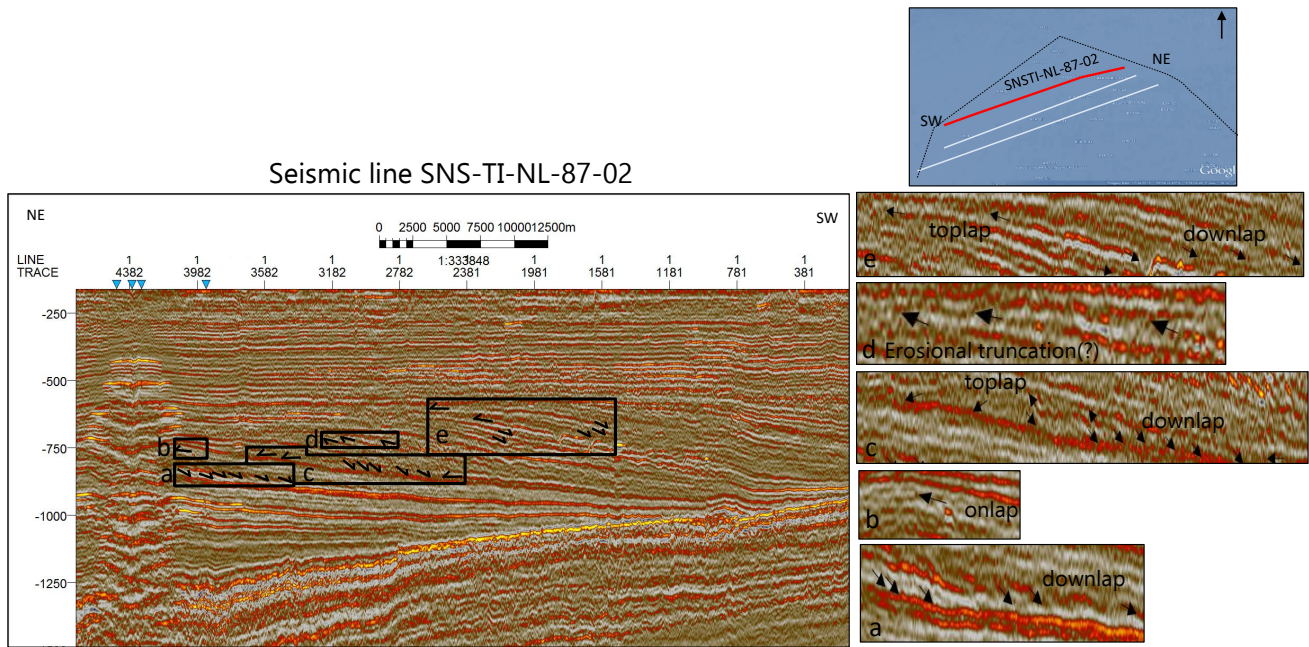

Figure B.2: Identification of stratal terminations on seismic line SNSTI-NL-87-02

Identification of incised valleys in seismic line 23 which transects seismic line ABT-91-03 where the stratigraphic interpretation has taken place.
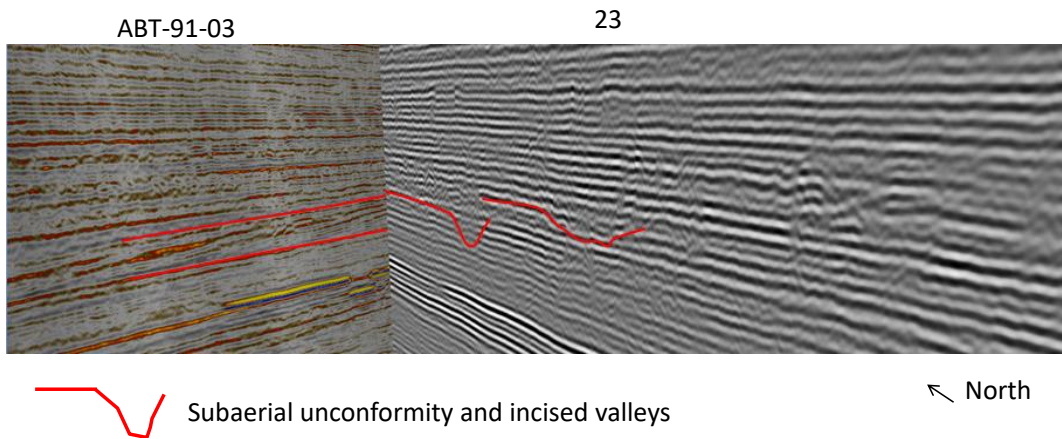

Figure B.3: Link of the incised valleys with the stratigraphic surfaces. Line 23 transects seismic line ABT-91-03.

Map showing the location where the incised valleys where identified in seismic line 23.
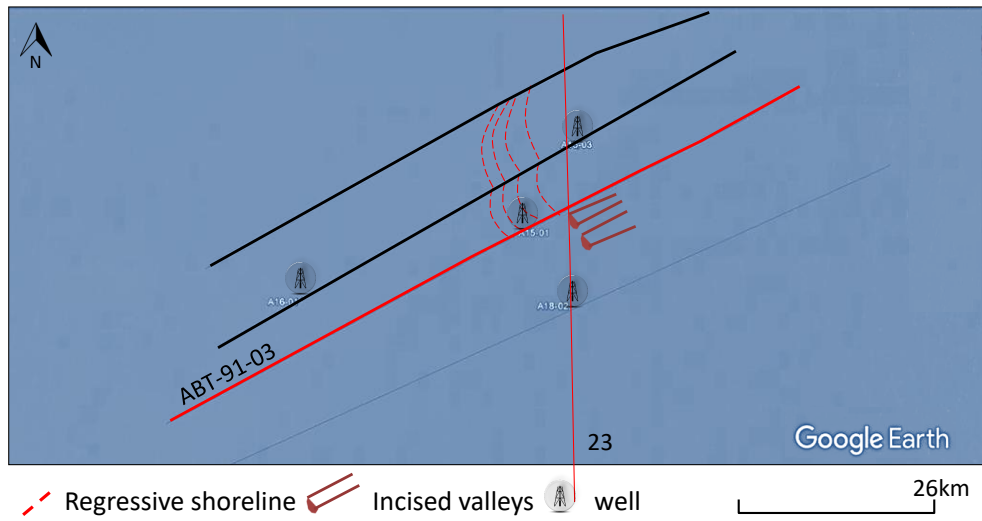

Figure B.4: Map showing the geographic location of the possible incised valleys and their formation with respect to the forced regressive clinoforms which are time equivalent.
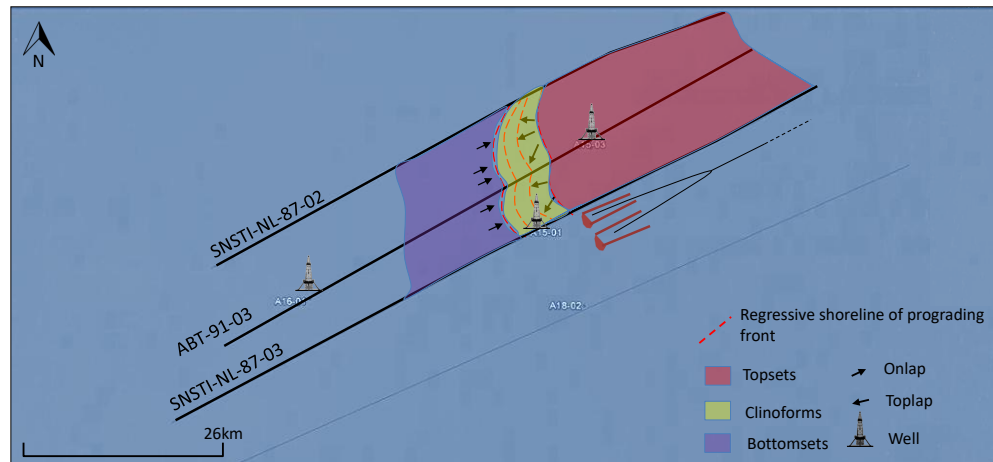

Figure B.5: Seismic facies map showing the time of the regressive shoreline migration and the prograding clinoforms. Also the stratal terminations are indicating with black arrows.

C

Appendix

The third part of the Appendix corresponds to Chapter 6 of the Geological Interpretation. The following map shows the wells that were analyzed in terms of the gamma ray response. These wells were selected because are transected by the examined seismic lines and therefore a more integrated image of the subsurface can be formed.
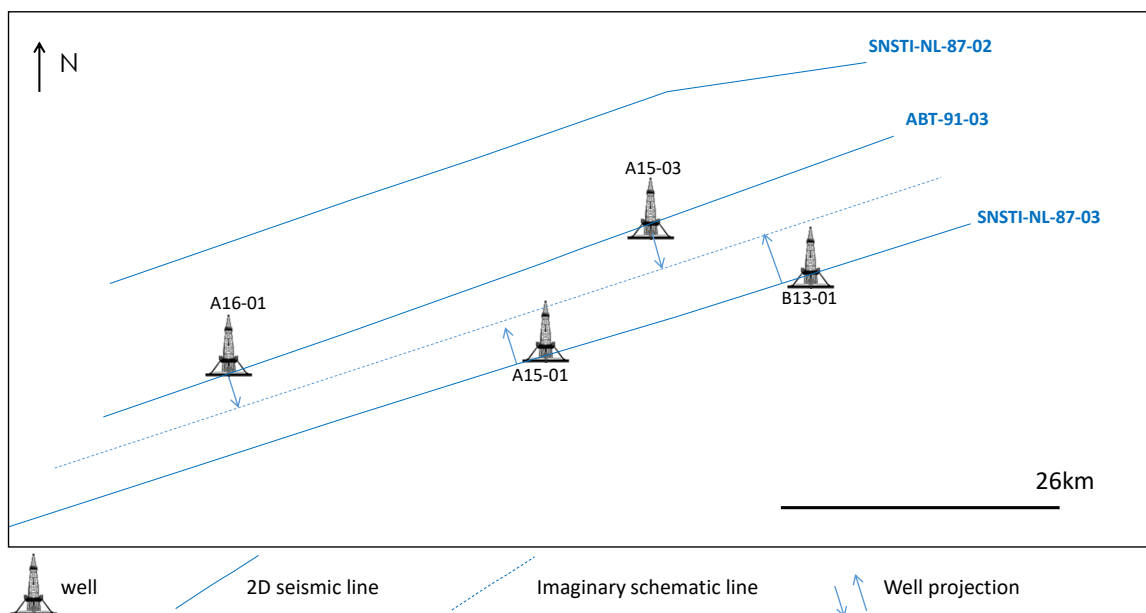

Figure C.1: Map showing the projection of wells from other parts of the delta into an imaginary line since all the three seismic lines are similar.
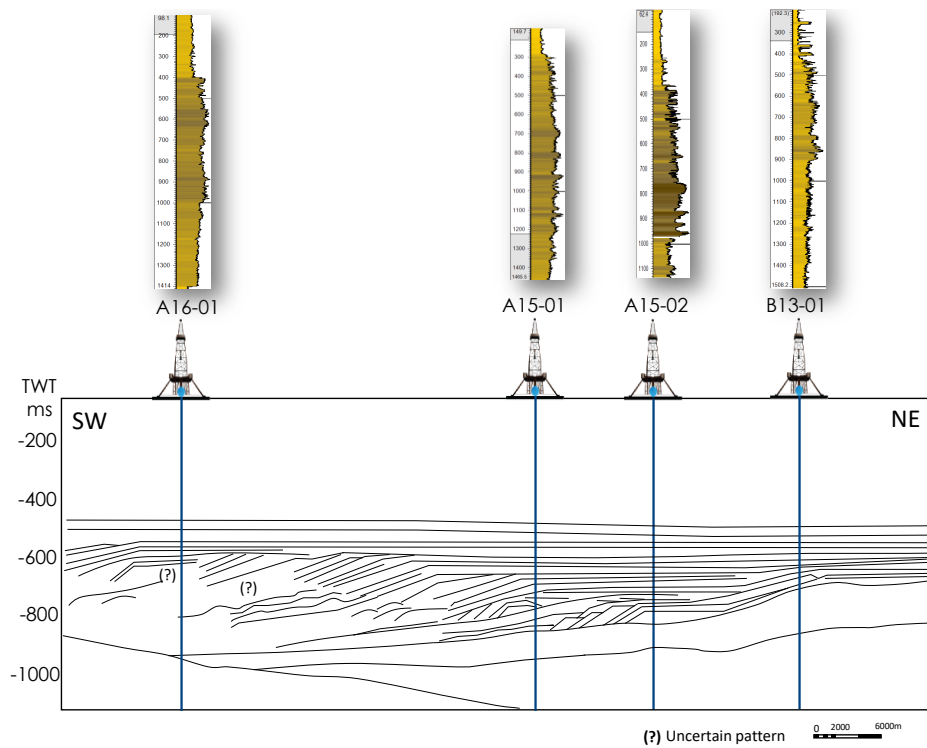
Figure C.2: Schematic illustration of the deltaic architecture and the depiction of other wells in different parts of the delta. The gamma ray response of each well corresponds to the interpreted depositional environments.

Sequence Unit 2

The second sequence unit ranges from 750m to 665m depth and it consists of two different gamma ray trends with the deeper showing gradually lower values and therefore a coarsening upward trend. The shallower trend shows a more irregular constant pattern with small lower values in between. The unit contains a sidewall sample (SWS 21) which has been characterized as subarkose sandstone. Generally as it is shown in figure C.3 the lithology starts to become slightly coarser with intercalation of a more sandy lithology. By combining this information and the seismic image it is visible that this unit corresponds to the prograding-aggrading clinoform-topset package of the Lowstand-Highstand system tracts. However the presence of one core sample (subarkose sandstone) at this interval cannot verify the coarsening and shallowing upward trend. The combination of the seismic image showing the prograding clinoforms with the presence of a clay-rich lithology with subarkose sandstone intercalation indicates a pro-deltaic environment.
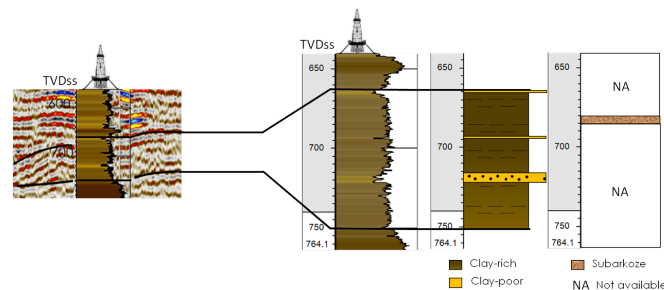

Figure C.3: Illustration of the integrated data set. There is only one core sample of a subarkozic sandstone at log depths around 680m.

Sequence Unit 3

The third sequence is different that the others since on seismic is not visible this abrupt change in gamma ray around 625m depth. The seismic sequence unit is one while the gamma ray can be divided to subsequences 3a and 3b with the dotted line comprising a candidate sequence boundary. On seismic this part is unclear due to low quality or erosion of strata. The gamma ray in terms of lithology consists of alternations between coarser and finer units which probably correspond to a silty sandstone and claystone respectively. Nevertheless the absent of core in this part does not allow the use of a rock characterization and thus the lithofacies interpretation will be based the two other type of data. By combining the seismic and well data it is concluded that there is a transgressive clay rich lithology followed by a prograding clay-free one.
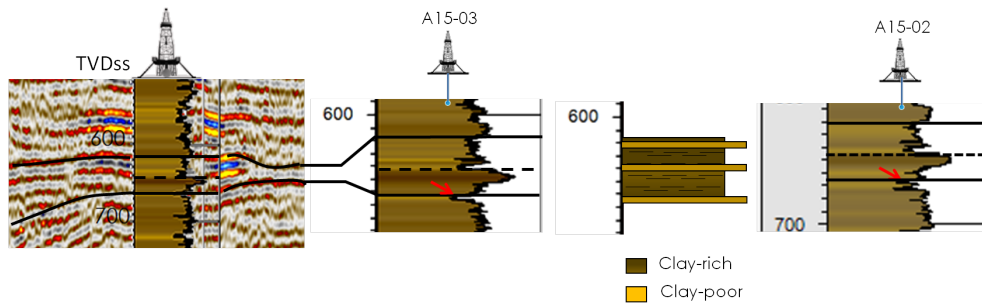

Figure C.4: Illustration of the two type of data and comparison to the well A15-02 which is transected by seismic line ABT-91-03. There is no available core at this depth.

Sequence Unit 4

The forth sequence unit, ranging from 640 to 555m depth shows a consecutive pattern of coarsening and fining upward trends. The higher values can reach a maximum of 144 GAPI while the minimum of around 72 GAPI. This difference in response must be lithology driven with "cleaner" ones between "dirtier". The core samples for this units were taken at log depths between 628m and 572m. The deeper samples at 628.46m and 616.28m log depth correspond to claystone and siltstone respectively. From depths around 592.32m the lithology starts to become coarser with the presence of feldspar sandstone. Claystone has also been recorder around this depth. At 592.65m and 591.35m depth the lithology shifts to siltstone with intercalation of claystone at depths around 572m. These short and consecutive alternations of siltstones, sandstones and claystone, as well as the progradation of the delta westwards based on the seismic image results into a delta front environment with silty and sandy lithologies. Due to the presence of slump deposits further west on seismic it becomes known that the well does not penetrate slope-related deposits. Figure C.5 shows the increase in silt and sand compare to the previous units which were more clay dominated. However by the spiky and coarsening-upward gamma ray trend with the presence of sand not being so dominant, the environment comes closer to shoreface-delta front than delta tops which are more sandy due to the river channels.

Sequence Unit 5

The fifth sequence unfortunately does not contain a core sample and therefore the lithology cannot be linked. Nevertheless, the abrupt change in gamma ray indicating clay-free lithologies has increased compare to the previous section and the trend becomes more blocky and coarser. Knowing from seismic that the delta had been prograding even more westwards and that the gamma ray trend shows these characteristics the environment can be described as delta front with transition to delta tops.
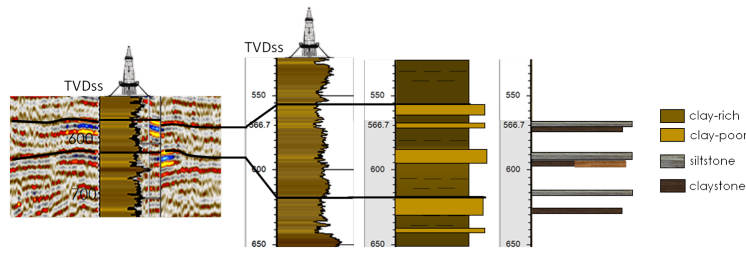
Figure C.5: The illustrated interval contains the majority of the core samples and shows the variety in lithology from claystones to siltstones and silty sandstones.
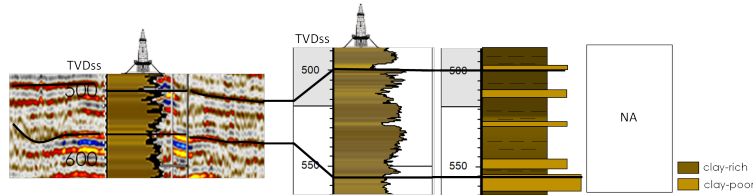

Figure C.6: The interval shows the integration of the two type of data since there are no core samples available at this depth. Alternations of poor and rich-clay lithologies are depicted in the gamma ray log.

Sequence Unit 6

This unit is characterized by a significant coarsening upward gamma ray trend which also shows a blocky shape. This type of response shows the influence of a distributary channelized environment on the delta top. It is also known from seismic that the delta continued prograding to the west. The core sample has been taken at 485m depth and corresponds to a subarkosic sandstone.
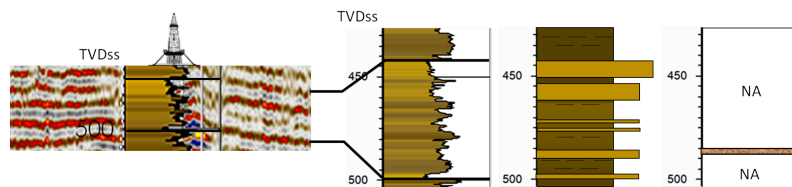

Figure C.7: The interval shows the integration of the two type of data since there are no core samples available at this depth. Alternations of poor and rich-clay lithologies are depicted in the gamma ray log.

Sequence Unit 7

The last sequence is characterized by large blocky gamma ray trends of a coarse lithology which are characteristic of a distributary channel fill environment. The seismic shows similar image as the previous unit. Based on the two types of data the influence by a fluvial environment is visible. On top of the unit characteristic large blocky patterns of a sandy lithology represent the fluvial plain.
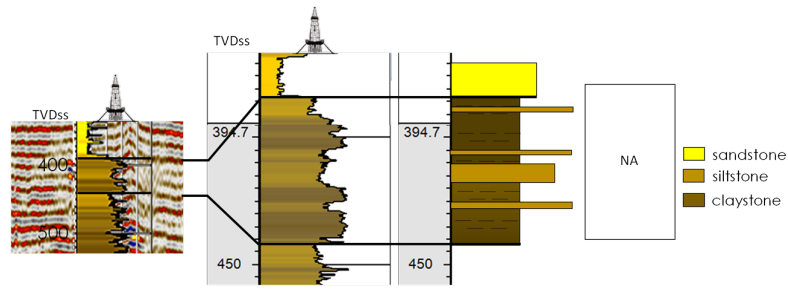
Figure C.8: The gamma ray response shows a characteristic coarsening upward trend of clay-free lithologies. There is no available core data at this depth.

The last part of the third Appendix contains sections that correspond to the Estimation of Seismic Volumes. The following figure shows the polygon shapes drew for each seismic unit in seismic lines ABT-91-03 and SNSTI-NL-87-03. Reconstruction of the less certain sea level changes curve by linear interpolation of constant time intervals it is also depicted in Figure C.11.
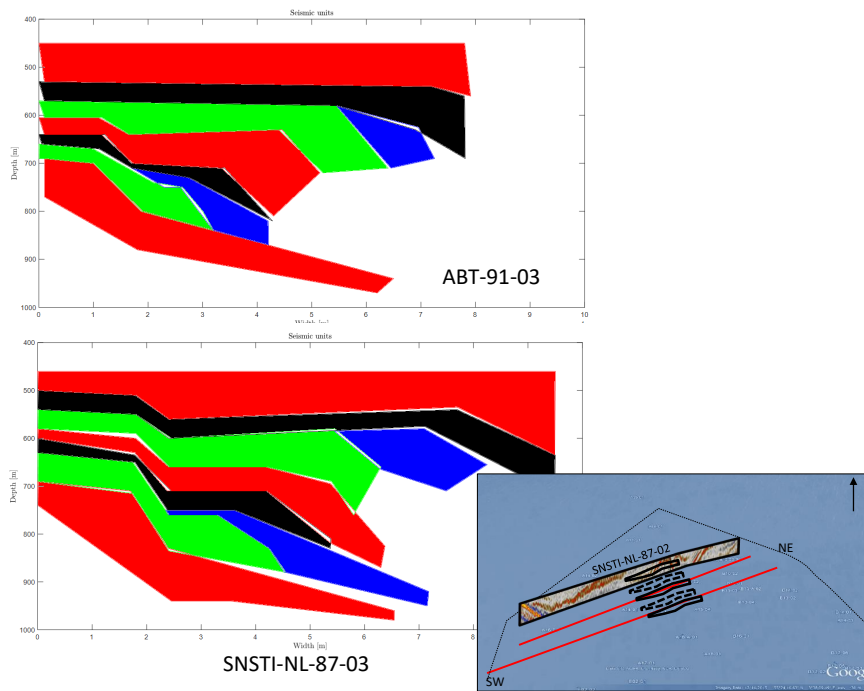

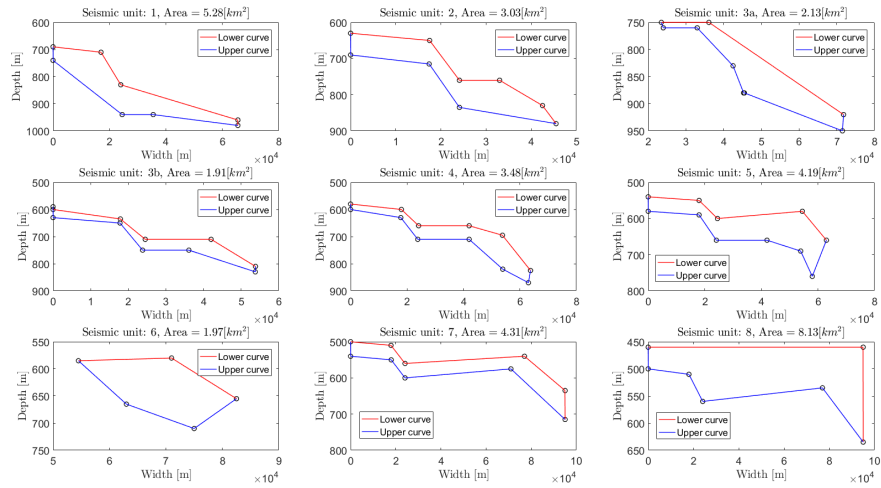Figure C.9: Surface areas of seismic units for seismic lines ABT-91-03 and SNSTI-NL-87-03

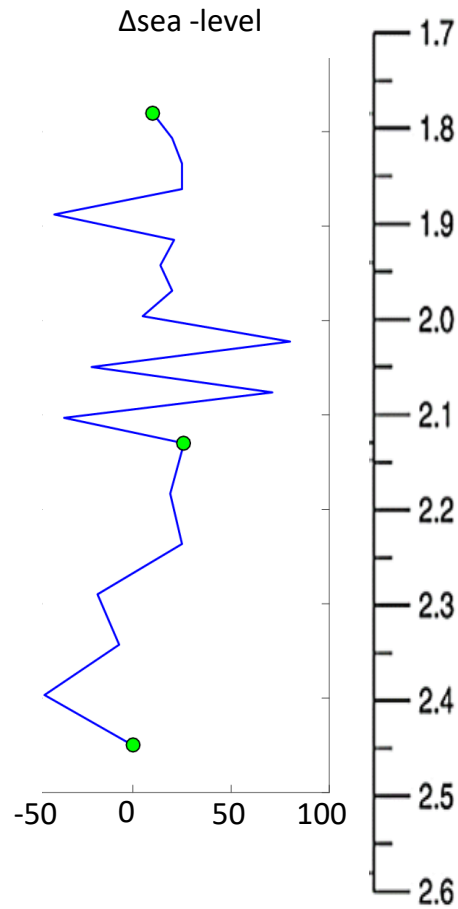Figure C.10: Calculation of the surface area of each unit by using a lower and upper curve

Figure C.11: Sea level curve of lower resolution reconstructed by this study

References

Badley, M. E. (1985). Practical seismic interpretation.

Bally, A. W. (1980). *Basins and subsidence-a summary.* Wiley Online Library.

Benvenuti, A., Kombrink, H., Ten Veen, J., Munsterman, D., Bardi, F., & Benvenuti, M. (2012). Late cenozoic shelf delta development and mass transport deposits in the dutch offshore area–results of 3d seismic interpretation. *Netherlands Journal of Geosciences*, *91*(4), 591–608.

Bijlsma, S. (1981). Fluvial sedimentation from the fennoscandian area into the north-west european basin during the late cenozoic. *Geologie en Mijnbouw*, *60*(4), 337–345.

Brooks, J., & Glennie, K. W. (1987). *Petroleum geology of north west europe: Proceedings of the 3rd conference on petroleum geology of north west europe held at the barbican centre, london, 26-29 october 1986* (Vol. 1). Graham & Trotman.

Cant, D. (1992). Subsurface facies analysis. *Facies Models, Response to Sea Level Changes. Geol. Assoc. Canada*, 27–45.

Carvajal, C. R., & Steel, R. J. (2006). Thick turbidite successions from supply-dominated shelves during sea-level highstand. *Geology*, *34*(8), 665–668.

Catuneanu, O. (2006). *Principles of sequence stratigraphy.* Elsevier.

Catuneanu, O., Abreu, V., Bhattacharya, J., Blum, M., Dalrymple, R., Eriksson, P., . . . others (2009). Towards the standardization of sequence stratigraphy. *Earth-Science Reviews*, *92*(1), 1–33.

Clausen, O., & Huuse, M. (1999). Topography of the top chalk surface on-and offshore denmark. *Marine and Petroleum Geology*, *16*(7), 677–691.

Clausen, O. R., Nielsen, O. B., Huuse, M., & Michelsen, O. (2000). Geological indications for palaeogene uplift in the eastern north sea basin. *Global and Planetary Change*, *24*(3), 175–187.

Cloetingh, S., Ziegler, P., Beekman, F., Andriessen, P., Matenco, L., Bada, G., . . . Sokoutis, D. (2005). Lithospheric memory, state of stress and rheology: neotectonic controls on europe's intraplate continental topography. *Quaternary Science Reviews*, *24*(3), 241–304.

Davis, A. (1992). Shallow gas: an overview. *Continental Shelf Research*, *12*(10), 1077–1079.

Ehlers, J., Grube, A., Stephan, H.-J., & Wansa, S. (2011). Pleistocene glaciations of north germany–new results. *Quaternary Glaciations: Extent and Chronology—A Closer Look: Developments in Quaternary Science*, *15*, 149–162.

Emery, D., & Myers, K. (2009). *Sequence stratigraphy.* John Wiley & Sons.

Gibbard, P., & Lewin, J. (2009). River incision and terrace formation in the late cenozoic of europe. *Tectonophysics*, *474*(1), 41–55.

Gibbard, P. L., & Lewin, J. (2016). Filling the north sea basin: Cenozoic sediment sources and river styles (andré dumont medallist lecture 2014). *Geologica Belgica*.

Hall, A. M., Gilg, H. A., Fallick, A. E., & Merritt, J. W. (2015). Kaolins in gravels and saprolites in north-east scotland: Evidence from stable h and o isotopes for palaeocene–miocene deep weathering. *Palaeogeography, Palaeoclimatology, Palaeoecology*, *424*, 6–16.

Harding, R., & Huuse, M. (2015). Salt on the move: Multi stage evolution of salt diapirs in the netherlands north sea. *Marine and Petroleum Geology*, *61*, 39–55.

Head, M. J., & Gibbard, P. L. (2015). Early–middle pleistocene transitions: linking terrestrial and marine realms. *Quaternary International*, *389*, 7–46.

Hijma, M. P., Cohen, K. M., Roebroeks, W., Westerhoff, W. E., & Busschers, F. S. (2012). Pleistocene rhine–thames landscapes: geological background for hominin occupation of the southern north sea region. *Journal of Quaternary Science*, *27*(1), 17–39.

Huuse, M., Redfern, J., Le Heron, D., Dixon, R., Moscariello, A., & Craig, J. (2012). Glaciogenic reservoirs and hydrocarbon systems..

Japsen, P. (1999). Overpressured cenozoic shale mapped from velocity anomalies relative to a baseline for marine shale, north sea. *Petroleum Geoscience*, *5*(4), 321–336.

Johannessen, E. P., & Steel, R. J. (2005). Shelf-margin clinoforms and prediction of deepwater sands. *Basin Research*, *17*(4), 521–550.

Kesel, R. H., & Gemmell, A. M. (1981). The 'pliocene'gravels of buchan: a reappraisal. *Scottish Journal of Geology*, *17*(3), 185–203.

Kirby, G., & Swallow, P. (1987). Tectonism and sedimentation in the flamborough head region of northeast england. *Proceedings of the Yorkshire Geological Society*, *46*(4), 301–309.

Knox, R., Bosch, A., Rasmussen, E., Heilmann-Clausen, C., Hiss, M., De Lugt, I., . . . others (2010b). *Petroleum geological atlas of the southern permian basin area.* Chapter.

Knox, R., Bosch, J., Rasmussen, E. S., Heilmann-Clausen, C., Hiss, M., De Lugt, I., . . . others (2010a). Cenozoic. In *Petroleum geological atlas of the southern permian basin area.* EAGE Publications bv.

Kuhlmann, G., Langereis, C., Munsterman, D., van Leeuwen, R. J., Verreussel, R., Meulenkamp, J., & Wong, T. (2006). Chronostratigraphy of late neogene sediments in the southern north sea basin and paleoenvironmental interpretations. *Palaeogeography, Palaeoclimatology, Palaeoecology*, *239*(3), 426–455.

Kuhlmann, G., & Wong, T. E. (2008). Pliocene paleoenvironment evolution as interpreted from 3d-seismic data in the southern north sea, dutch offshore sector. *Marine and Petroleum Geology*, *25*(2), 173–189.

Leckie, D. A. (1994). Canterbury plains, new zealand–implications for sequence stratigraphic models. *AAPG bulletin*, *78*(8), 1240–1256.

Mattern, F. (2005). Ancient sand-rich submarine fans: depositional systems, models, identification, and analysis. *Earth-Science Reviews*, *70*(3), 167–202.

Medvedev, S., & Hartz, E. H. (2015). Evolution of topography of post-devonian scandinavia: Effects and rates of erosion. *Geomorphology*, *231*, 229–245.

Miall, A. D., & Arush, M. (2001). The castlegate sandstone of the book cliffs, utah: sequence stratigraphy, paleogeography, and tectonic controls. *Journal of Sedimentary Research*, *71*(4), 537–548.

Mitchum Jr, R., Vail, P., & Sangree, J. (1977). Seismic stratigraphy and global changes of sea level: Part 6. stratigraphic interpretation of seismic reflection patterns in depositional sequences: Section 2. application of seismic reflection configuration to stratigraphic interpretation.

Overeem, I., Weltje, G. J., Bishop-Kay, C., & Kroonenberg, S. (2001). The late cenozoic eridanos delta system in the southern north sea basin: a climate signal in sediment supply? *Basin Research*, *13*(3), 293–312.

Pegrum, R., & Spencer, A. (1990). Hydrocarbon plays in the northern north sea. *Geological Society, London, Special Publications*, *50*(1), 441–470.

Pereira, L. A. G. R. (2009). *Seismic attributes in hydrocarbon reservoirs characterization* (Unpublished master's thesis). Universidade de Aveiro.

Rasmussen, E. (2004). The interplay between true eustatic sea-level changes, tectonics, and climatic changes: what is the dominating factor in sequence formation of the upper oligocene–miocene succession in the eastern north sea basin, denmark? *Global and Planetary Change*, *41*(1), 15–30.

Rasmussen, E., & Dybkjær, K. (2014). Patterns of cenozoic sediment flux from western scandinavia: discussion. *Basin Research*, *26*(2), 338–346.

Remmelts, G. (1995). Fault-related salt tectonics in the southern north sea, the netherlands.

Rudwick, M. (1996). Geological travel and theoretical innovation: The role ofliminal'experience. *Social studies of science*, *26*(1), 143–159.

Schroot, B., & Schüttenhelm, R. (2003). Expressions of shallow gas in the netherlands north sea. *Netherlands Journal of Geosciences*, *82*(1), 91–105.

Sørensen, J. C., Gregersen, U., Breiner, M., & Michelsen, O. (1997). High-frequency sequence stratigraphy of upper cenozoic deposits in the central and southeastern north sea areas. *Marine and Petroleum Geology*, *14*(2), 99–123.

Steel, R., & Olsen, T. (2002). Clinoforms, clinoform trajectories and deepwater sands. In *Sequence-stratigraphic models for exploration and production: Evolving methodology, emerging models and application histories: Gulf coast section sepm 22nd research conference, houston, texas* (pp. 367–381).

Thöle, H., Gaedicke, C., Kuhlmann, G., & Reinhardt, L. (2014). Late cenozoic sedimentary evolution of the german north sea–a seismic stratigraphic approach. *Newsletters on Stratigraphy*, *47*(3), 299–329.

Tropeano, M., Pieri, P., Pomar, L., & Sabato, L. (2002). The offlap break position vs sea level: a discussion. In *Egs general assembly conference abstracts* (Vol. 27).

Vail, P. R. (1987). Seismic stratigraphy interpretation using sequence stratigraphy: Part 1: Seismic stratigraphy interpretation procedure.

Van Der Molen, A. S. (2004). *Sedimentary development, seismic stratigraphy and burial compaction of the chalk group in the netherlands north sea area*. UU Dept. of Earth Sciences.

Van Wagoner, J., Mitchum Jr, R., Posamentier, H., & Vail, P. (1987). Seismic stratigraphy interpretation using sequence stratigraphy: Part 2: Key definitions of sequence stratigraphy.

Van Wagoner, J. C. (1995). Overview of sequence stratigraphy of foreland basin deposits: terminology, summary of papers, and glossary of sequence stratigraphy.

Van Wagoner, J. C., Mitchum, R., Campion, K., & Rahmanian, V. (1990). Siliciclastic sequence stratigraphy in well logs, cores, and outcrops: concepts for high-resolution correlation of time and facies.

Vinken, R. (1988). The northwest european tertiary basin:-results of the international geological correlation-programme, project no. 124.

Zachos, J., Pagani, M., Sloan, L., Thomas, E., & Billups, K. (2001). Trends, rhythms, and aberrations in global climate 65 ma to present. *Science*, *292*(5517), 686–693.

Zeng, H., & Backus, M. M. (2005). Interpretive advantages of 90-phase wavelets: Part 1—modeling. *Geophysics*, *70*(3), C7–C15.

Zhu, Y., Bhattacharya, J. P., Li, W., Lapen, T. J., Jicha, B. R., & Singer, B. S. (2012). Milankovitch-scale sequence stratigraphy and stepped forced regressions of the turonian ferron notom deltaic complex, south-central utah, usa. *Journal of Sedimentary Research*, *82*(9), 723–746.

Ziegler, P. A. (1990). Geological atlas of western and central europe..